Evaluating Sulfotransferases Metabolism *In Vitro*, Method Development and Application in Anti-doping Research

Inaugural-Dissertation

to obtain the academic degree

Doctor rerum naturalium (Dr. rer. nat.)

submitted to the Department of Biology, Chemistry, Pharmacy

of Freie Universität Berlin

by

Yanan Sun

2023

2

Research of the present study was conducted from 2017 until 2020 at School of Pharmaceutical Science and Technology of Tianjin University, and from 2020 to 2023 at the Institute of Pharmacy of the Freie Universität Berlin, under supervision of Prof. Dr. Maria Kristina Parr and Prof. Dr. Matthias Bureik.

1st Reviewer: Prof. Dr. Maria Kristina Parr

2nd Reviewer: Prof. Dr. Matthias Bureik

Date of defence: 13.11.2023

Table of Contents

Abbreviations

A

AAS ....Anabolic androgenic steroids
ABP ....Athlete Biological Passport
AMP .... Adenosine monophosphate
APS...Adenosine-5′-phosphosulfate
ATP...Adenosine triphosphate

C

cDNA .... Complementary DNA
CYP ....Cytochrome P450

D

DHEA .... Dehydroepiandrosterone

E

E.Coli... *Escherichia coli*
EMM .... Edinburgh minimal medium
ER.. Endoplasmic reticulum

G

GC-MS/(MS)........................... Gas chromatography coupled with (tandem) mass spectrometry

H

His ....Histidine
HPLC...High-performance liquid chromatography

L

LC-ESI-QQQ-MS ....Liquid chromatography hyphenated by electrospray ionization to a triple quadrupole mass spectrometer
LC-ESI-QTOF-MS..................Liquid chromatography coupled by electrospray ionization to a quadrupole time-flight-mass spectrometer

LC-MS(/MS) .... liquid chromatography coupled by (tandem) mass spectrometry
LC-QTOF ....liquid chromatography coupled by a quadrupole time-flight-mass spectrometer
Lys ....Lysine

M

M2 .... 17α-methyl-5β-androstan-3α,17β-diol
MT .... Methyltestosterone

O

OATPs ....Organic-anion-transporting polypeptides

P

PAP .... 3′-phosphoadenosine-5′- phosphate
PAPS... 3'-phosphoadenosine-5'-phosphosulfate

Q

qNMR...Quantitative nuclear magnetic resonance spectroscopy

S

S. pombe .... *Schizosaccharomyces pombe*
S.cerevisiae ....*Saccharomyces cerevisiae*
S2.. 17α-methyl-5β-androstan-3α,17β-diol, 3α-sulfate
S3.. 17α-methyl-5α-androstan-3β,17β-diol, 3α-sulfate
S4.. 17α-methyl-5β-androstan-3β,17β-diol, 3α-sulfate
Ser... Serine
SFC-MS/MS.....Supercritical fluid chromatography hyphenated by tandem mass spectrometry
SULTs .... Sulfotransferases

U

UGTs ....Glucuronosyltransferases

W

WADA .... World Anti-Doping Agency

1 Introduction and aims of this project

Humans are constantly exposed to various xenobiotics, including environmental compounds like pollen, food, drugs, and pharmaceuticals. The metabolic processes occurring within the human body play a crucial role in regulating the activity and toxicity of these xenobiotics, facilitating their excretion before they accumulate to toxic levels. The metabolic pathway can be divided into two phases: phase I (functionalization) and phase II (conjugation) metabolism. Phase II metabolism involves two main pathways, glucuronidation and sulfonation, catalyzed by glucuronosyltransferases (UGTs) and sulfotransferases (SULTs) respectively. Despite its significant role in both drug and doping compound metabolism, SULT catalyzed metabolism has not received sufficient attention over the years. This study focuses on the evaluation of the enzymatic functionality of human SULTs based on a recombinant fission yeast expression system, specifically in relation to doping compounds. The research aims to shed light on the role of human SULTs in drug metabolism and enhance our understanding of the significance of this pathway in regulating the metabolism of xenobiotics.

The misuse of doping substances and methods is not only unethical and against the principles of fair competition but also poses significant health risks to athletes [1]. Anti-doping testing is typically performed through the direct detection of administrated doping substances or their metabolites [2]. Since numerous doping compounds undergo extensive metabolism after administration and remain nearly undetectable as parental compounds, their metabolites play an essential role in extending the detection window and are often considered preferred analytes. Detecting sulfate metabolites, particularly sulfate steroids (for their thermal instability), requires enzymatic or chemical hydrolysis of sulfates [3] as a pre-treatment. These processes can result in the degradation of certain analytes or the generation of undesired by-products, thus, additional purification steps prior to instrumental detection are necessary to avoid the by-product effects on analyte detection [3-5]. Therefore, direct analysis of sulfate metabolites from urine excretion is desirable in anti-doping research.

Despite the benefits of direct detection of sulfate metabolites, a significant challenge arises from the lack of sulfo-conjugates as standard reference compounds. Chemical synthesis of sulfate metabolites is considered efficient for compounds with only one potential conjugation

site [6-8]. By contrast, accurately synthesizing from compounds with multiple conjugation sites becomes problematic due to the potential side products, which may share a similar structure with the desired product and pose challenges in their separation [9, 10]. Thanks to the regioselectivity of enzymes, biosynthesis allows the synthesis of specific sulfate metabolites for compounds with multiple conjugation sites. In this work, I aimed to investigate a potential biosynthetic method as a viable alternative to the chemical synthesis of sulfate metabolites, mainly focusing on sulfo-conjugates of doping substances. The new method enhances the performance of SULT metabolite identification in doping control analysis and it also presents novel perspectives and valuable contributions for future research in this field.

2   Theoretical background

2.1   *Overview of human sulfotransferases*

SULTs are a class of phase II enzymes which catalyze the transferring of a sulfonate moiety from the cofactor 3'-phosphoadenosine-5'-phosphosulfate (PAPS) to a hydroxyl or amine group of a small molecule (Figure 1). The sulfonate moiety on the small molecule's scaffold increases the hydrophilicity of the compound, allowing rapid excretion from the human body through biological fluids.
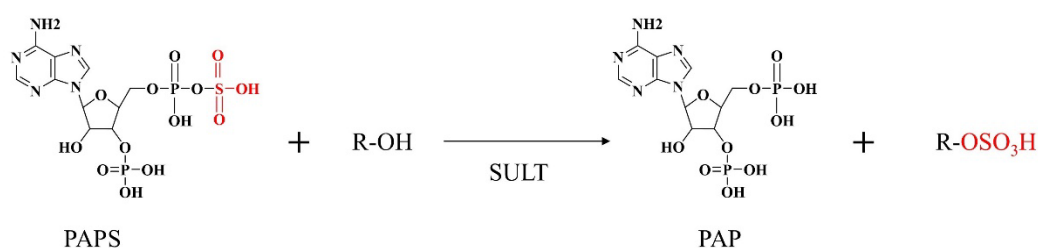

Figure 1. SULT catalyzed sulfonation. In this reaction, a sulfonate moiety is transferred from cofactor PAPS to an alcohol acceptor, generating 3'-phosphoadenosine-5'- phosphate (PAP) and the corresponding sulfate.

Before the mid-1990s, SULTs were classified mostly based on substrate specificity [11]. However, the overlapping substrate specificity among SULT isoforms resulted in a chaotic nomenclature. With the advent of molecular cloning and nucleotide/amino acid sequence analysis, all SULTs are now classified in different gene families within the SULT gene superfamily [12]. In humans, there are 14 SULT isoforms belonging to the families SULT1, SULT2, SULT4, and SULT6 [11]. Each SULT isoform has distinguished characteristics that give them substrate selectivity. For instance, members of the SULT1 family generally have a higher affinity for phenolic compounds. In comparison, the members of the SULT2 family demonstrated to have a higher affinity for steroid compounds [11]. SULT4A1 and SULT6B1 are the only known human isoforms in the SULT4 and SULT6 families, respectively. Despite numerous studies, the enzymatic characteristics of SULT4A1 and SULT6B1 were not identified

for a long time. Within the present work, the enzymatic functionality of these two enzymes has been demonstrated for the first time.

SULTs play a crucial role in both exogenous and endogenous metabolism. Sulfonation is a fundamental metabolic pathway for xenobiotics and endogenous compounds. Many active pharmaceutical ingredients are sulfonated in the human body; examples are non-steroidal anti-inflammatory drugs [13], breast cancer drugs [14], and phytopharmaceuticals such as liguzinediol [15]. Furthermore, SULTs are also relevant for the metabolism of some pollutants [16] and carcinogens [17]. In endogenous metabolism, SULTs are responsible for maintaining the homeostatic range of various important compounds, such as steroids, secosteroids, catecholamines, serotonin, and tyrosine-containing peptides [18].

SULTs have a wide distribution in tissues. The classification, main tissue localization, and typical substrates of SULT isoforms in humans are described in Table 1. While SULT1A1 abounds in the liver, the expression of SULT1A2 and SULT1C3 is mainly in the small intestine, and certain SULTs are found in other tissues such as colon, kidney, stomach, or skin. The broad distribution of SULTs in the human body underlines their importance and multi-functionality.

Table 1. Classification, main tissue localization, and typical substrates of SULT isoforms.

SULT subfamily	SULT isoform	Main tissue localization	Typical substrates
SULT1A	SULT1A1	Liver, adrenal gland [19]	Polyphenols [11], minoxidil [20]
	SULT1A2	Small intestine, liver [21]	Phenols [11], aromatic hydroxylamines and hydroxamic acids [22],
	SULT1A3	Brain [19], small intestine [21]	Catecholamines, dopamine [23]
SULT1B	SULT1B1	Colon, small intestine [21]	Phenols [11], thyroid hormones [24]
SULT1C	SULT1C2	Fetal kidney and liver [24], stomach [21]	p-Nitrophenol [25]
	SULT1C3a	Small intestine, colon [26]	-
	SULT1C3d	-	Benzylic alcohols [27]
	SULT1C4	Ovary, kidney [28]	Estrogens, flavonoids [29]
SULT1E	SULT1E1	Ileum, liver [21]	Estrogens [30]
SULT2A	SULT2A1	Liver, adrenal gland [21]	Hydroxysteroids, Butorphanol [31]
SULT2B	SULT2B1a	Colon, ovary [32]	Hydroxysteroids [33]
	SULT2B1b	Prostate, skin [34]	Hydroxysteroids [33]
SULT4A	SULT4A1	Brain [35]	-
SULT6B	SULT6B1	Spermatids [36, 37]	-

[*]- : No tissue localization or no substrate is reported

2.1.1   Structural and mechanistic studies

As the first resolved SULTs crystal structure, murine SULT1E1 was determined during the 1990s [38]. Subsequently, based on this template, the first human SULT structure, SULT1A3, was identified. Since then, over 35 crystal structures of human SULT isoforms were reported [39]. The mechanism of SULT catalyzation is still ambiguous. The reaction takes place through the nucleophilic attack of the substrate on the sulfate group of PAPS, proceeding primarily with the involvement of four residues: Histidine (His) 109, Lysine (Lys) 48, Lys107, and Serine (Ser)

135 (human SULT1B1 residue numbering, Figure 2), which exhibit a high degree of conservation across active human SULTs [40, 41].

His109 has been identified as the catalytic base responsible for the deprotonation of the substrate's hydroxy group [40]. Lys105 plays a role in substrate positioning and contributes to stabilizing the transition state by interacting with an oxygen atom of the sulfate [40, 42]. Lys48 is assumed to serve as a proton donor to the bridging oxygen, acting as a catalytic acid and aiding in the stabilization of the transition state, thereby facilitating the hydrolysis of the sulfonate-PAP bond [42]. Ser135 can regulate the hydrolysis of PAPS by modulating the position of Lys48 [42, 43]. Among different SULT isoforms, the illustration of reactive amino acid residues may be slightly different. The mechanistic models for four different isoforms in Manuscript II describe such differences in detail.
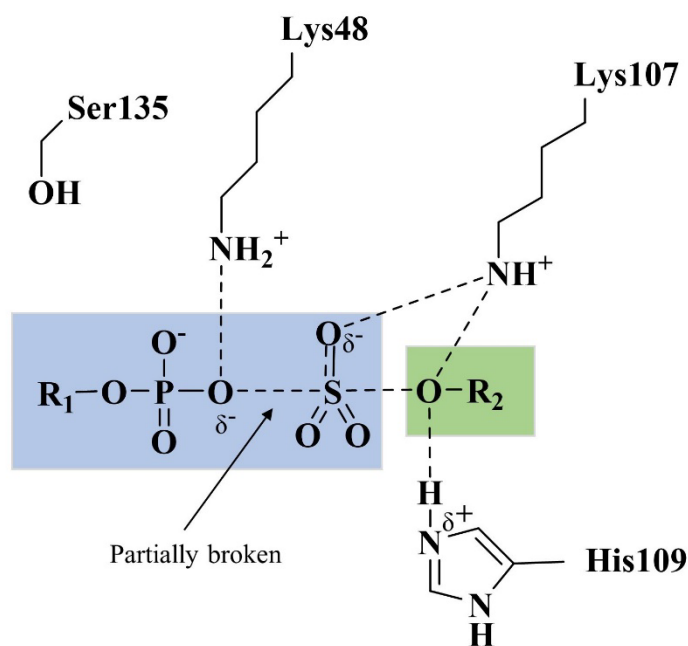
Figure 2. Reaction mechanism of SULT catalyzed sulfonation, taking human SULT1B1 as example. The blue box highlights the cofactor PAPS, while the green box highlights the recipient substrate [11].

All SULT structures are spherical in nature. An overlay of the structures of four SULT isoforms is presented in Figure 3. The substrate binding pocket and the PAPS binding pocket comprise

the two entrances of SULTs. The structural comparison of the displayed four enzymes indicates that their backbone positions exhibit high similarity, except for three loops surrounding substrate binding pocket. The differences between the three loops significantly affect substrate selectivity and stereoselectivity. Some domains are conserved across all isoforms, including the binding-substrate pocket (active site), PAPS binding pocket, and the dimerization domain (not shown) [11]. Understanding the structural and mechanistic basis for the specificity of human SULTs is essential to explore their role in maintaining homeostasis and regulating drug metabolism, which may aid in medication safety and the development of novel therapeutics.
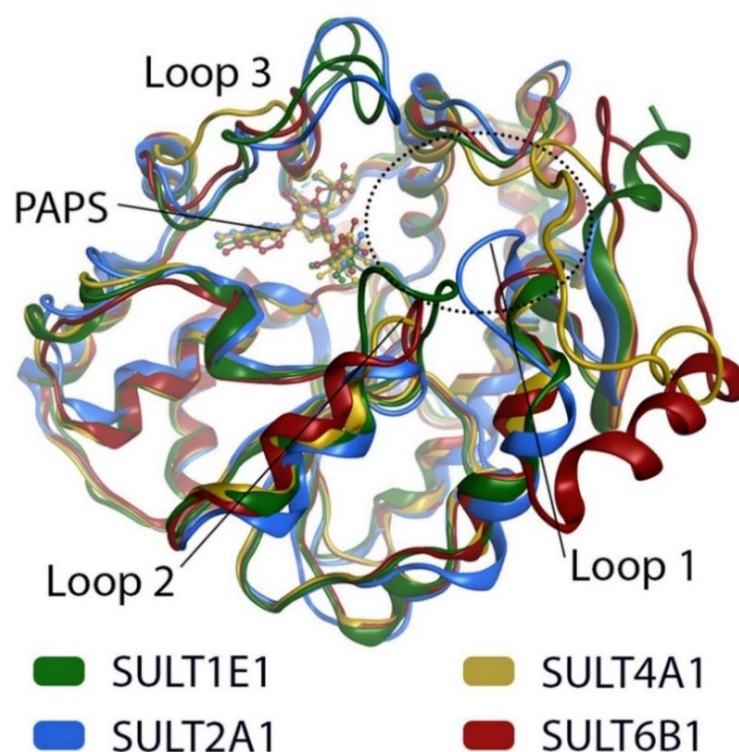
Figure 3. Overlay of the structures of four SULT isoforms, SULT1E1 (green), SULT4A1 (yellow), SULT2A1 (blue), and SULT6B1 (red). The dotted circle indicates substrate binding pocket.

2.1.2 *The generation and metabolism of cofactor PAPS*

As a sulfo-moiety donor, the cofactor PAPS is necessary for SULT reactions. The production of high-energy PAPS involves a two-step process. First, adenylation: adenosine-5′-phosphosulfate (APS) is generated through adenosine triphosphate (ATP) sulfonation catalyzed

by ATP sulfurylase. Second, phosphorylation of APS to PAPS by APS kinase [44]. The generated PAPS is subjected to SULT sulfonation. The PAP resulting from PAPS is subsequently dephosphorylated to adenosine monophosphate (AMP) and rephosphorylated in a few enzymatic steps to regenerate ATP. The formed sulfo-conjugates of substrates by SULT catalyzed sulfonation may be de-sulfated by sulfatases or secreted via organic-anion-transporting polypeptides (OATPs). The generation and metabolism of PAPS in mammalian cells are shown in Figure 4 [45].
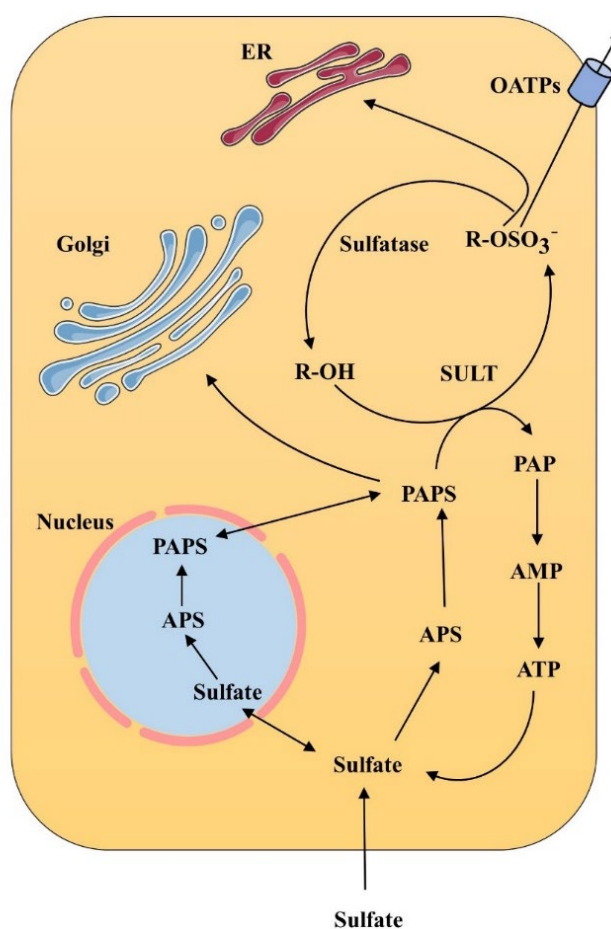
Figure 4. Sulfonation pathway in mammalian cells. Apart from involving sulfonation in cytoplasm, PAPS can be channeled into the Golgi apparatus (as indicated). Sulfated compounds can subsequently either be de-sulfated in the cytoplasma or in the endoplasmic reticulum (ER) or excreted through OATPs.

Sulfate activation to APS or PAPS is crucial not only for sulfation pathways but also for the primary assimilation of sulfate in plants, algae, bacteria, and fungi [46]. In particular, PAPS plays a vital role in sulfate reduction and cysteine synthesis in fungi and certain bacteria [47]. As a sulfo-moiety donor, PAPS is required for the sulfonation by cytosolic SULTs (see above) and also in the sulfation catalyzed by membrane-bound sulfotransferases in the Golgi [48]. Exogenous PAPS is often needed for *in vitro* studies of SULT metabolism and can be costly. Hence, we have developed and optimized a new approach that integrates SULT-dependent biotransformation with PAPS production *in situ*, utilizing the ability of synthesizing PAPS in fission yeast cells. Further information and specific details can be found in Manuscript III.

2.2   *In vitro studies on metabolism*

In vitro metabolism studies are generally carried out using organ preparations, such as homogenised human liver fractions and liver microsomes, or recombinantly expressed enzymes using microorganisms or *in vitro* cells as hosts, or isolated enzymes. Compared to *in vivo* studies, *in vitro* techniques offer advantages with respect to low cost and fast results. In addition, *in vitro* research avoids unpredicted adverse effects that may arise from administering potentially harmful drugs (without clear toxicity profiles) to human volunteers or experimental animals. Therefore, *in vitro* studies are generally conducted as an alternative or preliminary step before proceeding to *in vivo* studies.

- **Organ preparations** for metabolism investigation are mostly derived from liver, which is the main metabolic organ. Nevertheless, preparations of small intestine, kidney, or lungs are also applied for certain metabolic research [31]. These assays are characterized by a rapid reaction time and low substrate amount requirements, but cofactor addition might be mandatory. Hepatocytes, which are cells derived from the main parenchymal tissue of the liver, are used either fresh or after cryopreservation for disease research, drug screening, and predictive drug toxicology [49-51]. Human liver microsomes are subcellular fractions derived from the ER of hepatic cells that are obtained through homogenized liver followed by differential centrifugation. The S9 fraction is the supernatant fraction obtained from an organ homogenate (liver, intestine, or kidney) with 9000 g centrifuging

for 20 min in a suitable medium [52]. As cytosolic enzymes, most SULT isoforms are localized in the liver S9 fraction. Therefore, in this study, human liver S9 fraction is used for substrate screening of SULTs (Manuscript II).

- **Isolated enzymes** can be obtained through protein/peptide chemical synthesis or by isolating recombinant enzymes. In metabolism studies, isolated enzymes offer the advantages of low substrate amount requirements, and direct and efficient enzymatic reactions. Therefore, they are typically applied in evaluating metabolic pathways and kinetic studies. However, the drawbacks are obvious. For the enzymes that are not commercially available like SULTs, in-house production is required. Thus, the complex procedure involved in generating targeted enzymes and the subsequent purification is time consuming and expensive.

- **Recombinant expression systems** are typically either gene-modified microorganisms or *in vitro* cell lines. Both prokaryotic and eukaryotic microorganisms, such as *Escherichia coli* (*E.Coli*) [53], *Caenorhabditis elegans* [54], *Saccharomyces cerevisiae (S.cerevisiae)* [20] are commonly employed as host cells in metabolite synthesis. In comparison to an isolated enzyme assay, no isolation of enzymes is required in this model. Thus, it reduces the experimental process. However, undesired side products generated by host cells might pose a problem in the later analysis and purification of targeted metabolites.

2.2.1   Recombinant fission yeast expression system

Yeasts are eukaryotic unicellular fungi that encompass more than 1500 species. As one of the earliest applied microorganisms, yeasts have been extensively used in our daily lives for thousands of years. Beyond their traditional uses in baking, beer or wine production, yeasts have recently also found applications laboratory research and in the pharmaceutical industry as carrier cells, food additives, and even in treating enteropathy [55-57]. These applications are resulting from their abundant bioactive substances, such as proteins, vitamins, and enzymes. In laboratory research, yeasts are also some of the most used recipient cells. As eukaryotic cells, yeast can offer more precise protein folding than bacteria. Moreover, they can conduct posttranslational modifications on heterologous proteins, such as phosphorylation or

glycosylation [58]. Compared to mammalian cells, yeast cells are easier to manipulate, have simpler growth conditions, and much faster reproductive cycles.

Two important yeast species for biological research are the budding yeast *S. cerevisiae* and the fission yeast *Schizosaccharomyces pombe* (*S. pombe*). The cell cycles of both are presented in Figure 5. Both species have diverged from each other hundreds of million years ago [59]. According to gene sequence, cell cycle, and chromosome structure [60], *S. pombe* is as closely related to humans as it is to *S. cerevisiae*. Like other yeasts, both are suitable hosts for the recombinant expression of some foreign genes but not for others [61].
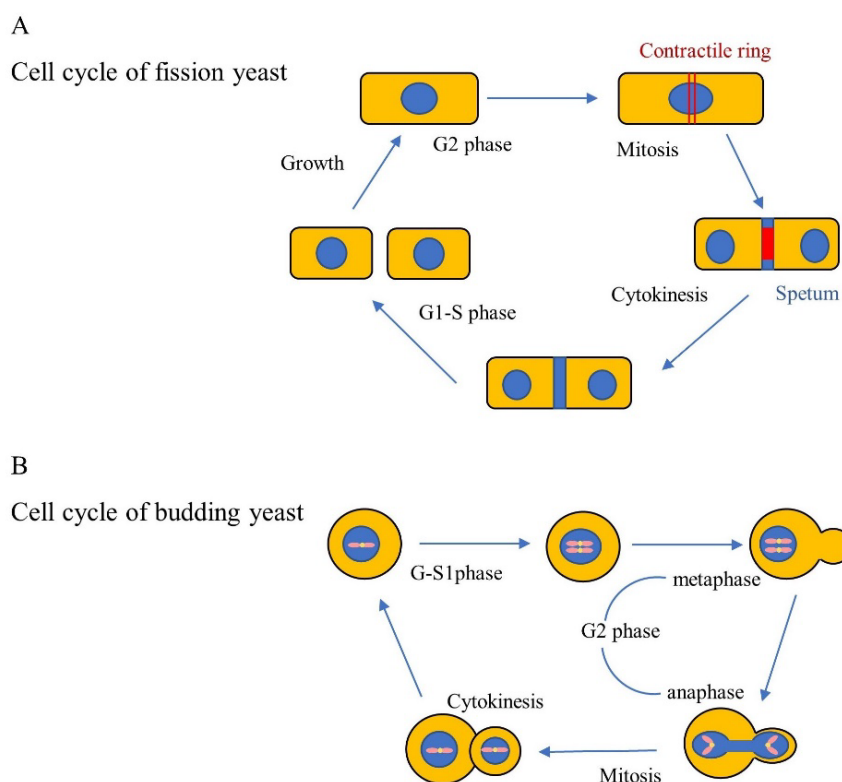
Figure 5. Cell cycle of fission yeast and budding yeast. A) presents the cell cycle of fission yeast. During mitosis, cell growth halts, and chromosomes are segregated by the mitotic spindle based on the contractile ring (red); during cytokinesis, as the contractile ring constricts, the medial septum (blue) grows inward [62]. B) presents the cell cycle of budding yeast. G₁-S phase involves preparation and DNA replication; G₂ phase is further divided into metaphase and anaphase, facilitating the preparation of mitosis [63].

Previously, Bureik *et al.* have successfully used fission yeast *S. pombe* for the functional expression of orphan cytochrome P450 (CYP) enzymes like CYP2A7, CYP4Z1, CYP4A22, and CYP20A1 [64-66], and a complete set of human UGTs [67, 68]. Therefore, fission yeast is considered as a promising host for the recombinant expression of human SULTs.

The generation of a complete set of recombinant fission yeast strains, each expressing one of the 14 human SULTs, is demonstrated in Manuscript II. Expression vectors employed were the integrative vector pCAD1 [69] and replicating vector pREP1 [70]. For both vectors, the cloning sites of the targeted SULT complementary DNAs (cDNA) are *Nde*I and *Bam*HI (Figure 6).
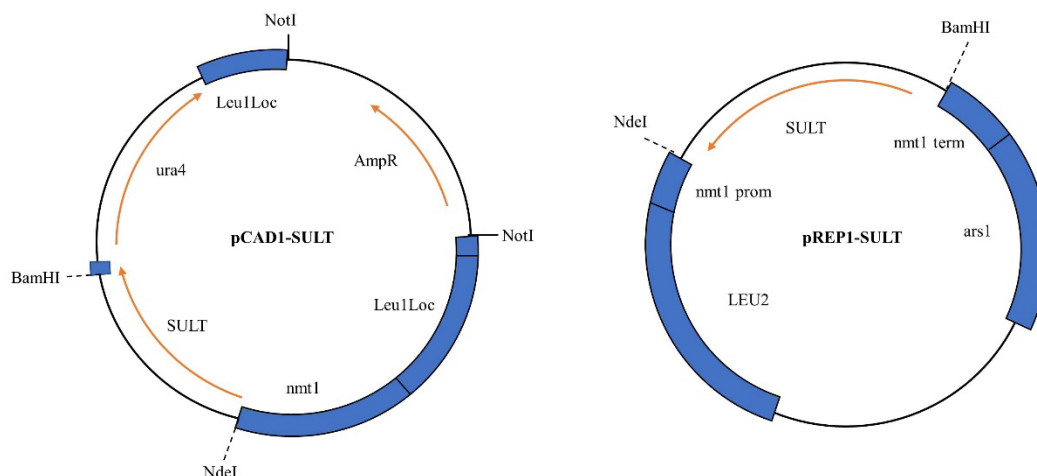

Figure 6. Vector map of pCAD1-SULT pREP1-SULT. In pCAD1-SULT, Leu1Loc indicates the gene fragments of the leu1 gene, which serve as integration target sequence; AmpR encodes β-lactamase; nmt1, nmt1 promoter; ura4 encodes orotidine monophosphate decarboxylase, which complements ura4.dl18 in S. pombe. In pREP1-SULT, nmt1 prom, nmt1 promoter; nmt1 term, nmt1 terminator; ars1, origin of replication [71]. S. cerevisiae LEU2 encodes β-isopropylmalate dehydrogenase and therefore complements mutations in the S. pombe leu1 gene.

To construct recombinant fission yeast, the vector pCAD1 needs to be digested with *Not*I enzyme to yield a long integration fragment (approximately 6.0 kb) containing the expression cassette, the *ura4* maker and franking *leu1* sequences. Successful transformants can be selected

using Edinburgh minimal medium (EMM) with leucine additive, as the targeted integration of pCAD1 by homologous recombination occurs at the *leu1* locus. Subsequently, recombinant pREP1 plasmids with the same enzyme cDNA introduced were transformed into the newly created strains. Like the fission yeast *leu1* gene, the *LEU2* gene of *S. cerevisiae* encodes β-isopropylmalate dehydrogenase and therefore complements *leu1* defects in *S. pombe*, but without a danger of homologous recombination due to the very diverse nucleotide sequences of the two genes. Therefore, transformants can be identified by growth on EMM without leucine supplement.

Consequently, each of the 14 double-expressor strains contains an integrated expression unit and an autosomal expression plasmid for the same SULT. Double-expressor strains provide a more robust expression of the targeted enzyme, while avoiding the need for amino acid supplements.

2.2.2   *Whole-cell biotransformation and enzyme bags*

Whole-cell biotransformation is extensively applied for metabolite biosynthesis due to its low cost and scalability. The intracellular level of the cofactor PAPS was proven to be sufficiently high for sulfonation in both budding yeast [20] and fission yeast (Manuscript II). Thus, exogenous PAPS is not necessary for sulfonation in whole-cell biotransformation using recombinant yeast strains. Due to the active state of the cells during the enzymatic reaction, regrowth and continuous production are feasible, which also results in cost-efficiency.

However, this approach has drawbacks such as low sensitivity and inefficiency due to the multilayer structural cell wall and cell membrane of yeast, which can hinder substrate entry into the cytoplasm, which is especially relevant in hydrophilic substrates. Moreover, the newly generated (and even more hydrophilic) metabolites might not be expelled efficiently from the cells for the same reason. A biotransformation method employing permeabilized fission yeast cells (enzyme bags) was developed to overcome these challenges. This method allows small molecules (such as substrates, cofactors, and products) to move freely between the assay medium and the interior of the cells, while large molecules (such as enzymes) are retained inside the cells. As a result, the enzyme bag assay has higher sensitivity and shorter reaction times. The effectiveness of this enzyme bags assay has already been demonstrated for CYPs

[65, 66] and UGTs [72] in previous studies. In this study, several enzyme bag assays were developed for different purposes (Manuscript II and Manuscript III).

2.2.3   *In silico studies on metabolism*

An *in silico* study is one performed via simulation on a computer. Associated with *in vitro* or *in vivo* studies, *in silico* experiments are widely applied in metabolic research. These experiments predict drug metabolic processes and assess potential adverse drug reactions by employing mathematical models and computer simulations. One example of molecular modelling experiments presented in Manuscript II was performed by Dr. David Machalz from the group of Prof. Dr. Wolber (FU Berlin). Docking experiments can help to understand the mechanism of enzymatic reactions. By visualizing enzymatic structures, substrates, cofactors, and inhibitors in three-dimensional space, the findings obtained from *in vivo* and *in vitro* studies can also be more effectively and intuitively illustrated. This integration of *in silico* methodologies with experimental approaches enhances our understanding of complex biochemical processes and provides valuable insights into drug metabolism and related phenomena.

2.3   *Doping control analysis*

The misuse of performance-enhancing drugs is a prevalent issue in sports and daily life [73]. This behaviour is strictly prohibited in sports, as it violates the spirit of sportsmanship and results in unfair competition [74]. Furthermore, the misuse of certain drugs can pose a health risk to both elite and recreational athletes. The term "doping" encompasses the utilization of prohibited substances or methods. Therefore, doping control analysis is of paramount importance in maintaining the integrity of sports and safeguarding the health of athletes by discouraging the misuse of doping substances, especially those that can cause serious side effects. The World Anti-Doping Program and the "World Anti-Doping Code" are implemented to protect the fundamental rights of athletes to participate doping-free sport and ensure harmonized, coordinated and effective anti-doping programs [74]. To ensure the generation of valid test results and to promote harmonization in analytical resting samples by laboratories and Athlete Biological Passport (ABP), the World Anti-Doping Agency (WADA) has published International Standards for Laboratories [75].

Analysis of urine samples has always been the preferred approach in anti-doping detection, as metabolites of most doping substance are excreted via kidney [1]. Blood samples may also be available, but urines offer the advantages of accessibility and non-invasive sample collection. Gas chromatography coupled with (tandem) mass spectrometry (GC-MS/(MS)) is one of the typical approaches for detecting targeted metabolites in urine sample. Sample preparation including hydrolysis, derivatization, or extraction is commonly required to obtain detectable analytes, increase sensitivity, or remove undesired impurities that may influence the detection of targeted analytes [3, 4]. A detailed introduction to sample preparation and GC-MS(/MS) techniques can be found in Manuscript I. However, inadequate hydrolysis and potential loss of analytes during each step of sample preparation can result in inaccurate detection or analyte concentrations below the limits of detection of GC-MS(/MS) [4]. Moreover, derivatization agents may lead to the formation of certain adducts which can interfere with the subsequent analytical detection [76]. Recently, a multi-target approach using liquid chromatography coupled by (tandem) mass spectrometry (LC-MS(/MS)), known as "dilute-and-inject" or "dilute-and-shoot", has been developed [77, 78]. This method allows for high-throughput and cost-efficient screening by direct injection of urine samples, without the need for sample pre-treatment. However, reference materials for identification and quantitation of targeted analytes are required in both GC-MS(/MS) and LC-MS(/MS) methods.

2.3.1   *Sulfotransferases metabolism in doping control analysis*

The study of SULT metabolism in doping control analysis has attracted increasing attention. The number of publications relevant to SULT metabolism in doping control analysis display an obvious increase over the last two decades (Figure 7). SULTs are widely involved in the metabolism of doping substances, including the sulfonation of anabolic androgenic steroids (AAS, such as boldenone and stanozolol) [79, 80], stimulants (such as octopamine) [81], beta-2-agonists (such as salbutamol and terbutaline) [9, 82, 83], and beta blockers (such as propranolol) [81].
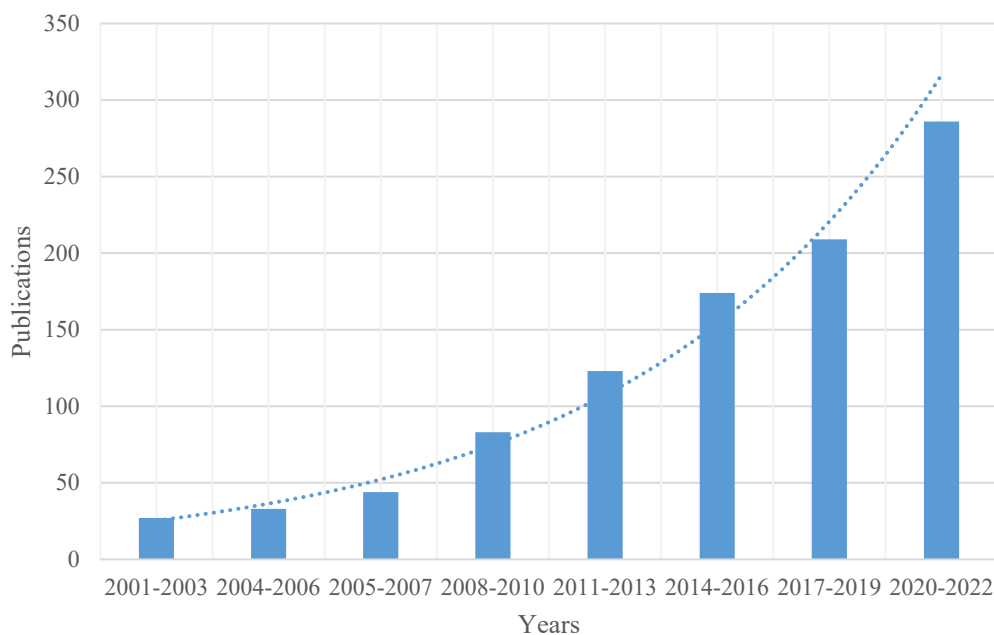
Figure 7. Number of publications relevant to SULT metabolism in doping control analysis from 2000 to 2022. The data originates from the PubMed database [84].

Most SULT metabolites of doping substances are reported as monoconjugates, although the presence of bis-sulfates has been recognized since the 1960s [85, 86]. As the most commonly misused doping substances, AAS are excreted from human body mainly as glucuronide or sulfate conjugates [73, 87]. While glucuronidation is considered the predominant pathway for AAS metabolism, sulfonation is reported to play a crucial role in the metabolism of steroids possessing a 3β-hydroxy function, such as dehydroepiandrosterone (DHEA) [88]. Other steroids, including androsterone, etiocholanolone, and testosterone, have been reported to be excreted as sulfates and glucuronides in similar percentages [89, 90]. Hence, the study of SULT metabolism and the detection of sulfo-conjugates are of high importance in doping control analysis.

In anti-doping detection, finding the best marker for detecting prohibited drug misuse is always important. Monitoring of SULT metabolites may provide alternative markers for detecting specific doping compounds or extending the detection window [91-93]. Sulfate conjugates associated with plasma proteins lead to an extended residence time in the body compared to glucuronic acid-conjugated metabolites [4]. Analyzing these sulfate conjugates may improve

the detection time window for specific metabolites. Detecting long-term metabolites makes it harder for athletes abusing prohibited drugs to remain undetected, thus promoting fairness in sports.

Analysis of SULT metabolites in anti-doping research is generally performed using GC-MS(/MS) [4, 94], LC-MS(/MS) [7, 80], and supercritical fluid chromatography hyphenated by tandem mass spectrometry (SFC-MS/MS) [81, 95]. As mentioned previously, detecting sulfate metabolites using GC-MS(/MS) requires complex pre-treatment processes. Direct LC-MS(/MS) or SFC-MS/MS analysis is a promising alternative, whereas many reference materials of SULT metabolites are not commercially available or are costly.

2.4   Synthesis of reference materials

Reference materials of metabolites of doping compounds play a vital role in anti-doping research and relevant fields by enabling accurate and convenient identification and quantitation of targeted analytes in biological fluids. As mentioned in Chapter 2.3, phase II conjugates may undergo hydrolysis to release the corresponding phase I metabolites or parental compounds, prior to GC-MS(/MS) detection. Thus, reference materials of the corresponding released compounds are required in this approach. The direct detection using LC-MS(/MS) or SFC-MS/MS requires reference materials of the targeted metabolites. In cases where commercial reference materials are unavailable, chemical or biological synthesis is necessary. For more comprehensive information, refer to Manuscript I.

2.4.1   Chemical synthesis

Chemical synthesis is usually the method of choice to obtain the reference materials of SULT metabolites for anti-doping analysis due to its efficiency and cost-effectiveness. Several methods have been developed using a pyridine complex of sulfur trioxide [6, 9, 80], sulfuric acid and carbodiimides [96], sulfamic acid [97], or sulfurylimidazolium salts [98, 99] as sulfo-moiety donors. Chemically synthesized sulfated references have been widely applied for analytical method development, identification, and quantitation of the relevant metabolites in doping control samples [9, 100, 101]. Metabolites with a single conjugation site can generally be effectively synthesized chemically [8, 102, 103]. However, chemical synthesis may not be as efficient for compounds with multiple potential conjugation sites due to the challenge of

separating the desired compound from (complex) side products [9]. Further information can be found in Manuscript I.

2.4.2   Biological synthesis

Biological synthesis is an alternative approach. Utilizing enzyme catalyzed synthesis, this approach generally exhibits good regioselectivity, thus, minimizing the occurrence of isomeric side products. Additionally, biosynthesis is considered greener than chemical synthesis since enzymatic reactions are inherently safer, carried out at mild conditions and commonly take place in aqueous solution, which reduces the use of harmful organic solvents [104]. *In vitro* biosynthesis involves an enzyme-catalyzed process using tissues, cells, isolated enzymes, or recombinant microorganisms, respectively, to convert substrates to targeted products [68, 105]. The application of biosynthesis in various fields such as drug production, vaccine research, food science or agriculture has drawn increasing attention from scientists in many fields [105, 106]. For mass production, microorganism-based biosynthesis may achieve low costs and high efficiency, which is referred to as fermentation- or microorganism-engineering.

In industrial production and laboratory-scale experiments, bioreactors are typically applied for biosynthesis. Bioreactors provide an isolated and sterilized environment, allowing for precise monitoring of multiple fermentation parameters such as pH, oxygen, and temperature for biosynthesis. Whole-cell biotransformation is the general approach for production using bioreactors [105]. The successful synthesis of long-term metabolites of metandienone and oral-Turinabol in a bioreactor using whole-cell biotransformation has been reported [107, 108]. In addition to whole-cell biotransformation, organ S9 fraction [31, 109] and isolated enzyme [110] assays are commonly employed in the biosynthesis of sulfo-conjugates, although scaled-up production has never been reported. This thesis presents a novel approach for the biosynthesis of sulfo-conjugates using enzyme bags with *in situ* production of PAPS (Manuscript III). This developed approach holds promise for scaled-up biosynthesis of sulfate metabolites.

3   Manuscripts

3.1   Manuscript I: "Relevance of Sulfotransferase Metabolism for Doping Analysis"

Yanan Sun, Maria Kristina Parr & Matthias Bureik

State: In preparation

Abstract: The misuse of doping compounds in human and animal sports events has become a significant threat to fair competitions as well as the well-being of athletes and animals involved. In the fight against doping, phase I or phase II metabolites are often used as markers to trace back the administration of small molecule drugs that are prohibited as doping in sports. Confronted with an increasing number of prohibited substances and biomarkers to screen on, new high-throughput, cost-effective, and fast methods must be implemented by anti-doping laboratories. The latest generation of analytical techniques addresses the limitations of instrumental detection limits, enhancing the efficiency of metabolite identification. Furthermore, novel approaches for analytical sample preparation and reference materials synthesis are constantly being developed. The importance of sulfotransferase (SULT) metabolism in doping control analysis has recently garnered increasing attention. This review provides an overview of the relevance of SULT metabolism in anti-doping research, while also presenting both conventional and cutting-edge methods for sample preparation and analytical detection. Additionally, research on methods for the production of sulfated metabolites via chemical synthesis and both *in vivo*- and *in vitro*-techniques are discussed with an emphasis on recent publications.

Relevance of Sulfotransferase Metabolism for Doping Analysis

Yanan Sun[1,2], Maria Kristina Parr[2,*] & Matthias Bureik[1,*]

[1] School of Pharmaceutical Science and Technology, Health Sciences Platform, Tianjin University, Tianjin 30072, China, matthias@tju.edu.cn (M.B.)

[2] Pharmaceutical and Medicinal Chemistry (Pharmaceutical Analyses), Institute of Pharmacy, Freie Universität Berlin, Germany, suny72@zedat.fu-berlin.de (Y.S.), maria.parr@fu-berlin.de (M.K.P.)

* Correspondence: maria.parr@fu-berlin.de, +49 30 838 57686 (M.K.P.) and matthias@tju.edu.cn, +86 155 2268 6706 (M.B.).

Abstract

The misuse of doping compounds in human and animal sports events has become a significant threat to fair competitions as well as the well-being of athletes and animals involved. In the fight against doping, phase I or phase II metabolites are often used as markers to trace back the administration of small molecule drugs that are prohibited as doping in sports. Confronted with an increasing number of prohibited substances and biomarkers to screen on, new high-throughput, cost-effective, and fast methods must be implemented by anti-doping laboratories. The latest generation of analytical techniques addresses the limitations of instrumental detection limits, enhancing the efficiency of metabolite identification. Furthermore, novel approaches for analytical sample preparation and reference materials synthesis are constantly being developed. The importance of sulfotransferase (SULT) metabolism in doping control analysis has recently garnered increasing attention. This review provides an overview of the relevance of SULT metabolism in anti-doping research, while also presenting both conventional and cutting-edge methods for sample preparation and analytical detection. Additionally, research on methods for the production of sulfated metabolites via chemical synthesis and both *in vivo*- and *in vitro*-techniques are discussed with an emphasis on recent publications.

1. Introduction

The fight against doping in sports originated in the 1960s. During the 1960 Roma Summer Olympic Games, a Danish cyclist collapsed and died after taking a stimulating "cocktail" containing Ronicol (nicotinyl alcohol) and an amphetamine-like substance [2]. This incident marked a turning point, leading to a gradual recognition of the numerous hazards associated with doping. Since the early 1970s, the anti-doping fight was coordinated under the leadership of the International Olympic Committee (IOC). In 1999, the world anti-doping agency (WADA) was established. Since then, WADA has become the most important organization in coordinating and regulating anti-doping activities internationally.

The misuse of doping substances and methods is not only unethical and against fair competition in sports but also poses health risks to both elite and recreational athletes. A vast variety of doping agents have been identified, including anabolic androgenic steroids (AAS), peptide hormones, growth factors, stimulants, and beta-2 agonists. Achieving accurate and efficient doping control in sports faces a considerable challenge, primarily due to the multitude of compounds that need to be screened. Hence, comprehensive analytical methods allowing for short reporting times, affordable costs, and high-throughput screening for different classes of prohibited substances are desirable.

Most doping compounds undergo extensive metabolism following administration, rendering them nearly undetectable as parent compounds. Consequently, metabolites serve as the primary target analytes in sports drug tests. Metabolic reactions can be subdivided into phase I and II metabolism. Phase I (functionalization) reactions involve the transformation of parent compounds to more polar metabolites by unmasking or by introducing new functional groups. Whereas, phase II (conjugation) reactions consist of the attachment of hydrophilic moieties (often with a negative charge) to target compounds, thus facilitating the prompt and efficient excretion of resulting metabolites from the body via urine and bile. Glucuronidation and sulfonation are the two main metabolic pathways of phase II metabolism and are catalyzed by uridine diphosphate (UDP) glucuronosyltransferases (UGTs) and sulfotransferases (SULTs), respectively. Phase II metabolism is the main metabolic pathway for steroids, as only a small number of steroids excreted in urine are in their original form. For instance, at least 97% of androgens are present as phase II conjugates [3]. Certain substances may undergo phase II metabolism directly, but in many cases, compounds go through phase I metabolism prior to phase II conjugation. For example, in the case of testosterone, phase I metabolism involves A-ring reduction and oxidation at the C17 hydroxy group, followed by sulfate or glucuronide conjugation [4] (Error! Reference source not found.). Similarly, synthetic AAS are typically metabolized through glucuronidation or sulfonation [5]. It is generally assumed that sulfonation serves as the primary phase II route for 3β-hydroxy steroids, while 3α-hydroxy groups in steroids mainly undergo

glucuronidation [6, 7]. Among these two groups of metabolites, most studies in humans were so far dedicated to investigations of glucuronidated steroids. The steroidal module of the Athletes' Biological passport (ABP) also relies on urinary steroids excreted as glucuronides [8, 9]

In humans, 14 SULTs are belonging to the families SULT1, SULT2, SULT4, and SULT6, respectively, whereas SULT3 and SULT5 family members are not present [1]. Substrates for all twelve human SULT1 and SULT2 family members have been previously described. Recent findings from our group have also identified substrates for SULT4A1 and SULT6B1 [10], confirming that all human SULTs are enzymatically active. The activity of SULTs is dependent on the presence of the cofactor 3'-phosphoadenosine-5'-phosphosulfate (PAPS), which provides the sulfo-moiety that is being transferred onto the substrate. Among the SULT families, the members of the SULT2 family exhibit a higher affinity for steroidal compounds, while the SULT1 family demonstrates a stronger affinity for phenolic compounds [1]. Consequently, the SULT2 family is deemed to play a more significant role in the metabolism of steroidal doping compounds.
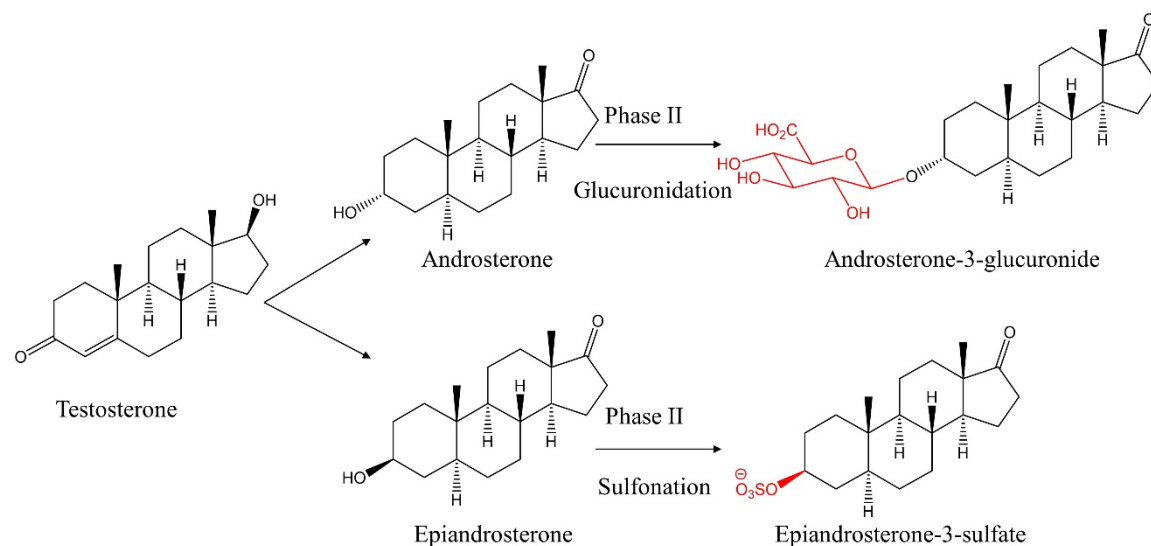

Figure 8. Metabolism of testosterone with phase I and phase II reactions (sulfate and glucuronide conjugation).

While SULTs play a vital role in drug metabolism, their significance in anti-doping research has long been overlooked. Most known SULT metabolites of prohibited drugs are monoconjugates, although the occurrence of bis-sulfate has been recognized since the 1960s [11, 12]. Recent studies have focused on the sulfation pathways of various doping substances [13, 14], leading to the discovery of several endogenous and exogenous steroid sulfates. These findings have contributed to the detection of the misuse of endogenous androgenic anabolic steroids (EAAS) [15] and AAS including boldenone [16, 17], clostebol [18, 19], stanozolol, and danazol [20, 21]. In this review, we summarize the methodologies of anti-doping research relevant to SULT metabolism, involving the developments and challenges in sample preparation, reference synthesis and analytical techniques.

2. Sample preparation

The original samples that are analyzed for the possible presence of sulfo-conjugates (such as biological fluids) sometimes cannot be directly injected into analytical instruments. Instead, pretreatment is often required for getting detectable analytes, increasing sensitivity, or preventing the instruments from damage. Generally, three approaches are used for this purpose: Hydrolysis, derivatization, and extraction. In the case of conjugated steroids, hydrolysis or deconjugation is commonly performed due to their degradation under high temperatures required for gas chromatography (GC) analysis [3]. Hydrolysis or deconjugation of phase II sulfo-conjugates generally leads to corresponding phase I metabolites. For some doping substances, the absence of reference compounds of SULT metabolites makes it easier to detect phase I metabolites instead of sulfo-conjugates in both identification and quantitation analysis. Hydrolysis can be carried out using enzymatic or chemical methods. Enzymatic hydrolysis typically involves the use of catalysts derived from mammalian (e.g., beef liver extracts), microbial (e.g., *Escherichia coli*), or mollusk origin (e.g., *Helix pomatia*, *Paanalolgate*, *Haliotis* or *Ampullaria*) [3]. Among these, the digestive fluid of *Helix pomatia* (*H. pomatia*) is commonly employed. However, the sulfatases presented in it do not hydrolyze all steroid sulfates, as 3α,5α-bis-sulfates, and C19 steroids sulfated at

C17 were reported to be resistant to hydrolysis [22-24]. Additionally, there are concerns regarding the conversion and degradation of steroid sulfates due to the presence of additional enzymatic activities in *H. pomatia* preparations. [3, 25, 26]. To address these challenges, an expressed and purified arylsulfatase derived from *Pseudomonas aeruginosa* was utilized [27]. This purified arylsulfatase specifically exhibits sulfatase activity, enabling the selective hydrolysis of sulfo-conjugates. However, it is not universally effective, as it was only successful in hydrolyzing six out of the nine tested steroid sulfates (in the study cited above). In addition to enzymatic approaches, chemical hydrolysis has been widely employed as well. Hot acid, such as hydrochloric or sulfuric acid, was initially used for chemical hydrolysis of sulfo-conjugates [28]. More recently, solvolysis in an organic environment has emerged as an alternative method, offering superior steroid recovery compared to hot acid hydrolysis [3, 29, 30]. Solvolysis generally utilizes ethyl acetate under acidic condition with heating below 55 °C. Study has reported solvolysis efficiencies exceeding 60% for most steroid sulfates [31]. However, the strongly acidic conditions may result in the degradation of certain analytes, additionally raising the problem of matrix-derived interference in the subsequent analytical detection [3, 24].

Liquid-liquid extraction (LLE) is commonly performed to remove such interferences [18, 31, 32], while solid-phase extraction (SPE) is typically carried out to purify the biological fluid or chemically synthesized samples prior to injection into analytical instruments [33-35]. Following hydrolysis, derivatization is often employed to enhance the sensitivity, thermostability, volatility, and standardization of analytes. Based on the individual properties of the compound and the detection system, the derivatization of steroids can be accomplished using silylation or acylation reactions. Silylation, employed various trimethylsilyating (TMS) reagents, including *N,O*-bis(trimethylsilyl)-trifluoroacetamide (BSTFA) [3], *N*-methyl-*N*-trifluoroacetamide (MSTFA) [36, 37], and methyloxime-trimethylsilyl (MO-TMS) [38], dominates the steroid derivatization approach in GC/MS analysis. Recently, deconjugation followed by derivatization, or direct derivatization using TMS, MO-TMS, trifluoroacetyl, with solvolysis as deconjugation methods has been investigated [38]. A novel approach

involving simultaneous deconjugation/derivatization with MO-TMS followed by TMS derivatization was established to overcome the additional enol TMS ether formation of keto sterols in direct TMS derivatization. Although silylation is widely applied for sample preparation of gas chromatography-(tandem) mass spectrometry (GC-MS(/MS)), the reagents are considered incompatible with gas chromatography/combustion/isotopic ratio mass spectrometry (GC/C/IRMS) due to the incomplete combustion caused by the deposition of silicon on the copper wire [3]. As an alternative, acetylation generates the derivates with good stability and chromatographic properties. Compared to silylation, only two carbon atoms are introduced in acetylation instead of three, resulting in a lesser impact on the overall carbon isotope ratio [39].

3. Generation of reference materials

The detection of sulfate metabolites in doping control analysis is generally performed with GC-MS(/MS) after the pretreatment processes. However, the low efficiency of hydrolysis and the instability of certain analytes can lead to very low or undetectable levels in GC-MS(/MS) analysis. Directly analysis using liquid chromatography coupled with (tandem) mass spectrometry (LC-MS(/MS)) holds promise as an alternative approach. Nevertheless, the lack of available reference materials poses a challenge for the direct analysis of sulfate metabolites, especially in terms of quantitating analytes in biological fluids. Many of the references are either not commercially available, or costly, such as 4-hydroxy propranolol sulfate (around 250 $/mg). Therefore, the synthesis of reference materials of sulfate metabolites is desired.

3.1 Chemical synthesis

Chemical synthesis of sulfated doping metabolites has been widely applied due to its cost-effectiveness and high yield. Numerous methods have been developed for the production of sulfate metabolites, including reactions involving chlorosulfonic acid [40], amine or pyridine complex of sulfur trioxide [41-44] sulfuric acid and carbodiimides [45], sulfamic acid [46], or more recently, sulfurylimidazolium salts [47, 48]. Although these reactions effectively yield the desired sulfate compounds, significant chemical expertise, specialized reagents [47, 48], or complicated

purification methods are often required. Additionally, exposure to harsh or hazardous conditions can occur sporadically [40, 44, 45]. Not long ago, a simple and adequate method for small-scale synthesis and purification of steroid sulfate compounds was reported [35]. In this study, synthesis was performed with a solution of sulfur trioxide pyridine complex (SO3•py) in dimethylformamide (DMF), to which the parental steroid and 1,4-dioxane were added. After 4 hours of stirring at room temperature, the reaction products were purified by SPE, and eluted as corresponding ammonia salts (Figure 2). Through this method, sixteen steroid sulfates were synthesized with high efficiency, including the sulfo-conjugates of the designer steroids furazadrol (17β-hydroxyandrostan-[2,3-d]isoxazole), isofurazadrol (17β-hydroxyandrostan[3,2-c])isoxazole) and trenazone (17β-hydroxyestra-4,9-dien-3-one). This method was also employed in another study aimed at analyzing sulfate metabolites of oxandrolone and danazol [20]. The same approach with slight modifications was utilized for the synthesis of sulfated tetrahydro methyl testosterone with the sulfation at position 3,
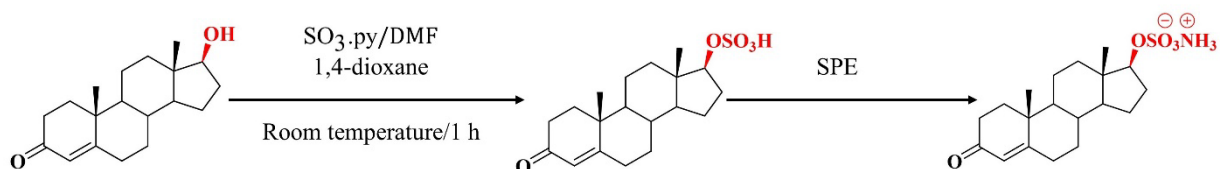
Figure 9. Graphical abstract of sulfate metabolites synthesized with SO3•py and purified by SPE.

resulting in the synthesis of six isomers [4]. Additionally, the method demonstrated efficacy in the synthesis of steroid bis-sulfates [14], although the sulfation at the 17-hydroxy group is considered slower than that at the 3-hydroxy group [4]. Mixed steroid sulfate glucuronide metabolites were primarily produced through the general chemical process for small-scale synthesis, followed by treatment with *Escherichia coli* (*E. coli*) E504G glucuronyl synthase for glucuronidation [49].

In addition to human sport events, the abuse of illegal drugs is also a significant issue in animal sports. A recent study evaluated the sulfonation of the three arylpropionamide-based selective androgen receptor modulators (SARMs) in horse

urine, and the chemical synthesis of their sulfo-conjugated metabolites was also reported [50]. The targeted metabolites were synthesized through selective *O*-sulfation using SO$_3$•py (Figure 3). Subsequently, the products were purified by high-performance liquid chromatography (HPLC) and further characterized through ^{19}F nuclear magnetic resonance (NMR) [51].
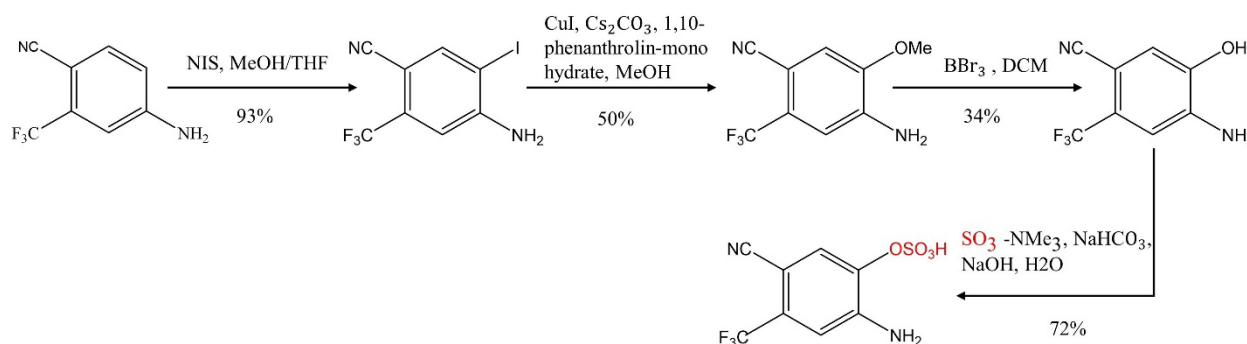

Figure 10. The scheme of chemical synthesis of sulfated metabolites and yield ratio in each step.

A complete set of eighteen 3- and 21-monosulfates, including their double-conjugated form of tetrahydrocortisol, tetrahydro-11-deoxycortisol, and tetrahydrocortisone in the 5α- and 5β-series was synthesized chemically [52]. Two years later, synthesis of 3- and 21-monosulfates of allo-tetrahydrocorticosteroids labeled with four or five deuterium atoms was accomplished as well [53]. The sulfation reactions were carried out by reacting sulfur trioxide–trimethylamine with dry pyridine. Whereas deuterium-labeled products were achieved by hydrogen-deuterium exchange reaction of active methylene groups with NaOD in CH$_3$OD, followed by reduction with NaBD$_4$. These isotope-labeled analogs have the potential to serve as internal standards in LC-MS analysis for clinical and biochemical studies.

Non-steroidal sulfo-conjugates, like phenethylamine sulfates [51] and terbutaline sulfates [54], have been chemically synthesized and monitored in doping controls. Phenethylamine represents the basic structure of various drugs with stimulant-like properties. The sulfonation of 2-amino-1-(4-hydroxyphenyl) ethan-1-one, 2-(4-hydroxyphenyl) acetamide, 2-(3-hydroxyphenyl) acetamide, and d$_6$-hordenine was conducted using SO3•py in DMF for 1 h [51]. As a reference for detection of SULT

metabolites in urine sample, all possible terbutaline sulfates including mono-, dis- and tri-sulfates were synthesized through the reaction of terbutaline and sulfur trioxide [54]. Pure fractions of phenolic sulfo-conjugated terbutaline and benzylic esterified sulfo-conjugated terbutaline were obtained using a gravity column.

The study of analytical methods using chemically synthesized metabolites can contribute to the precise and effective analysis of *in vivo* samples. In one study, sulfate steroids with a wide range of different substitution patterns and stereo-chemistries were synthesized and characterized by GC-MS through a non-hydrolyzing method [55]. However, steroids with a 17α-hydroxy function in combination with a 17β methyl group (e.g., 17β-methyltestosterone, 17β-oxandrolone, and epimetendiol) were not synthesized successfully. The research of Hongguang Bi suggested that sulfate esters capable of undergoing elimination to form stable cation intermediates (such as tertiary alcohols) are considered unstable and challenging to synthesize [56].

3.2 *In vivo* synthesis

The chemical synthesis of sulfate metabolites offers the benefits of cost-effectiveness and rapid outcomes. However, this strategy is generally efficient for doping compounds with a single conjugation site. Conversely, compounds with multiple conjugation sites are not effectively synthesized through chemical processes due to the production of side products and need for complex purification processes [54] (Figure 4). Nevertheless, owing the advantage of enzymatic regio-selectivity, biosynthesis holds promise for resolving this issue [57].

Direct detection of drug metabolites from urine, blood, or plasma after administration and metabolization by human volunteers (or test animals) is the most common way to obtain standards for anti-doping analysis. Among these bodily fluids, urine offers the advantage of accessibility and painless sample collection, making it the preferred choice for doping control detection. In the context of sporting events, the detection of long-term metabolites is crucial to prevent the unnoticed misuse of drugs. SULTs metabolism involves binding to plasma proteins, thus, it is supposed to prolong the presence of metabolites in the body and extending the detection window of specific

doping compounds [31, 58]. For instance, epiandrosterone sulfate was indicated as a long-term metabolite, prolonging the detectability of testosterone, 4-androstenedione, and dihydrotestosterone misuse [59]. Epiandrosterone was depleted for a significantly longer timespan in carbon isotope ratio mass spectrometry (CIR-MS), compared to current routine protocols in sports drug testing.

SARMs were also investigated *in vivo* through the urinary approach. The steroidal compound YK11 was reported to possess SARM and myostatin inhibitor-like characteristics, and fourteen deuterated urinary metabolites (including five sulfate metabolites) were detected in humans [36].
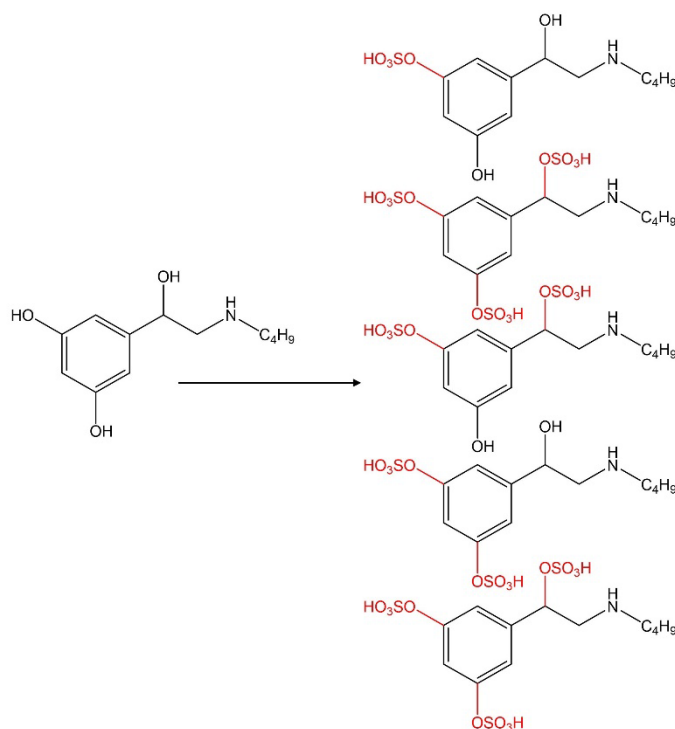
Figure 11. Potential sulfated products of terbutaline in chemical synthesis.

In the urinary steroid metabolome, steroid bis-sulfates are significant but are relatively minor constituents and have received limited research attention. Nevertheless, evaluation of urinary steroidal metabolites (especially bis-sulfates) presents the potential for application in the diagnosis of pathologies related to their biosynthesis [13]. Endogenous bis-sulfate metabolites of select steroids were analyzed in human urine using constant ion loss (CIL) monitoring from the molecular dianion and used as

markers for the prenatal diagnosis of disorders leading to reduced estriol production [13].

As a β_2-agonist, Tretoquinol has been extensively studied for its metabolism in various animal species, including rats [60, 61], guinea pigs [60], rabbits [61], and horses [62]. Recently, tretoquinol and its metabolites in human urine were investigated using LC-MS [63]. The study identified both the sulfo-conjugates of the parent compound and the sulfated phase I metabolite (O-methylated tretoquinol sulfate).

In vivo studies have investigated the differences in SULT metabolism of testosterone between Caucasian and Asian populations, highlighting potential variations based on race. Notably, a longer detection time of the ratio of androsterone sulfate/testosterone sulfate in the Caucasian population was observed, whereas Asian volunteers showed much shorter detection times (or sulfates concentrations below the quantitation limit). Only two Asian test subjects exhibited similar or longer detection times compared to their Caucasian counterparts [64]. Hence, the potential of sulfate metabolites and the selection of the best marker of testosterone significantly depend on the ethnicity and the individual. Different administration routes of prohibited drugs, such as oral [36, 59], transdermal [59], or intramuscular application [64], have been investigated. Animal studies involving cows [65] and horses [66] have also been conducted. Identifying multiple metabolites from matrices can be demanding, thus, chemically synthesized metabolites are served as standard references to aid in the final identification of metabolites detected in *in vivo* studies. For example, in the sulfonation of the arylpropionamide-based SARM compounds mentioned before, urinary sulfated metabolites were identified using ultra high-performance liquid chromatography hyphenated by quadrupole time-flight-mass spectrometer (UHPLC/QTOF). Those metabolites were further matched with authentic standards specifically synthesized for this purpose [50]. In another report, three sulfate metabolites of methylnortestosterone were identified in human urine, and one long-term metabolite (17α-methyl-5β-estrane-3α,17β-diol-3α sulfate) was produced chemically [29].

Even though *in vivo* generation is widely applied to anti-doping studies owing to its precise target directness and regioselectivity, the disadvantages are apparent as well.

The metabolism of doping compounds typically takes days, resulting in a slow response time. Additionally, the associated costs are relatively high, and the identification of various metabolites from complex matrices such as blood or urine can be inconvenient. Furthermore, the toxicological effects of most prohibited drugs are still unclear. Rashly using them on human volunteers or experimental animals may cause unpredicted adverse effects. For analysis, the low amounts of metabolites obtained from administration trials and the arduous process of purification procedures add further complexity to such *in vivo* studies.

3.3 Biological synthesis *in vitro*

The utilization of in vitro biological synthesis techniques offers a cost-effective, efficient, and safer approach for generating sulfated metabolites as reference materials. Additionally, *in vitro* generation occurs in a cleaner matrix compared to the *in vivo* environment, thereby requiring simpler pretreatment processes prior to instrumental analysis. *In vitro* synthesis has been used since 1940s [67]. In the last two decades, it has become a viable alternative to *in vivo* studies. Organ preparation, isolated enzyme and genetically unmodified microorganism are generally employed in *in vitro* studies.

In vitro assays employing liver preparations such as hepatocytes, liver microsomes, or homogenized liver fractions are used to develop analytical methods for drug screening in biological fluids, early clinical development and anti-doping screening [4]. Additionally, preparations from lung, kidney or small intestine are frequently utilized as well [68]. In one study, human liver microsomes (HLMs) and S9 fractions were utilized to establish a screening method for the detection of the designer drug 3,4-methylenedioxypyrovalerone (MPDV) in urinary samples [69]. MPDV is a stimulant belonging to the cathinone class and has similar pharmacological characteristics as methylphenidate and methylenedioxymethamphetamine, which are prohibited by WADA [70].

The generation of phase II metabolites with horse liver homogenates was first reported in 2016, using morphine as one of the model substrates [71]. In this study, morphine glucuronides were detected rather than morphine sulfates. In contrast, human liver S9

fractions readily produce the corresponding morphine sulfates [68]. In the subsequent study, sulfonation of eight opioid drugs, including morphine, was evaluated using HepG2 human hepatoma cells and human liver samples. Five of these compounds (hydromorphone, oxymorphone, butorphanol, nalorphine, and naltrexone) presented more abundant sulfation in HepG2 compared to the other three drugs. Furthermore, the enzymatic assays demonstrated that SULT1A1 is the main isoform responsible for sulfonation of oxymorphone, nalbuphine, nalorphine, and naltrexone. SULT1A3 was found to calalyze the sulfonation of morphine, while hydromorphone was sulfated by SULT2A1, along with butorphanol and levorphanol. Therefore, this study, corroborates the notion that sulfation indeed plays an essential role in the metabolism of morphine and other opioid drugs.

In addition to using preparations from human or animal tissues, the synthesis of metabolites using genetically modified microorganisms has been occasionally employed in anti-doping studies. One example is the production of SARM S1 glucuronides through biotransformation with the fungus *Caenorhabditis elegans (C. elegans)* [72]. However, there are more examples where isolated SULT isoforms were obtained through molecular cloning, recombinant expression in a microbial host, and subsequent enzyme purification [73, 74]. Common microbial hosts for recombinant protein production, such as the bacterium *E. coli* [75] and the two yeast species *Saccharomyces cerevisiae* (*S. cerevisiae*) [57] and *Schizosaccharomyces pombe* (*S. Pombe*) [10, 76], have also been used for the recombinant expression of human SULTs and the production of sulfo-conjugates. Interestingly, in both yeasts, the intracellular level of the (expensive) cofactor PAPS was found to be sufficiently high to allow for sulfate metabolite production by whole-cell biotransformation [10, 57]. These findings are of importance as whole-cell biotransformation has the potential for scale-up production through fermentation.

As an example of the sulfation of a doping compound, the biotransformation of fenoterol with recombinant SULT1A1 and SULT1A3 led to the generation of two mono-sulfates and one bis-sulfate by each enzyme [77]. A more systematic analysis of the sulfation of ractopamine and salbutamol with eleven purified human SULTs was

also reported [78]. It was found that four isoforms could metabolize ractopamine, while only SULT1A3 showed sulfation activity towards salbutamol. Although purified enzymes provide clear insights into the specific activities of certain isoforms towards substrates, the processes of cloning, expression, and purification can be complicated and time-consuming, especially for laboratories not specialized in molecular biology. Therefore, *in vitro* preparations from tissues are often employed for initial quick tests on targeted substrates as they are readily commercially available.

As mentioned above, there is a significant disparity in the number of publications focusing on in vitro sulfation and sulfate metabolites of doping compounds compared to those on doping compound glucuronidation and the corresponding glucuronides. One obvious reason for this discrepancy is likely the high cost of the cofactor PAPS as compared to UDP glucuronic acid. Hence, a low-cost sulfate metabolite generation system is undoubtedly desirable. Two recently described PAPS generation systems may provide a suitable solution [76, 79]. In an elegant study published in 2018, *in vitro* sulfonation reactions with human, equine, or canine liver S9 fractions were performed
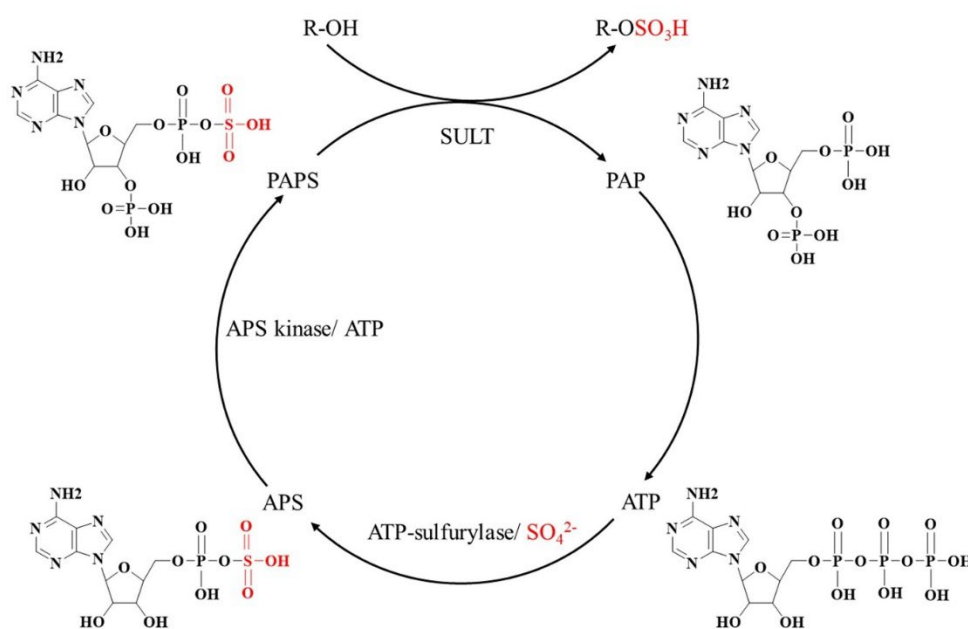

Figure 12. Two biosynthesis of PAPS from ATP and sulfate by ATP-sulfurylase and APS kinase, followed by SULT-dependent sulfonation [1].

using ATP and Na_2SO_4 instead of PAPS (Figure 5). As a result, six steroidal sulfates including androsterone 3-sulfate and etiocholanolone 3-sulfate were produced. The generation of PAPS can be divided in two steps: adenosine-5′-phosphosulfate (APS) generated from ATP and sulfate under the catalyzation of ATP-sulfurylase, followed by APS kinese catalyzed PAPS production from APS and ATP. A recent report from our group illustrates an *in vitro* biosynthesis approach that combines SULT-dependent biotransformation using recombinant and permeabilized fission yeast cells with PAPS production *in situ* [76]. An optimal approach was developed with a higher space-time yield and lower experimental cost compared to the original biotransformation where PAPS had to be supplied. Furthermore, certain SULTs were utilized to demonstrate the sulfonation of various test compounds, such as 4-hydroxypropranolol, salbutamol, and dehydroepiandrosterone. This productive and low-cost *in vitro* sulfo-conjugation system is expected to contribute to the up-scaling of sulfate metabolite production and possibly also to the prediction of novel metabolites.

4. Analytical techniques

The metabolites obtained from biosynthesis or chemical synthesis, or *in vivo* samples are generally evaluated using a variety of analytical instruments. Less than three decades ago, anti-doping analysis mainly relied on GC-MS. While different analytical techniques are now employed for the growing number of prohibited drugs, GC-MS remains the fundamental method for detecting steroid sulfo-conjugates. Pretreatment of sulfo-conjugates including hydrolysis or derivatization is generally required prior to GC-MS analysis, due to their minimal volatility (see chapter 2 above). In anti-doping analysis, various approaches using GC combined with different ionization sources, involving atmospheric-pressure chemical ionization (APCI) source [80], atmospheric-pressure photoionization (APPI) source [81, 82], ESI source [83], and electron ionization (EI) source [55, 84]. Recently, the limits of detection of GC-EI-MS/(MS) are considered sufficiently lower than the minimum required performance levels. Compared to LC-ESI-MS(/MS), GC-EI-MS(/MS) showed greater sensitivity for the majority of tested steroids [83]. Analysis of non-hydrolyzed sulfated steroids has been

reported to use either GC coupled by chemical ionization to a triple quadrupole mass spectrometer (GC-CI-QQQ) or low energy−EI−GC−QTOF (LE−EI−GC−QTOF) [55]. Based on the common GC-MS behavior of non-hydrolyzed sulfated steroids, two applications were evaluated: the discovery of (new) sulfated metabolites of mesterolone and expanding AAS abuse detection windows. GC-MS was found to possess higher structural elucidating power and more inclusion in screening methods compared to LC-MS. Multidimensional GC has been employed for achieving high peak purity [59]. In this approach, several capillary columns (usually two) are utilized instead of one. CIR-MS was combined with GC to analyze the labeled epiandrosterone sulfate in testosterone misuse detection. This study contributed to extending the detection window of testosterone misuse to up to 8 days.

Advanced LC-MS techniques in anti-doping research were developed during the 1990s [85, 86]. Numerous new applications and strategies in doping control analysis have been developed based on LC-MS (/MS), especially for determining doping metabolites that are barely detectable or undetectable by GC-MS. In contrast to GC-MS, LC-MS allows the direct detection of conjugates without hydrolysis or derivatization. UHPLC hyphenated with high sensitive MS such as QQQ, TOF or ion trap mass analyzers (Orbitrap) is frequently applied in LC-MS (/MS) strategies. Nowadays, a simple high-throughput and low-cost method called "dilute-and-inject" (or "dilute-and-shoot") was investigated, which requires no sample pretreatment and is increasingly applied in anti-doping screening [87, 88]. The detection of steroid sulfate metabolites in urine samples has always been a challenge, not just for their chemical and isomeric diversity but also for the existing degradation artifacts and endogenous interferences resulting in ambiguous peaks in MS/MS analysis [14, 15, 16]. A latest study combined LC-HRMS with ion mobility (LC-IM-HRMS) to increase the peak capacity and selectivity, thus, improving identifications of intact sulfate metabolites, especially in the case of low concentration and differentiating isomers [89]. In 2017, the UHPLC-MS/MS CIL method for direct and untargeted detection of steroid bis(sulfate) metabolites was introduced [14]. Compared to the precursor ion scan method that used precursors of m/z 97, the CIL method is based on the constant loss of HSO_4^- and was found to be

more sensitive. Besides bis-sulfates, further phase II metabolites comprising steroid bis-glucuronides or mixed conjugates such as sulfate glucuronides were detected as endogenous human urinary metabolites [49].

Although HPLC/UHPLC is widely applied in doping control analysis, it shows limited resolution capabilities for some high polar metabolites due to the insufficient interaction in conventional reversed-phase (RP) columns [90]. As an orthogonal separation technique, supercritical fluid chromatography (SFC) may overcome this issue. SFC utilizes a mobile phase consisting of a supercritical fluid (such as CO_2) and an organic modifier. The physical characteristics of supercritical fluid, such as low viscosity and high diffusivity, and high solvating power, lead to a faster running time and higher resolution compared to HPLC [91]. SFC hyphenated (tandem) mass spectrometer (SFC-MS/(MS)) has been introduced into the field of anti-doping research in the last decade. With high separation power, it plays an increasingly important role in the analysis of doping metabolite, including sulfo-conjugates [65, 90, 92-94] and their enantiomers analysis [94, 95]. Parr and her team analyzed numerous analytes, including doping sulfo-conjugates like fenoterol sulfate, octopamine sulfate, phenylephrine sulfate, propranolol-4 hydroxy sulfate, and tyramine sulfate, using both SFC-MS/MS and LC-MS/MS. The results indicated that SFC-MS/MS exhibited better retention compared to LC-MS/MS for highly polar compounds like octopamine sulfate [90]. In the analysis of endogenous steroids and steroid sulfates, SFC demonstrated superior selectivity compared to GC or LC [94]. In total, 51 steroids and steroid sulfates were distinguished, including enantiomers in biological fluids.

5. **Summary**

The investigation of SULT metabolism of doping compounds is a relatively new and promising research field that is likely to increasingly contribute to anti-doping research. In recent years, new metabolites have been discovered, and efficient and accurate analytical methods have been established and refined for anti-doping analysis. Studies focused on SULTs metabolism of doping compounds, employing chemical, *in vivo*, and *in vitro* approaches (or a combination thereof) are being reported with greater frequency

(Table 1). Currently, there are two compelling possibilities to address the issue of the costly cofactor PAPS: *In vitro* synthesis using more affordable substrates or *in vitro* synthesis through whole-cell biotransformation using recombinant yeasts. Thus, we expect SULT metabolism of doping compounds to significantly increase in importance for anti-doping analysis in the future.

Table 2. Summary of SULTs metabolism in doping analysis and analytical technic.

Classification	Doping compounds	Sulfate metabolites	Methods	Reference
Anabolic agents	4-chlorometandienone (4Cl-MTD)	Six sulfate metabolites were identified. Five of them were detected in urine.	Human urine, LC-MS/MS, GC-MS/MS	[96]
	Testosterone	14 endogenous steroid sulfates were identified.	Human urine, LC-MS, SPE	[64]
	Clostebol	Eight sulfate conjugates were identified, seven of them were unreported, one conjugate was considered as long-term metabolite.	Human urine, LC-QTOF MS/MS	[19]
	Methylnortestosterone	Three new sulfate metabolites were detected, one of them were synthesized in chemical way.	Human urine, chemical synthesis, GC-MS and LC-QTOF-MS	[29]
	Superdrol	Three sulfate metabolites were identified from equine liver S9 fractions.	Equine liver S9 fractions, PAPS generation system, UPLC-MS	[79]
	Furazadrol	Three sulfated metabolites of furazadrol were identified from the urine of thoroughbred racehorses.	Thoroughbred racehorses' urine, NMR, LC-MS	[66]
	Oxandrolone and danazol	New sulfate metabolite of oxandrolone was identified and danazol metabolites sulfated ethisterone and 2-hydroxymethyl	Human urine, chemical synthesis, LC-MS, GC-MS	[20]

		ethisterone were detected in urine and synthesized.		
	Trenbolone, nandrolone, boldenone, methenolone, mesterolone, and drostanolone	Nine sulfate conjugates were synthesized in chemical way.	Chemical synthesis, HPLC-MS/MS	[20]
	Tibolone	Bis-sulfates of 23 steroid metabolites were synthesized (including bisulfatedmetabolits of tibolone), urine samples were also detected	Chemical synthesis, UHPLC-QQQ	[14]
	DHEA	51 steroids and steroid sulfates (including DHEA sulfate and analog DHEA sulfate) were detected and the analytical method was optimized	Derivatization, GC-MS, SFC-MS/MS	[94]
		Seven analytes in urine in the sulphated fraction were quantified.	Solvolysis, derivatization, human urine, GC-QTOF	[31]
Selective androgen receptor modulators (SARMs)	SARM YK11	Five urinary sulfated metabolites were detected.	Human urine, GC-IRMS, GC-HRMS	[36]
	SARM S1, S4 (Andarine) and S22 (Ostarine/ Enobosarm)	Targeted metabolites were detected in urine samples and synthesized in chemical way.	Human urine, UPLC-QTOF-MS, NMR	[50]
	LGD-4033	Two tris-hydroxylated metabolites were identified in human urine; one of them was reported to be detected in horse urine and plasma.	Human urine, LC–HRMS	[97]
Stimulants	2-phenylethanamine	Two sulfate metabolites were identified in urine, 2-(3-hydroxyphenyl) acetamide sulfate was	Human urine, chemical synthesis, GC-MS and nitrogen phosphorus-specific detection (GC-	[51]

		synthesized in chemical way	MS/NPD), isotope-dilution LC-MS/MS	
	Octopamine	Mono- and disulfate of octopamine were detected in urine	Human urine, SFC-MS/MS, LC-MS/MS	[90]
Narcotics	Opioid drugs (morphine, hydromorphone, oxymorphone, butorphanol, nalbuphine, levorphanol, nalorphine, and naltrexone)	Differential sulfating activities towards the tested drugs were detected in human hepatoma cells and human organ fractions. SULT1A1 is the main SULT of sulfonation of oxymorphone, nalbuphine, nalorphine, and naltrexone, SULT1A3 for sulfonation of morphine and hydromorphone, and SULT2A1 for the sulfation of butorphanol and levorphanol	Human HepG2 hepatoma cells and organ samples, Thin-layer chromatography	[68]
Beta-2-agonists	Tretoquinol	Tretoquinol sulfate and O-methylated tretoquinol sulfate were identified	Human urine, LC-MS	[63]
	Salbutamol	Salbutamol-4-O-sulfate was synthesized	Recombinant fission yeast, LC-QQQ	[76]
	Terbutaline	Two mono-sulfoconjugates were synthesized, one of them was detected in urine sample.	Chemical synthesis, human urine, NMR, HR-LC-orbitrap-MS	[54]
		Enantioseparation of Terbutaline and its monosulfate conjugate was achieved	SFC	[95]
	Fenoterol	Two mono-sufoconjugates and one bis-sulfoconjufate were synthesised	Human S9 fractions, recombinant SULTs, LC-MS/MS	[77]
Beta blockers	Propranolol	Propranolol-4-OH sulfate was detected in urine and the reference was chemically synthesized	Human urine, chemically synthesize, SFC-	[90]

	MS/MS, LC-MS/MS

References

[1]   Tibbs ZE, Rohn-Glowacki KJ, Crittenden F, Guidry AL, Falany CN. Structural plasticity in the human cytosolic sulfotransferase dimer and its role in substrate selectivity and catalysis. *Drug metabolism and pharmacokinetics* 30 (2015) 3-20

[2]   Ljungqvist A. Brief History of Anti-Doping. *Medicine and sport science* 62 (2017) 1-10

[3]   Gomes RL, Meredith W, Snape CE, Sephton MA. Analysis of conjugated steroid androgens: deconjugation, derivatisation and associated issues. *Journal of pharmaceutical and biomedical analysis* 49 (2009) 1133-1140

[4]   Weththasinghe SA. Synthesis and in vitro metabolism studies of selected steroids for anti-doping analysis. in: *Research School of Chemistry*, Australian National University,   (2020)

[5]   Kuuranne T. Phase-II metabolism of androgens and its relevance for doping control analysis. *Handbook of experimental pharmacology* (2010) 65-75

[6]   Shackleton C, Marcos P, Gross M, Caprioli R. GC/MS steroid profiling: diagnosis of disorders affecting steroid synthesis and metabolism. *The encyclopedia of mass spectrometry* 8 (2011) 789-813

[7]   Schänzer W, Horning S, Opfermann G, Donike M. Gas chromatography/mass spectrometry identification of long-term excreted metabolites of the anabolic steroid 4-chloro-1, 2-dehydro-17α-methyltestosterone in humans. *The Journal of steroid biochemistry and molecular biology* 57 (1996) 363-376

[8]   Ponzetto F, Baume N, Schweizer C, Saugy M, Kuuranne T. Steroidal module of the athlete biological passport. *Current Opinion in Endocrine and Metabolic Research* 9 (2019) 14-21

[9]   Dvorak J, Baume N, Botré F, Broséus J, Budgett R, Frey WO, Geyer H, Harcourt PR, Ho D, Howman D. Time for change: a roadmap to guide the implementation of the World Anti-Doping Code 2015. *British Journal of Sports Medicine* 48 (2014) 801-806

[10]   Sun Y, Machalz D, Wolber G, Parr MK, Bureik M. Functional Expression of All Human Sulfotransferases in Fission Yeast, Assay Development, and Structural Models for Isoforms SULT4A1 and SULT6B1. *Biomolecules* 10 (2020) 1517

[11]   Pasqualini JR, Jayle M-F. Identification of 3β, 21-dihydroxy-5-pregnene-20-one disulfate in human urine. *The Journal of Clinical Investigation* 41 (1962) 981-987

[12]   Arcos M, Lieberman S. 5-Pregnene-3β, 20α-diol-3-sulfate-20-(2'-acetamido-2'-deoxy-α-D-glucoside) and 5-Pregnene-3β, 20α-diol-3, 20-disulfate. Two Novel Urinary Conjugates. *Biochemistry* 6 (1967) 2032-2039

[13]   Pozo OJ, Marcos J, Khymenets O, Pranata A, Fitzgerald CC, Mcleod MD, Shackleton C. SULFATION PATHWAYS: Alternate steroid sulfation pathways targeted by LC-MS/MS analysis of disulfates: application to prenatal diagnosis of steroid synthesis disorders. *Journal of molecular endocrinology* 61 (2018) M1-M12

[14]   Mcleod MD, Waller CC, Esquivel A, Balcells G, Ventura R, Segura J, Pozo OSJ. Constant ion loss method for the untargeted detection of bis-sulfate metabolites. *Analytical chemistry* 89 (2017) 1602-1609

[15]   Esquivel A, Alechaga E, Monfort N, Ventura R. Direct quantitation of endogenous steroid

sulfates in human urine by liquid chromatography-electrospray tandem mass spectrometry. *Drug testing and analysis* 10 (2018) 1734-1743

[16] Gomez C, Pozo OJ, Geyer H, Marcos J, Thevis M, Schanzer W, Segura J, Ventura R. New potential markers for the detection of boldenone misuse. *J Steroid Biochem Mol Biol* 132 (2012) 239-246

[17] Gomez C, Pozo OJ, Marcos J, Segura J, Ventura R. Alternative long-term markers for the detection of methyltestosterone misuse. *Steroids* 78 (2013) 44-52

[18] Balcells G, Pozo OJ, Garrostas L, Esquivel A, Matabosch X, Kotronoulas A, Joglar J, Ventura R. Detection and characterization of clostebol sulfate metabolites in Caucasian population. *Journal of chromatography. B, Analytical technologies in the biomedical and life sciences* 1022 (2016) 54-63

[19] Lu J, Fernandez-Alvarez M, Yang S, He G, Xu Y, Aguilera R. New clostebol metabolites in human urine by liquid chromatography time-of-flight tandem mass spectrometry and their application for doping control. *Journal of mass spectrometry : JMS* 50 (2015) 191-197

[20] Rzeppa S, Viet L. Analysis of sulfate metabolites of the doping agents oxandrolone and danazol using high performance liquid chromatography coupled to tandem mass spectrometry. *Journal of chromatography. B, Analytical technologies in the biomedical and life sciences* 1029-1030 (2016) 1-9

[21] Balcells G, Matabosch X, Ventura R. Detection of stanozolol O- and N-sulfate metabolites and their evaluation as additional markers in doping control. *Drug testing and analysis* 9 (2017) 1001-1010

[22] Shackleton C. Profiling steroid hormones and urinary steroids. *Journal of Chromatography B: Biomedical Sciences and Applications* 379 (1986) 91-156

[23] Cawley LP, Faucette W, Musser BO, Beckloff S. Steric hindrance of the sulfatase of Helix pomatia on some 17-ketosteroid sulfate conjugates. *American Journal of Clinical Pathology* 52 (1969) 652-655

[24] Cawley AT, Kazlauskas R, Trout GJ, George AV. Determination of urinary steroid sulfate metabolites using ion paired extraction. *Journal of Chromatography B* 825 (2005) 1-10

[25] Choi MH, Chung BC. Bringing GC–MS profiling of steroids into clinical applications. *Mass Spectrometry Reviews* 34 (2015) 219-236

[26] Christakoudi S, Cowan DA, Taylor NF. Sodium ascorbate improves yield of urinary steroids during hydrolysis with Helix pomatia juice. *Steroids* 73 (2008) 309-319

[27] Stevenson BJ, Waller CC, Ma P, Li K, Cawley AT, Ollis DL, Mcleod MD. Pseudomonas aeruginosa arylsulfatase: a purified enzyme for the mild hydrolysis of steroid sulfates. *Drug testing and analysis* 7 (2015) 903-911

[28] Venturelli E, Cavalleri A, Secreto G. Methods for urinary testosterone analysis. *Journal of Chromatography B: Biomedical Sciences and Applications* 671 (1995) 363-380

[29] Sakellariou P, Kiousi P, Fragkaki AG, Lyris E, Petrou M, Georgakopoulos C, Angelis YS. Alternative markers for Methylnortestosterone misuse in human urine. *Drug testing and analysis* 12 (2020) 1544-1553

[30] Hauser B, Deschner T, Boesch C. Development of a liquid chromatography–tandem mass spectrometry method for the determination of 23 endogenous steroids in small quantities of primate urine. *Journal of Chromatography B* 862 (2008) 100-112

[31] Martinez-Brito D, Notarianni ML, Iannone M, De La Torre X, Botre F. Validation of steroid

sulfates deconjugation for metabolic studies. Application to human urine samples. *Journal of pharmacological and toxicological methods* 106 (2020) 106938

[32] Fragkaki A, Angelis Y, Kiousi P, Georgakopoulos C, Lyris E. Comparison of sulfo-conjugated and gluco-conjugated urinary metabolites for detection of methenolone misuse in doping control by LC-HRMS, GC-MS and GC-HRMS. *Journal of Mass Spectrometry* 50 (2015) 740-748

[33] Pedersen M, Frandsen HL, Andersen JH. Optimised deconjugation of androgenic steroid conjugates in bovine urine. *Food additives & contaminants. Part A, Chemistry, analysis, control, exposure & risk assessment* 34 (2017) 482-488

[34] Rzeppa S, Heinrich G, Hemmersbach P. Analysis of anabolic androgenic steroids as sulfate conjugates using high performance liquid chromatography coupled to tandem mass spectrometry. *Drug testing and analysis* 7 (2015) 1030-1039

[35] Waller CC, Mcleod MD. A simple method for the small scale synthesis and solid-phase extraction purification of steroid sulfates. *Steroids* 92 (2014) 74-80

[36] Piper T, Dib J, Putz M, Fusshöller G, Pop V, Lagojda A, Kuehne D, Geyer H, Schänzer W, Thevis M. Studies on the in vivo metabolism of the SARM YK11: Identification and characterization of metabolites potentially useful for doping controls. *Drug testing and analysis* 10 (2018) 1646-1656

[37] Mussell C, Wolff Briche CS, Hopley C, O'connor G. Analysis of 19-norandrosterone in human urine by gas chromatography–isotope-dilution mass spectrometry: method adopted by LGC for participation in the Comité Consultatif pour la Quantité de Matière (CCQM) Pilot Study P68. *Accreditation and quality assurance* 12 (2007) 469-474

[38] Junker J, Chong I, Kamp F, Steiner H, Giera M, Müller C, Bracher F. Comparison of strategies for the determination of sterol sulfates via GC-MS leading to a novel deconjugation-derivatization protocol. *Molecules* 24 (2019) 2353

[39] Becchi M, Aguilera R, Farizon Y, Flament MM, Casabianca H, James P. Gas chromatography/combustion/isotope-ratio mass spectrometry analysis of urinary steroids to detect misuse of testosterone in sport. *Rapid Communications in Mass Spectrometry* 8 (1994) 304-308

[40] Fieser LF. Naphthoquinone antimalarials; water-soluble derivatives of alcoholic and unsaturated compounds. *Journal of the American Chemical Society* 70 (1948) 3232-3237

[41] Sobel AE, Spoerri PE. Steryl sulfates. I. Preparation and properties. *Journal of the American Chemical Society* 63 (1941) 1259-1261

[42] Dusza J, Joseph J, Bernstein S. Steroid conjugates IV. The preparation of steroid sulfates with triethylamine-sulfur trioxide. *Steroids* 12 (1968) 49-61

[43] Dusza JP, Joseph JP, Bernstein S. The preparation of estradiol-17β sulfates with triethylamine-sulfur trioxide. *Steroids* 45 (1985) 303-315

[44] Dusza JP, Joseph JP, Bernstein S. A fusion method for the preparation of steroid sulfates. *Steroids* 45 (1985) 317-323

[45] Mumma RO. Preparation of sulfate esters. *Lipids* 1 (1966) 221-223

[46] Joseph JP, Dusza JP, Bernstein S. Steroid conjugates I. The use of sulfamic acid for the preparation of steroid sulfates. *Steroids* 7 (1966) 577-587

[47] Desoky AY, Hendel J, Ingram L, Taylor SD. Preparation of trifluoroethyl-and phenyl-protected sulfates using sulfuryl imidazolium salts. *Tetrahedron* 67 (2011) 1281-1287

[48]   Liu Y, Lien I-FF, Ruttgaizer S, Dove P, Taylor SD. Synthesis and protection of aryl sulfates using the 2, 2, 2-trichloroethyl moiety. *Organic letters* 6 (2004) 209-212

[49]   Pranata A, Fitzgerald CC, Khymenets O, Westley E, Anderson NJ, Ma P, Pozo OJ, Mcleod MD. Synthesis of steroid bisglucuronide and sulfate glucuronide reference materials: Unearthing neglected treasures of steroid metabolism. *Steroids* 143 (2019) 25-40

[50]   Garg N, Hansson A, Knych HK, Stanley SD, Thevis M, Bondesson U, Hedeland M, Globisch D. Structural elucidation of major selective androgen receptor modulator (SARM) metabolites for doping control. *Organic & biomolecular chemistry* 16 (2018) 698-702

[51]   Sigmund G, Dib J, Tretzel L, Piper T, Bosse C, Schänzer W, Thevis M. Monitoring 2-phenylethanamine and 2-(3-hydroxyphenyl) acetamide sulfate in doping controls. *Drug testing and analysis* 7 (2015) 1057-1062

[52]   Okihara R, Mitamura K, Hasegawa M, Mori M, Muto A, Kakiyama G, Ogawa S, Iida T, Shimada M, Mano N. Potential corticoid metabolites: chemical synthesis of 3-and 21-monosulfates and their double-conjugates of tetrahydrocorticosteroids in the 5α-and 5β-series. *Chemical and Pharmaceutical Bulletin* 58 (2010) 344-353

[53]   Mitamura K, Mabuchi T, Nagae K, Nakajima M, Matsumoto R, Fujioka S, Sato K, Satoh R, Iida T, Ogawa S. Synthesis of multiply deuterated 3-and 21-monosulfates of allo-tetrahydrocorticosteroids as internal standards for mass spectrometry. *Steroids* 77 (2012) 1423-1437

[54]   Orlovius AK, Guddat S, Parr MK, Kohler M, Gütschow M, Thevis M, Schänzer W. Terbutaline sulfoconjugate: characterization and urinary excretion monitored by LC/ESI-MS/MS. *Drug testing and analysis* 1 (2009) 568-575

[55]   Polet M, Van Gansbeke W, Albertsdóttir AD, Coppieters G, Deventer K, Van Eenoo P. Gas chromatography− mass spectrometry analysis of non-hydrolyzed sulfated steroids by degradation product formation. *Drug testing and analysis* 11 (2019) 1656-1665

[56]   Bi H, Massé R. Studies on anabolic steroids—12. Epimerization and degradation of anabolic 17β-sulfate-17α-methyl steroids in human: Qualitative and quantitative GC/MS analysis. *The Journal of steroid biochemistry and molecular biology* 42 (1992) 533-546

[57]   Nishikawa M, Masuyama Y, Nunome M, Yasuda K, Sakaki T, Ikushiro S. Whole-cell-dependent biosynthesis of sulfo-conjugate using human sulfotransferase expressing budding yeast. *Applied microbiology and biotechnology* 102 (2018) 723-732

[58]   Gomez C, Pozo O, Garrostas L, Segura J, Ventura R. A new sulphate metabolite as a long-term marker of metandienone misuse. *Steroids* 78 (2013) 1245-1253

[59]   Piper T, Putz M, Schänzer W, Pop V, Mcleod MD, Uduwela DR, Stevenson BJ, Thevis M. Epiandrosterone sulfate prolongs the detectability of testosterone, 4-androstenedione, and dihydrotestosterone misuse by means of carbon isotope ratio mass spectrometry. *Drug testing and analysis* 9 (2017) 1695-1703

[60]   Meshi T, Otsuka M, Sato Y. Studies on trimetoquinol. I. Distribution, excretion and metabolism of trimetoquinol. *Biochemical pharmacology* 19 12 (1970) 2937-2948

[61]   Satoh C, Nagao T, Kono T, Kiyomoto A. Studies on trimetoquinol. II. The metabolic fate of trimetoquinol. *Chemical and Pharmaceutical Bulletin* 19 (1971) 667-675

[62]   Camargo F, Lehner A, Harkins J, Hughes C, Karpiesiuk W, Boyles J, Woods W, Tobin T. Chromatographic detection of Trimetoquinol (Inolin®) and its major urinary metabolites in the horse: a preliminary report. *Chromatographia* 60 (2004) 371-378

[63]   Okano M, Miyamoto A, Sato M, Kageyama S. Analysis of tretoquinol and its metabolites in human urine by liquid chromatography–tandem mass spectrometry. *Drug testing and analysis* 11 (2019) 1724-1730

[64]   Esquivel A, Alechaga É, Monfort N, Yang S, Xing Y, Moutian W, Ventura R. Evaluation of sulfate metabolites as markers of intramuscular testosterone administration in Caucasian and Asian populations. *Drug testing and analysis* 11 (2019) 1218-1230

[65]   Doué M, Dervilly-Pinel G, Pouponneau K, Monteau F, Le Bizec B. Analysis of glucuronide and sulfate steroids in urine by ultra-high-performance supercritical-fluid chromatography hyphenated tandem mass spectrometry. *Analytical and bioanalytical chemistry* 407 (2015) 4473-4484

[66]   Waller CC, Cawley AT, Suann CJ, Ma P, Mcleod MD. In vivo and in vitro metabolism of the designer anabolic steroid furazadrol in thoroughbred racehorses. *Journal of pharmaceutical and biomedical analysis* 124 (2016) 198-206

[67]   Borsook H, Dubnoff JW. The biological synthesis of hippuric acid in vitro. *Journal of Biological Chemistry* 132 (1940) 307-324

[68]   Kurogi K, Chepak A, Hanrahan MT, Liu M-Y, Sakakibara Y, Suiko M, Liu M-C. Sulfation of opioid drugs by human cytosolic sulfotransferases: metabolic labeling study and enzymatic analysis. *European journal of pharmaceutical sciences* 62 (2014) 40-48

[69]   Strano-Rossi S, Cadwallader AB, De La Torre X, Botrè F. Toxicological determination and in vitro metabolism of the designer drug methylenedioxypyrovalerone (MPDV) by gas chromatography/mass spectrometry and liquid chromatography/quadrupole time-of-flight mass spectrometry. *Rapid Communications in Mass Spectrometry* 24 (2010) 2706-2714

[70]   Wada. International standard-the prohibited list 2019. (2019)

[71]   Wong JK, Chan GH, Leung DK, Tang FP, Wan TS. Generation of phase II in vitro metabolites using homogenized horse liver. *Drug testing and analysis* 8 (2016) 241-247

[72]   Rydevik A, Lagojda A, Thevis M, Bondesson U, Hedeland M. Isolation and characterization of a β-glucuronide of hydroxylated SARM S1 produced using a combination of biotransformation and chemical oxidation. *Journal of pharmaceutical and biomedical analysis* 98 (2014) 36-39

[73]   Pai TG, Sugahara T, Suiko M, Sakakibara Y, Xu F, Liu M-C. Differential xenoestrogen-sulfating activities of the human cytosolic sulfotransferases: molecular cloning, expression, and purification of human SULT2B1a and SULT2B1b sulfotransferases. *Biochimica et Biophysica Acta (BBA)-General Subjects* 1573 (2002) 165-170

[74]   Falany CN, Falany JL, Wang J, Hedström J, Von Euler Chelpin H, Swedmark S. Studies on sulfation of synthesized metabolites from the local anesthetics ropivacaine and lidocaine using human cloned sulfotransferases. *Drug metabolism and disposition* 27 (1999) 1057-1063

[75]   Taskinen J, Ethell BT, Pihlavisto P, Hood AM, Burchell B, Coughtrie MW. Conjugation of catechols by recombinant human sulfotransferases, UDP-glucuronosyltransferases, and soluble catechol O-methyltransferase: structure-conjugation relationships and predictive models. *Drug Metab Dispos* 31 (2003) 1187-1197

[76]   Parr M, Sun Y, Harps L, Bureik M. Human sulfotransferase assays with PAPS production in situ. *Frontiers in Molecular Biosciences* 9-2022   107

[77]   Orlovius A, Guddat S, Gütschow M, Thevis M, Schänzer W. In vitro synthesis and characterisation of three fenoterol sulfoconjugates detected in fenoterol post-administration urine samples. *Analytical and bioanalytical chemistry* 405 (2013) 9477-9487

[78]   Ko K, Kurogi K, Davidson G, Liu MY, Sakakibara Y, Suiko M, Liu MC. Sulfation of ractopamine and salbutamol by the human cytosolic sulfotransferases. *The Journal of Biochemistry* 152 (2012) 275-283

[79]   Weththasinghe SA, Waller CC, Fam HL, Stevenson BJ, Cawley AT, Mcleod MD. Replacing PAPS: In vitro phase II sulfation of steroids with the liver S9 fraction employing ATP and sodium sulfate. *Drug testing and analysis* 10 (2018) 330-339

[80]   Raro M, Portolés T, Sancho J, Pitarch E, Hernández F, Marcos J, Ventura R, Gómez C, Segura J, Pozo O. Mass spectrometric behavior of anabolic androgenic steroids using gas chromatography coupled to atmospheric pressure chemical ionization source. Part I: ionization. *Journal of Mass Spectrometry* 49 (2014) 509-521

[81]   Hintikka L, Haapala M, Franssila S, Kuuranne T, Leinonen A, Kostiainen R. Feasibility of gas chromatography–microchip atmospheric pressure photoionization-mass spectrometry in analysis of anabolic steroids. *Journal of Chromatography A* 1217 (2010) 8290-8297

[82]   Hintikka L, Haapala M, Kuuranne T, Leinonen A, Kostiainen R. Analysis of anabolic steroids in urine by gas chromatography–microchip atmospheric pressure photoionization-mass spectrometry with chlorobenzene as dopant. *Journal of Chromatography A* 1312 (2013) 111-117

[83]   Cha E, Kim S, Kim HJ, Lee KM, Kim KH, Kwon OS, Lee J. Sensitivity of GC-EI/MS, GC-EI/MS/MS, LC-ESI/MS/MS, LC-Ag+ CIS/MS/MS, and GC-ESI/MS/MS for analysis of anabolic steroids in doping control. *Drug testing and analysis* 7 (2015) 1040-1049

[84]   Thevis M, Schänzer W. Mass spectrometry in sports drug testing: structure characterization and analytical assays. *Mass spectrometry reviews* 26 (2007) 79-107

[85]   Barrón D, Barbosa J, Pascual J, Segura J. Direct determination of anabolic steroids in human urine by on-line solid-phase extraction/liquid chromatography/mass spectrometry. *Journal of mass spectrometry* 31 (1996) 309-319

[86]   Ventura R, Fraisse D, Becchi M, Paisse O, Segura J. Approach to the analysis of diuretics and masking agents by high-performance liquid chromatography—mass spectrometry in doping control. *Journal of Chromatography B: Biomedical Sciences and Applications* 562 (1991) 723-736

[87]   Görgens C, Guddat S, Orlovius A-K, Sigmund G, Thomas A, Thevis M, Schänzer W. "Dilute-and-inject" multi-target screening assay for highly polar doping agents using hydrophilic interaction liquid chromatography high resolution/high accuracy mass spectrometry for sports drug testing. *Analytical and bioanalytical chemistry* 407 (2015) 5365-5379

[88]   Alcántara-Durán J, Moreno-González D, Beneito-Cambra M, García-Reyes JF. Dilute-and-shoot coupled to nanoflow liquid chromatography high resolution mass spectrometry for the determination of drugs of abuse and sport drugs in human urine. *Talanta* 182 (2018) 218-224

[89]   Davis Jr DE, Leaptrot KL, Koomen DC, May JC, Cavalcanti GDA, Padilha MC, Pereira HM, Mclean JA. Multidimensional Separations of Intact Phase II Steroid Metabolites Utilizing LC–Ion Mobility–HRMS. *Analytical chemistry* 93 (2021) 10990-10998

[90]   Parr MK, Wuest B, Naegele E, Joseph JF, Wenzel M, Schmidt AH, Stanic M, De La Torre X, Botrè F. SFC-MS/MS as an orthogonal technique for improved screening of polar analytes in anti-doping control. *Analytical and bioanalytical chemistry* 408 (2016) 6789-6797

[91]   Lee ML, Markides KE. Analytical supercritical fluid chromatography and extraction. in, Citeseer, (1990)

[92]   Nováková L, Rentsch M, Perrenoud AG-G, Nicoli R, Saugy M, Veuthey JL, Guillarme D. Ultra high performance supercritical fluid chromatography coupled with tandem mass spectrometry for screening of doping agents. II: analysis of biological samples. *Analytica Chimica Acta* 853 (2015) 647-659

[93]   Xhaferaj M, Naegele E, Parr MK. Ion exchange in supercritical fluid chromatography tandem mass spectrometry (SFC-MS/MS): Application for polar and ionic drugs and metabolites in forensic and anti-doping analysis. *Journal of Chromatography A* 1614 (2020) 460726

[94]   Teubel J, Wüst B, Schipke CG, Peters O, Parr MK. Methods in endogenous steroid profiling–A comparison of gas chromatography mass spectrometry (GC–MS) with supercritical fluid chromatography tandem mass spectrometry (SFC-MS/MS). *Journal of Chromatography A* 1554 (2018) 101-116

[95]   Aboushady D, Hanafi RS, Parr MK. Quality by Design approach for Enantioseparation of Terbutaline and its Sulfate Conjugate Metabolite for Bioanalytical Application using Supercritical Fluid Chromatography. *Journal of Chromatography A* (2022) 463285

[96]   Balcells G, Gómez C, Garrostas L, Pozo ÓJ, Ventura R. Sulfate metabolites as alternative markers for the detection of 4-chlorometandienone misuse in doping control. *Drug testing and analysis* 9 (2017) 983-993

[97]   Fragkaki AG, Sakellariou P, Kiousi P, Kioukia-Fougia N, Tsivou M, Petrou M, Angelis Y. Human in vivo metabolism study of LGD-4033. *Drug testing and analysis* 10 (2018) 1635-1645

3.2 Manuscript II: "Functional Expression of All Human Sulfotransferases in Fission Yeast, Assay Development, and Structural Models for Isoforms SULT4A1 and SULT6B1"

Yanan Sun, David Machalz, Gerhard Wolber, Maria Kristina Parr, Matthias Bureik

Abstract: Cytosolic sulfotransferases (SULTs) catalyze phase II (conjugation) reactions of drugs and endogenous compounds. A complete set of recombinant fission yeast strains each expressing one of the 14 human SULTs was generated, including SULT4A1 and SULT6B1. Sulfation of test substrates by whole-cell biotransformation was successfully demonstrated for all enzymes for which substrates were previously known. The results proved that the intracellular production of the cofactor 3′-phosphoadenosine 5′-phosphosulfate (PAPS) necessary for SULT activity in fission yeast is sufficiently high to support metabolite production. A modified variant of sulfotransferase assay was also developed that employs permeabilized fission yeast cells (enzyme bags). Using this approach, SULT4A1-dependent sulfation of 1-naphthol was observed. Additionally, a new and convenient SULT activity assay is presented. It is based on the sulfation of a proluciferin compound, which was catalyzed by SULT1E1, SULT2A1, SULT4A1, and SULT6B1. For the latter two enzymes this study represents the first demonstration of their enzymatic functionality. Furthermore, the first catalytically competent homology models for SULT4A1 and SULT6B1 in complex with PAPS are reported. Through mechanistic molecular modeling driven by substrate docking, we pinned down the increased activity levels of these two isoforms to optimized substrate binding.

biomolecules

MDPI

Article

Functional Expression of All Human Sulfotransferases in Fission Yeast, Assay Development, and Structural Models for Isoforms SULT4A1 and SULT6B1

Yanan Sun [1,2], David Machalz [3], Gerhard Wolber [3], Maria Kristina Parr [2,*] and Matthias Bureik [1,*]

1   School of Pharmaceutical Science and Technology, Health Sciences Platform, Tianjin University, Tianjin 300072, China; suny72@zedat.fu-berlin.de
2   Pharmaceutical and Medicinal Chemistry (Pharmaceutical Analyses), Institute of Pharmacy, Freie Universitaet Berlin, 14195 Berlin, Germany
3   Pharmaceutical and Medicinal Chemistry (Computer-Aided Drug Design), Institute of Pharmacy, Freie Universitaet Berlin, 14195 Berlin, Germany; david.machalz@fu-berlin.de (D.M.); gerhard.wolber@fu-berlin.de (G.W.)
*   Correspondence: maria.parr@fu-berlin.de (M.K.P.); matthias@tju.edu.cn (M.B.); Tel.: +49-30-838-57686 (M.K.P.); +86-22-87401835 (M.B.)

check for updates

Abstract: Cytosolic sulfotransferases (SULTs) catalyze phase II (conjugation) reactions of drugs and endogenous compounds. A complete set of recombinant fission yeast strains each expressing one of the 14 human SULTs was generated, including SULT4A1 and SULT6B1. Sulfation of test substrates by whole-cell biotransformation was successfully demonstrated for all enzymes for which substrates were previously known. The results proved that the intracellular production of the cofactor 3'-phosphoadenosine 5'-phosphosulfate (PAPS) necessary for SULT activity in fission yeast is sufficiently high to support metabolite production. A modified variant of sulfotransferase assay was also developed that employs permeabilized fission yeast cells (enzyme bags). Using this approach, SULT4A1-dependent sulfation of 1-naphthol was observed. Additionally, a new and convenient SULT activity assay is presented. It is based on the sulfation of a proluciferin compound, which was catalyzed by SULT1E1, SULT2A1, SULT4A1, and SULT6B1. For the latter two enzymes this study represents the first demonstration of their enzymatic functionality. Furthermore, the first catalytically competent homology models for SULT4A1 and SULT6B1 in complex with PAPS are reported. Through mechanistic molecular modeling driven by substrate docking, we pinned down the increased activity levels of these two isoforms to optimized substrate binding.

Keywords: drug metabolism; phase II; proluciferin; sulfation; sulfotransferase

1. Introduction

The plethora of biotransformations that together constitute human drug metabolism is subdivided into phase I (functionalization) and phase II (conjugation) reactions. The latter are carried out by Uridine 5'-diphospho-glucuronosyltransferases (UGTs), sulfotransferases, glutathione transferases, and other enzymes [1]. Cytosolic sulfotransferases (SULTs) catalyze the transfer of a sulfate group from the universal sulfate donor 3'-phosphoadenosine 5'-phosphosulfate (PAPS) to both endogenous and xenobiotic compounds [2]. In these reactions, the SO_3^- moiety is transferred to hydroxy or amino functions of small molecule substrates. While the majority of known sulfations lead to metabolites

with reduced biological activity compared to their parental compounds, there are also some examples of metabolic activation by this process [3]. There are 14 human SULTs that belong to the families SULT1, SULT2, SULT4, and SULT6, respectively, whereas SULT3 and SULT5 family members are not present in humans [4]. Most of the human SULTs are reported to be functionally expressed in *Escherichia coli* [5] or in *Saccharomyces cerevisiae* [6]. For two of these enzymes, namely, SULT4A1 and SULT6B1, no endogenous substrate nor activity data were ever reported before this study. Human SULT4A1 was originally identified in brain tissue [7] and displays a very high level of evolutionary conservation across species. More than a decade ago it was suggested that this enzyme might not be functional because it lacks part of one of the PAPS binding regions [8]. However, a severe phenotype and early postnatal death in SULT4A1 knock-out mice very recently revealed that SULT4A1 is an essential neuronal protein at least in this species [9]. Human SULT6B1 was first identified in 2004 [10] and belongs to a family that is also well conserved from mammals to fish, birds, and amphibians. In SULT6 enzymes, the sulfotransferase dimerization motif KXXXTVXXXE [11] is not retained, which suggests that they exist as monomers [2]. Human SULT6B1 is mainly expressed in the testes [10], whereas its mouse homologue is expressed in a variety of tissues [12]. The latter was reported to metabolize thyroxine and bithionol [12]. Previously, we successfully used fission yeast *Schizosaccharomyces pombe* for the functional expression of orphan cytochrome P450 (CYP) enzymes, such as CYP2A7, CYP4Z1, CYP4A22, and CYP20A1 [13–16], and UGTs such as UGT1A5 [17]. Homology models of these understudied enzymes guided by substrate activity data helped to increase knowledge on their functionality. There are two endogenous CYPs but no UGT or SULT homologues in fission yeast [18]. The aims of the present study were to evaluate fission yeast as a host for the recombinant expression of human SULTs and to assess its suitability for the functional production of SULT4A1 and SULT6B1. Furthermore, we aimed to rationalize our experimental results by modeling SULT–substrate complexes using homology modeling and substrate docking experiments.

2. Materials and Methods

2.1. Chemicals and Reagents

Na_2HPO_4, NH_4Cl, glucose, KH_2PO_4, NH_4I, and potassium hydrogen phthalate were from Chemart Chemical (Tianjin, China). $MgCl_2$ $6H_2O$, $CaCl_2$ $2H_2O$, KCl, Na_2SO_4, nicotinic acid, inositol, sodium pantothenate, biotin, $MnSO_4$, $ZnSO_4$ $7H_2O$, $FeCl_3$ $6H_2O$, KI, $CuSO_4$ $5H_2O$, H_3BO_3, MoO_4 $2H_2O$, citric acid, agar, and thiamine were from Kermel Chemical (Tianjin, China). Triton-X100 was from Leagene (Beijing, China). NH_4HCO_3 was from Jiangtian Chemical (Tianjin, China). Tris-HCl was from AKZ-Biotech (Tianjin, China). E.Z.N.A. Plasmid Mini Kit and E.Z.N.A. Cycle Pure Kit were from Omega Bio-tek (Norcross, GA, USA); *E. coli* cells were from General Biosystems (Anhui, China); 4-nitrophenol, 1-naphthol, 7-hydroxycoumarin, and dehydroepiandrosterone (DHEA) were from Accela ChemBio Co., Ltd. (Shanghai, China); UGT-Glo substrates A (GSA, 6-hydroxy-4-methylbenzo[*d*]thiazole-2-carbonitrile) and B (GSB, 6-((3-aminobenzyl)amino)benzo[*d*]thiazole-2-carbonitrile) were from Promega (Madison, WS, USA); S9 fractions of human liver cells were from Sekisui XenoTech (Kansas City, KS, USA). All other chemicals and reagents used were of the highest grade available.

2.2. Fission Yeast Media and General Techniques

General DNA manipulation methods were performed using standard techniques [19] and the preparation of media and basic manipulation methods of *S. pombe* were carried out as described [20]. Briefly, strains were generally cultivated at 30 °C in Edinburgh minimal medium (EMM) with supplements of 0.1 g/L final concentration as required. EMM was prepared with NH_4Cl (93.5 mM), glucose (2% *w/v*), Na_2HPO_4 (15.5 mM), potassium hydrogen phthalate (14.7 mM), and a given amount of a salt, vitamin, and mineral solution. Liquid cultures were kept shaking at 150 rpm. Thiamine was used at a concentration of 5 μM throughout.

2.3. Expression Plasmid Construction

Synthetic cDNAs encoding for each of the 14 human SULTs were synthesized by General Biosystem (Anhui, China) and cloned into both the integrative vector pCAD1 [21] and the replicating vector pREP1 [22] for expression in fission yeast. Both expression vectors contain the thiamine-repressible nmt1 promotor which allows for strong expression in *S. pombe* [23]. The correctness of all expression constructs was confirmed by automated sequencing.

2.4. Fission Yeast Strain Construction

Transformation of fission yeast was done using the lithium acetate method [24]. Briefly, strain NCYC2036 (genotype *h⁻ ura4-D18*) [25] was transformed with pCAD1-SULT expression constructs to yield a set of new strains which contained the SULT genes integrated into the *leu1* locus on chromosome II of fission yeast under control of the nmt1 promotor [23]. Correct chromosomal integration of the pCAD1 constructs into the *leu1* locus was confirmed by replica plating colonies on EMM lacking leucine. These 14 new strains were in turn transformed with the corresponding pREP1-SULT plasmids.

2.5. Whole-Cell Biotransformation in Shaking Flasks

Whole-cell biotransformation was essentially done as described previously [6]. Briefly, wet fission yeast cells were suspended at a concentration of 25% (*w/v*) in 100 mM potassium phosphate (KPi) buffer (pH 7.4) containing 1% (*w/v*) ammonium sulfate, and 8% (*w/v*) glucose. Substrate stock solution (100 mM in DMSO) was added to the cell suspension to a final concentration of 1 mM. Biotransformation was performed at 30 °C with shaking at 150 rpm for the times indicated. Afterwards, three volumes of acetonitrile were added to the reaction solution. After centrifugation at $10,000 \times g$ for 10 min, the supernatant was evaporated and the remaining pellet resolved in 50 µL of the solvent for the HPLC analysis.

2.6. Biotransformation with Enzyme Bags

This was essentially done as described in [17] with slight modifications. Briefly, fission yeast strains were grown in 10 mL liquid culture of EMM with supplements as needed at 30 °C and 230 rpm for 24 h. For each assay, 5×10^7 cells were transferred to 1.5 mL Eppendorf tubes, pelleted, and incubated in 1 mL of 0.3% Triton-X100 in Tris-KCl buffer (200 mM KCl, 100 mM Tris-Cl pH 7.8) at room temperature for 60 minutes at 150 rpm to allow permeabilization. Cells were then washed thrice with 1 mL of NH_4HCO_3 buffer (50 mM, pH 7.8) and directly used for SULT-dependent reactions. Enzyme bags were resuspended in 200 µL of NH_4HCO_3 buffer (50 mM, pH 7.8) containing 100 µM PAPS and substrate as indicated. For luminescence assays, enzyme bags were resuspended in 30 µL assay buffer (containing 8 µL 5 * UGT-Glo buffer, 100 µM PAPS, and either 10 µM UGT-Glo substrate A (GSA) or 50 µM UGT-Glo substrate B (GSB) as indicated). Biotransformations were done for 3 h at 37 °C in a shaking incubator (1000 rpm). Afterwards, the reaction mixtures were transferred to 1.5 mL Eppendorf tubes and centrifuged at $16,000 \times g$ for 1 min. The supernatants were then either analyzed by LC–MS or transferred to white 96-well microtiter plates for luminescence measurements.

2.7. HPLC–UV and LC–MS Analysis

Analytic instruments were composed of a micrOTOF focus mass spectrometer (BrukerDaltonics, Bremen, Germany) hyphenated by electrospray ionization (ESI) to a 1290 infinity II liquid chromatography system (Agilent, Santa Clara, CA, USA), equipped with a LiChrospher®100 reversed phase C18 column (5 µm, 4.0 × 125 mm, Merck KGaA, Darmstadt, Germany) or a Kromasil 100-5-C18 column (for analysis of 4-nitrophenol biotransformations, 5 µm, 4.6 × 250 mm, Akzo Noble, Arlöv, Sweden). Mobile phase flow rate was 0.5 mL/min. MS parameters were set using negative ion mode with spectra acquired over a mass range of *m/z* 50–1000; capillary voltage, +3500 V; drying gas temperature, 180 °C; dry gas flow, 6 L/min; nebulizing gas pressure, 1.2 bar. The accurate mass data of

molecular ions was calculated using Bruker Compass Data Analysis 4.1 (BrukerDaltonics, Bremen, Germany).

For the analysis of the biotransformations of 7-hydroxycoumarin and 4-methyl-7-hydroxycoumarin, the column compartment was maintained at 25 °C. Mobile phase A was water and mobile phase B was methanol. The following gradient mode was used: 0–2 min 10% B, 2–8 min 10–60% B, 8–10 min 60–10% B, 10–12 min 10% B. Detection was performed by UV at a wavelength of 320 nm.

For the analysis of 1-naphthol biotransformations the column was maintained at 25 °C. The mobile phase A was water with 0.2% acetic acid and mobile phase B was methanol with 0.2% acetic acid. The following gradient mode was used: 0–15 min 15–90% B, 15–18 min 90% B. Detection was performed by UV at a wavelength of 280 nm.

For the analysis of 4-nitrophenol biotransformations the column was maintained at 25 °C. The separation was performed with an isocratic mixture of water with 0.2% acetic acid and methanol (1:1, v/v) for 13 min. Detection was performed by UV at a wavelength of 280 nm.

For the analysis of DHEA biotransformations, the column was maintained at 35 °C. The mobile phase A was water with 0.1% formic acid and mobile phase B was 90% methanol and 10% water with 0.1% formic acid. The following gradient mode was used: 0–5 min 50% B, 5–10 min 50–100% B, 10–15% min 100% B.

For the analysis of GSA biotransformations a Q Exactive[TM] HF Combined Quadrupole Orbitrap Mass Spectrometer (Thermo Fisher, Waltham, MA, USA) and a Kromasil 100-5-C18 column (5 µm, 4.6 × 250 mm) were used. The column was maintained at 25 °C, and the flow rate was 0.5 mL/min. The mobile phase A was water and mobile phase B was methanol. The following gradient mode was used: 10–32 min 10–95% B, 32–35 min 95% B, 35–36 min 95–10% B, 36–40 min 10% B.

2.8. Bioluminescence Detection

Supernatants from the SULT-dependent biotransformations were transferred to white microtiter plates and an equal amount of reconstituted luciferin detection reagent was added to each well. Plates were then incubated at room temperature for 20 min and luminescence was recorded on a Magellan infinite 200Pro microplate reader (Tecan; Männedorf, Switzerland). In all cases reaction parameters (reaction times and enzyme concentrations) were within the linear range. All measurements were done at least three times in triplicate.

2.9. Statistical Analysis

All data are presented as mean ± SD. Statistical significance was determined using a two-tailed *t*-test. Differences were considered significant if $p < 0.05$. Statistical analysis was done using GraphPad Prism 5.01 (GraphPad Software, Inc., La Jolla, CA, USA).

2.10. Homology Modeling for SULT4A1 and SULT6B1

No experimentally solved 3D structure of the catalytically competent complex with cofactor PAPS exists for either SULT4A1 or SULT6B1. Hence, structural homology modeling was conducted on the I-TASSER [26–28] server. Input sequences for SULT4A1 (uniprot-id: Q9BR01) and SULT6B1 (uniprot-id: Q6IMI4) originated from uniprot [29]. Only the best model according to the C-score was further considered for both SULT enzymes (SULT4A1: 0.97, SULT6B1: 0.59). A high C-score assumes high model quality confidence and ranges from –5 to 2. The COFACTOR [30,31]/COACH [32] functionality of I-TASSER predicted the coordinates of adenosine-3′,5′-diphosphate (PAP), the depleted form of the cofactor commonly used for co-crystallization with SULTs, for the homology models of the two SULTs. For SULT4A1, COFACTOR/COACH suggests the PAP coordinates in SULT1A1 (PDB-id: 1LS6 [33]) and for SULT6B1 those in mouse SULT1D1 (PDB-id: 2ZPT [34]). For SULT4A1, side chain Tyr91 was rotated outwards of the catalytic pocket to allow for substrate positioning using the Rotamer function in MOE (Molecular Operating Environment 2019. 1; Chemical Computing Group ULC, Montreal, QC,

Canada). In a similar fashion, Lys65 and Trp70 in the SULT6B1 model were slightly optimized towards cofactor accommodation.

2.11. Substrate Docking Experiments

In order to suggest a binding mode hypothesis, molecular docking experiments of UGT-Glo substrate A (GSA) to the active sites of SULT1E1, SULT2A1, SULT4A1, and SULT6B1 were performed using GOLD [35] (v5.7.0; Genetic Optimization for Ligand Docking; CCDC Software, Cambridge, UK). For SULT1E1 and SULT2A1, the X-ray structure 4JVN [36] of SULT1E1 was used due to the high similarity of the co-crystallized substrate (2,6-dibromo-3-(2,4-dibromophenoxy)phenol) to GSA. For SULT4A1 and SULT6B1 the previously built homology models were used. PAPS was built manually in all three SULT structures based on the PAP coordinates and complexes were prepared using the Structure Preparation functionality in MOE. We performed 25 genetic algorithm (GA) runs at 200% search efficiency using the PLP scoring function. The active site was defined by a sphere with the sulfur atom of PAPS at its center and a radius of 18 Å. The algorithm was instructed to search for diverse solutions (substrate poses) with a root mean square difference (RMSD) of at least 1.5 Å. The obtained docking poses were energy minimized using the MMFF94 force field [37] and visually inspected in LigandScout [38–40] (v4.4; Inte:ligand, Vienna, Austria). Plausible and catalytically productive binding was assumed when the hydroxy group of GSA, which undergoes sulfation, formed a hydrogen bond with the catalytic histidine (SULT1E1: His107, SULT2A1: His99, SULT4A1: His111, SULT6B1: His118).

3. Results

3.1. Strain Construction

For each of the human SULT isoenzymes, the most frequently occurring allozyme was used. Sequences were taken from the NCBI database on 19 June 2018. In the case of more than one allozyme, isoform a was employed. Synthetic DNAs coding for each of the human SULTs were cloned into both the integrative vector pCAD1 [21] and the replicating vector pREP1 [22] to yield 28 new expression plasmids. The host strain NCYC2036 was transformed to uracil prototrophy and leucine auxotrophy by homologous integration of the pCAD1-based clones into the *leu1* locus [25]. These 14 strains were subsequently transformed to leucine prototrophy with the corresponding pREP1-based clones (all strains are listed in Table 1). As consequence, each one of the 14 double-expressor strains contains both an integrated expression unit and an autosomal expression plasmid for the same SULT. The suitability of these double-expressor strains was verified by the whole-cell biotransformation assays performed with YN2 and YN4. The former that bears only the integrated expression unit pCAD1 for SULT2A1, showed no activity towards 7-hydroxycoumarin, but the double-expressor strain YN4, yielded sulfated 7-hydroxycoumarin. Additionally, by this cloning strategy, non-auxotrophic strains are obtained, which facilitates their propagation.

Table 1. List of fission yeast strains used in this study.

Strain	Parental Strain	Expressed Proteins	Genotype	Reference
NCYC2036	None	None	h- ura4-D.18	[25]
YN5	NCYC2036	SULT1A1	h- ura4-D.18 leu1::pCAD1- SULT1A1	This study
YN6	NCYC2036	SULT1A2	h- ura4-D.18 leu1::pCAD1- SULT1A2	This study
YN7	NCYC2036	SULT1A3	h- ura4-D.18 leu1::pCAD1- SULT1A3	This study
YN1	NCYC2036	SULT1B1	h- ura4-D.18 leu1::pCAD1- SULT1B1	This study
YN8	NCYC2036	SULT1C2	h- ura4-D.18 leu1::pCAD1- SULT1C2	This study
YN9	NCYC2036	SULT1C3a	h- ura4-D.18 leu1::pCAD1- SULT1C3a	This study
YN10	NCYC2036	SULT1C3d	h- ura4-D.18 leu1::pCAD1- SULT1C3d	This study
YN11	NCYC2036	SULT1C4	h- ura4-D.18 leu1::pCAD1- SULT1C4	This study
YN12	NCYC2036	SULT1E1	h- ura4-D.18 leu1::pCAD1- SULT1E1	This study
YN2	NCYC2036	SULT2A1	h- ura4-D.18 leu1::pCAD1- SULT2A1	This study
YN13	NCYC2036	SULT2B1a	h- ura4-D.18 leu1::pCAD1- SULT2B1a	This study
YN14	NCYC2036	SULT2B1b	h- ura4-D.18 leu1::pCAD1- SULT2B1b	This study
YN17	NCYC2036	SULT4A1	h- ura4-D.18 leu1::pCAD1- SULT4A1	This study
YN15	NCYC2036	SULT6B1	h- ura4-D.18 leu1::pCAD1- SULT6B1	This study
YN18	YN5	SULT1A1 (twice)	h- ura4-D.18 leu1::pCAD1-SULT1A1/pREP1-SULT1A1	This study
YN19	YN6	SULT1A2 (twice)	h- ura4-D.18 leu1::pCAD1- SULT1A2/pREP1-SULT1A2	This study
YN20	YN7	SULT1A3 (twice)	h- ura4-D.18 leu1::pCAD1- SULT1A3/pREP1-SULT1A3	This study
YN3	YN1	SULT1B1 (twice)	h- ura4-D.18 leu1::pCAD1- SULT1B1/ pREP1-SULT1B1	This study
YN21	YN8	SULT1C2 (twice)	h- ura4-D.18 leu1::pCAD1- SULT1C2/pREP1-SULT1C2	This study
YN22	YN9	SULT1C3a (twice)	h- ura4-D.18 leu1::pCAD1- SULT1C3a/pREP1-SULT1C3a	This study
YN23	YN10	SULT1C3d (twice)	h- ura4-D.18 leu1::pCAD1- SULT1C3d/pREP1-SULT1C3b	This study
YN24	YN11	SULT1C4 (twice)	h- ura4-D.18 leu1::pCAD1- SULT1C4/pREP1-SULT1C4	This study
YN25	YN12	SULT1E1 (twice)	h- ura4-D.18 leu1::pCAD1- SULT1E1/pREP1-SULT1E1	This study
YN4	YN2	SULT2A1 (twice)	h- ura4-D.18 leu1::pCAD1- SULT2A1/pREP1-SULT2A1	This study
YN31	YN13	SULT2B1a (twice)	h- ura4-D.18 leu1::pCAD1- SULT2B1a/pREP1-SULT2B1a	This study
YN27	YN14	SULT2B1b (twice)	h- ura4-D.18 leu1::pCAD1- SULT2B1b/pREP1-SULT2B1b	This study
YN32	YN17	SULT4A1(twice)	h- ura4-D.18 leu1::pCAD1- SULT4A1/pREP1-SULT4A1	This study
YN29	YN15	SULT6B1 (twice)	h- ura4-D.18 leu1::pCAD1- SULT6B1/pREP1-SULT6B1	This study

3.2. Monitoring of SULT Activity Using Standard Test Substrates

In order to demonstrate the functionality of the human SULTs recombinantly expressed in fission yeast, sulfation activities of the strains expressing one of the twelve human SULT1 or SULT2 family members were tested using known standard substrates. The assay format for these positive control reactions was whole-cell biotransformation. Based on a recent publication on the recombinant expression of several human SULTs in baker's yeast, which demonstrated that the intracellular level of the cofactor PAPS is sufficiently high for sulfation reactions [6], it was hypothesized that the same might be true for fission yeast. The substrates tested were 4-nitrophenol (for SULT1A2, SULT1A3 SULT1C2, and SULT1C3a), 1-naphthol (for SULT1A1, SULT1C3d, and SULT1E1), 7-hydroxycoumarin (for SULT1B1, SULT1C4, and SULT2A1), and dehydroepiandrosterone (DHEA for SULT2B1a and SULT2B1b), respectively [8,41,42]. Product analysis was done by LC–MS. All SULTs of the families 1 and 2 were found to catalyze the generation of the expected sulfoconjugates. LC–MS chromatograms are shown for SULT1A3, SULT1E1, and SULT1B1, respectively (Figure 1). An additional assay format was developed which employs permeabilized fission yeast cells (enzyme bags) using a protocol similar to those previously reported for CYPs [43] and UGTs [17], but with the addition of the cofactor PAPS instead of NADPH or GSA. In these experiments SULT4A1 catalyzed the sulfation of 1-naphthol (Figure 2), but not of 4-nitrophenol, 7-hydroxycoumarin, or DHEA. To the best of our knowledge, 1-naphthol is therefore the first known substrate for this enzyme. Using SULT6B1, none of these substrates was converted to its sulfate in our assay. Control experiments with the parental strain NCYC2036 were carried out in parallel. In the genome of fission yeast there are no genes with homology to the SULT family and as expected, no formation of any sulfated substrates was seen in control experiments.

3.3. Sulfation of a Proluciferin Substrate by the S9 Fraction of Human Liver Cells

Proluciferin probe substrates for the convenient activity monitoring of CYPs or UGTs have been commercially available for many years. However, a similar test system for the determination of SULT activities was lacking. Since a considerable number of compounds are substrates for both UGTs and SULTs, we speculated that at least one of the two available UGT proluciferin substrates might also be a SULT substrate. In order to test this hypothesis, we performed sulfation reactions using the S9 fraction of human liver cells, the cofactor PAPS, and GSA or GSB. These experiments showed that GSA, but not GSB, is metabolized by the S9 fraction in a PAPS-dependent manner (Figure 3). Formation of sulfated GSA was also confirmed by LC–MS analysis ($C_9H_6N_2O_4S_2$, [M–H]$^-$ theor. = 268.96962, [M–H]$^-$ exp. = 268.96900, $\Delta m/z$ = 2.31 ppm). The reaction scheme for these experiments is shown in the graphical abstract of this manuscript. In conclusion, these data demonstrate that GSA is a substrate for SULTs contained in the S9 fraction of human liver cells.

3.4. Sulfation of a Proluciferin Substrate by Individual Human SULTs Recombinantly Expressed in Fission Yeast

In order to determine which human SULTs are capable of metabolizing the proluciferin substrate, all 14 fission yeast strains that contain two SULT expression units were tested for metabolization of GSA using the enzyme bag approach. Four of these strains showed a statistically significant substrate sulfation (Figure 4); those were YN25 (expressing SULT1E1), YN4 (SULT2A1), YN32 (SULT4A1), and YN29 (SULT6B1). Formation of sulfated GSA was also confirmed by LC–MS analysis (Figure 5). Together with data from the Genotype-Tissue Expression (GTEx) project, our data suggest that the sulfation of this substrate by S9 fractions is predominantly due to SULT2A1 activity, as expression levels of the other three SULTs in liver are much lower.
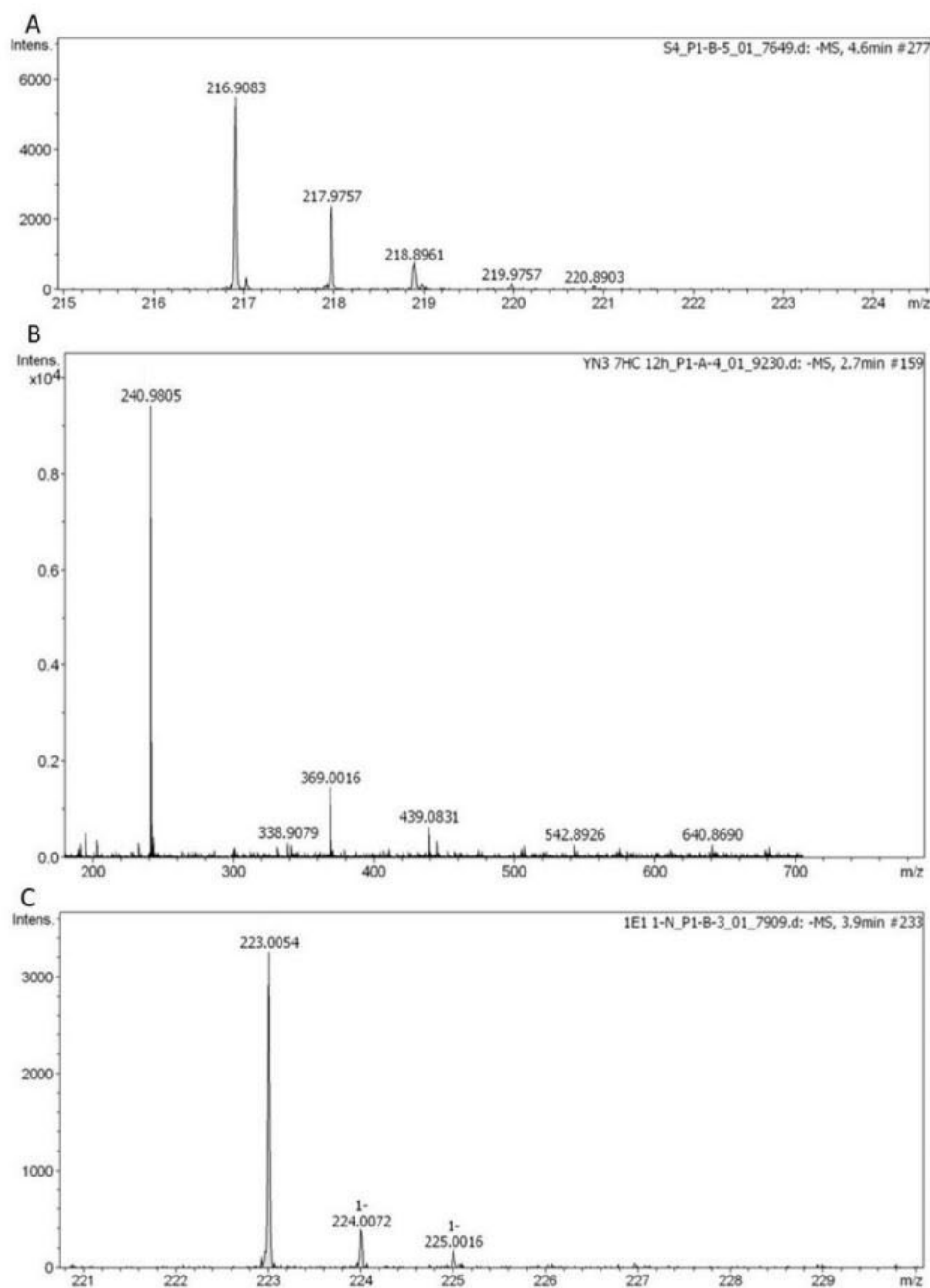
Figure 1. Exemplary results of standard SULT substrates metabolized in whole-cell biotransformations with human SULTs recombinantly expressed in fission yeast. (**A**) 4-nitrophenyl sulfate produced from 4-nitrophenol by SULT1A3 ($C_6H_5NO_6S$, $[M–H]^-$ theor. = 217.9765, $[M–H]^-$ exp. = 217.9757, $\Delta m/z = 3.67$ ppm). (**B**) 7-hydroxycoumarin sulfate produced from 7-hydroxycoumarin by SULT1B1 ($C_9H_6SO_6$, $[M–H]^-$ theor. = 240.9813, $[M–H]^-$ exp.= 240.9805, $\Delta m/z = 3.32$ ppm). (**C**) 1-naphthyl sulfate produced from 1-naphthol by SULT1E1 ($C_{10}H_8O_4S$, $[M–H]^-$ theor. = 223.0071, $[M–H]^-$ exp. = 223.0054, $\Delta m/z = 7.62$ ppm).
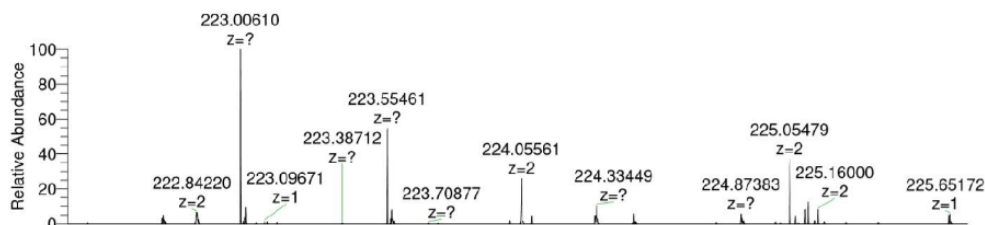
Figure 2. Mass spectrum of 1-naphthyl sulfate produced from 1-naphthol by enzyme bag biotransformation with human SULT4A1 ($C_{10}H_8O_4S$, $[M-H]^-$ theor. $= 223.00705$, $[M-H]^-$ exp. $= 223.00610$, $\Delta m/z = 4.26$ ppm).
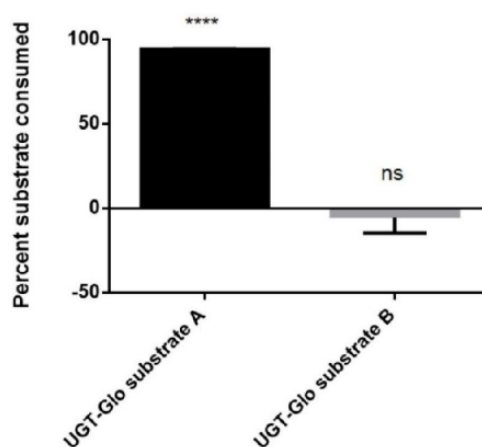
Figure 3. Biotransformation of GSA and GSB by the S9 fraction of human liver cells. Data shown were calculated from two independent experiments. **** $p < 0.0001$ vs. control (i.e., reaction samples without addition of PAPS); n.s.; not significant.
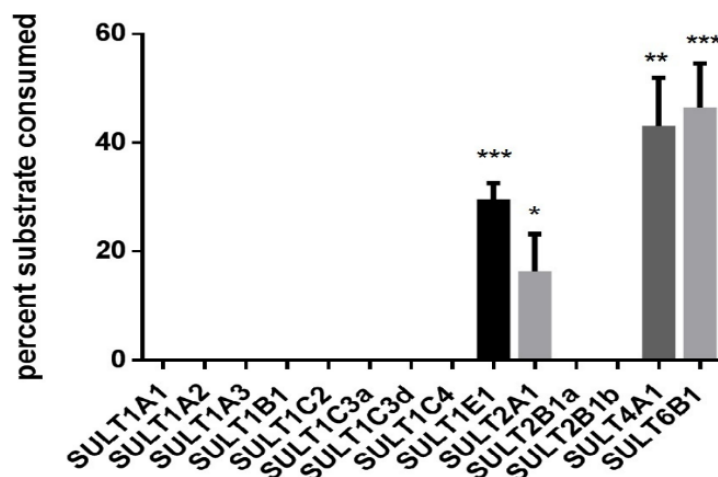
Figure 4. Activity of human SULT enzymes towards GSA. Enzyme bags were prepared from 14 fission yeast strains as indicated and activity was monitored by detecting luminescence. Data shown as percentage of substrate consumed after 3 h of reaction. Data shown were calculated from three independent experiments done in triplicate. * $p < 0.05$; ** $p < 0.01$; *** $p < 0.001$ vs. control (i.e., reaction samples without addition of PAPS).
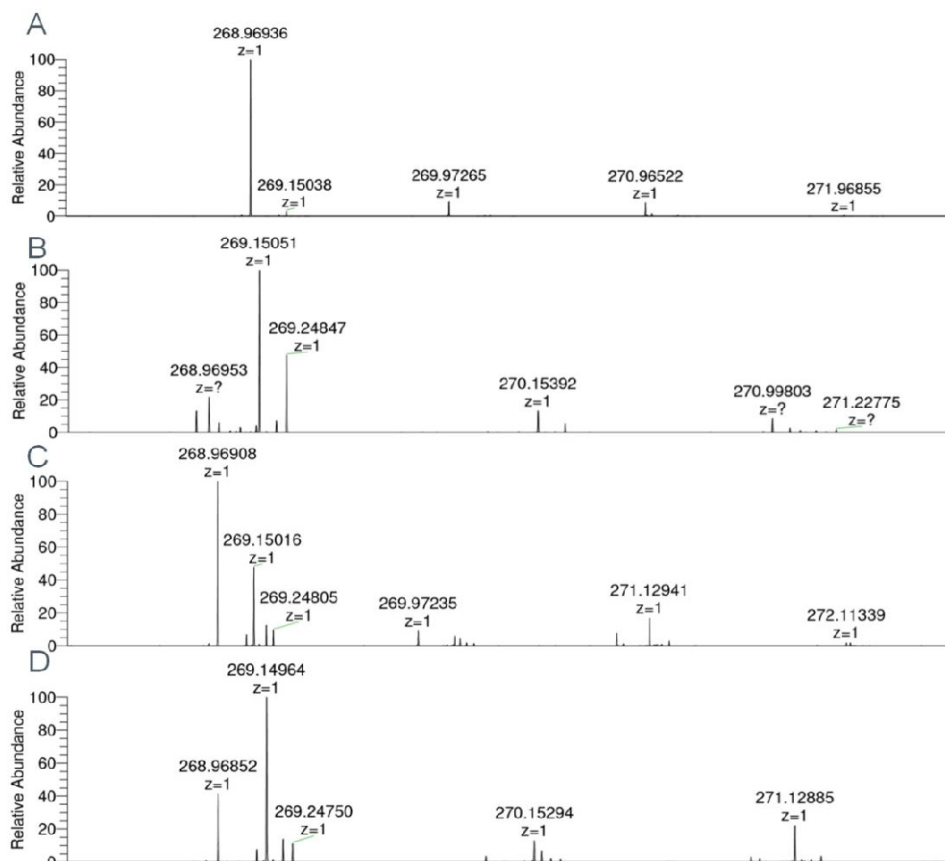
Figure 5. Mass spectra of 6-hydroxy-4-methyl-1,3-benzothiazole-2-carbonitrile sulfate (sulfated GSA) obtained by enzyme bag-catalyzed biotransformations with four human SULTs recombinantly expressed in fission yeast. (**A**) SULT1E1 ($C_9H_6N_2O_4S_2$, [M–H]$^-$ theor. = 268.96962, [M–H]$^-$ exp. = 268.96936, $\Delta m/z$ = 0.97 ppm). (**B**) SULT2A1 ([M–H]$^-$ exp. = 268.96953, $\Delta m/z$ = 0.33 ppm). (**C**) SULT4A1 ([M–H]$^-$ exp. = 268.96908, $\Delta m/z$ = 2.01 ppm). (**D**) SULT6B1 ([M–H]$^-$ exp. = 268.96852, $\Delta m/z$ = 4.09 ppm).

3.5. Comparative Mechanistic Modeling for SULT1E1, SULT2A1, SULT4A1, and SULT6B1

In order to rationalize the reported activity of GSA in SULT1E1, SULT2A1, SULT4A1, and SULT6B1, respectively, we performed mechanistic molecular modeling of the four respective enzyme substrate complexes. For SULT1E1 and SULT2A1 the available X-ray structures were used. The only available X-ray structure of SULT4A1 (PDB-id: 4JVN [36]) cannot accommodate the cofactor PAPS (Figure 6), and SULT6B1 has no solved X-ray structure. Hence, we designed homology models of SULT4A1 and SULT6B1 using the I-TASSER [26–28] server. A structural comparison of the four isoforms reveals that the backbone position is highly similar except for three loop regions that surround the substrate pocket (Figure 7A). High structural flexibility has been reported for loops 2 and 3 in SULT1E1 [44]. There are three prominent residue positions in the catalytic pocket (Figure 7B): Firstly, the conserved histidine crucial for the deprotonation of the substrate's hydroxy moiety (Figures 7B and 8E). Secondly, a lysine facilitating the sulfation of the substrate by holding the cofactor PAPS in place (Figures 7B and 8E), explaining its conservation. The residue in the third position is not conserved. In SULT1E1 (Figure 8A) and SULT4A1 (Figure 8C) the lysine at the third position likely interacts with PAPS and the substrate, thereby assisting the reaction. Ser97 in SULT2A1 (Figure 8B) and Ala116 in SULT6B1 (Figure 8D) in the same position cannot adopt this functionality. This does not seem to decrease the sulfation rate of

GSA in these two SULT isoforms (Figure 4). According to our homology model of SULT4A1, the rest of the active site comprises residues Glu14, Leu27, Pro28, Pro29, Phe30, Cys31, Pro54, Lys55, Val88, Glu90, Tyr91, Pro92, Lys109, His111, Tyr142, Phe145, Thr151, Met152, Gly171, and Tyr172. Surprisingly, the model of catalytically competent SULT4A1 resembled SULT1B1 (PDB-id: 3CKL) more than the X-ray structure of SULT4A1 (PDB-id: 1ZD1 [8]) according to TM-align [45], a program implemented in I-TASSER. The substrate pocket of SULT6B1 consists of the following further residues: Met39, Ser68, Tyr89, Phe92, Val94, Glu96, Cys97, Gly98, His118, Phe152, Pro157, Asp158, Trp179, His250, Val253, and Leu257, as suggested by the homology model.
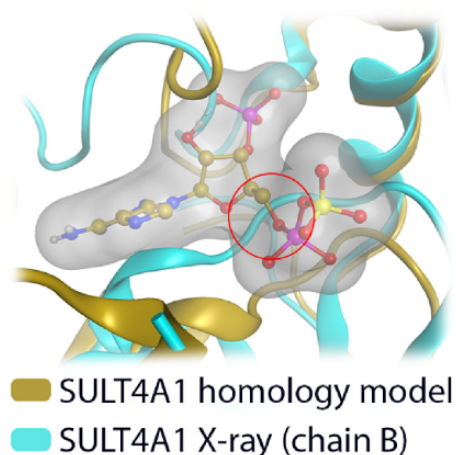
Figure 6. Comparison of our SULT4A1 homology model with the X-ray structure of SULT4A1 (PDB-id: 1ZD1 [8], chain B). The homology model can accommodate the cofactor PAPS, while in the X-ray structure it clashes with the protein backbone (red circle).
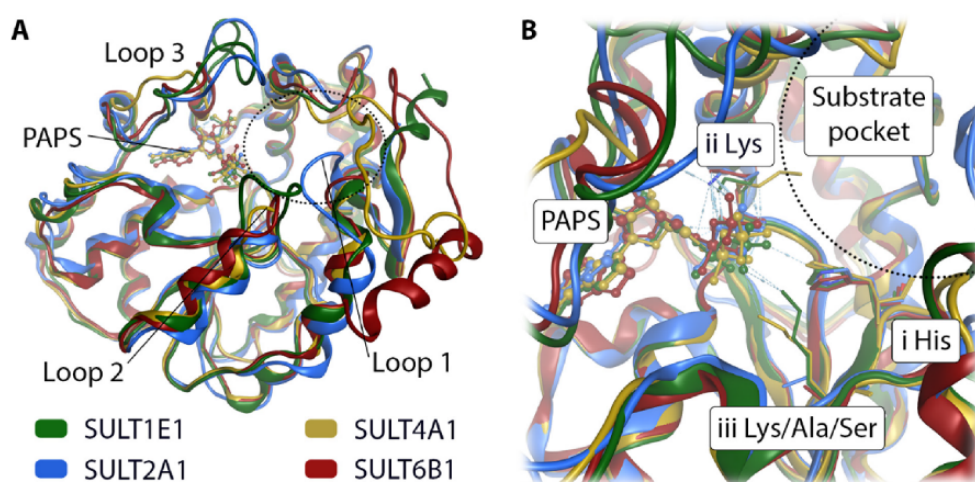
Figure 7. Superposition of four SULT isoforms with cofactor PAPS. SULT1E1 and SULT2A1 are X-ray structures taken from the PDB. SULT4A1 and SULT6B1 are homology models. (**A**) The view of the full structures shows deviations in three loops contributing to the binding site. (**B**) A closer look at the catalytic site shows the position of the conserved catalytically relevant histidine (i His). A lysine (ii Lys) is located in the vicinity of the substrate pocket (indicated by a dotted semicircle), while the second lysine is only present in SULT1E1 and SULT4A1 (iii Lys).
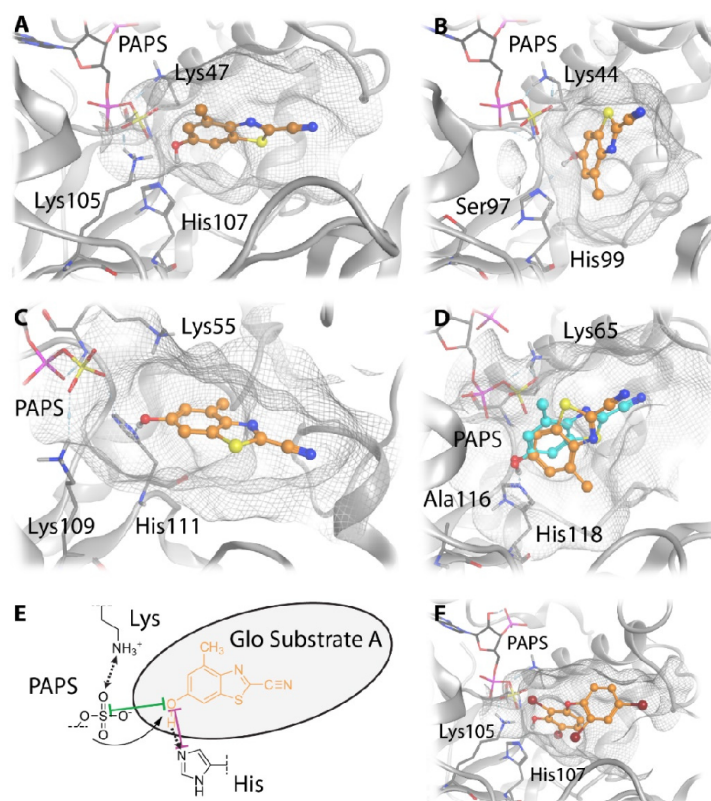
Figure 8. Suggested binding modes of GSA to four different SULT isoforms. (**A–D**) The most plausible docking poses of GSA to SULT1E1 (**A**), SULT2A1 (**B**), SULT4A1 (**C**), and SULT6B1 (**D**). (**E**) Distances of the hydroxy group of GSA to the catalytic histidine and the cofactor PAPS are displayed in a 2D substrate pocket depiction. (**F**) The X-ray binding mode of the co-crystallized ligand 2,6-dibromo-3-(2,4-dibromophenoxy) phenol to SULT1E1 is shown for comparison (PDB-id: 4JVN).

However, the catalytic histidine and cofactor-binding lysine are highly conserved in all four SULT isoforms, and differences in the third key residue position do not rationalize the observed activity trend of UGT-Glo substrate A. Hence, we docked this substrate to the active sites of the four SULT isoforms to suggest differences in the binding modes. The most plausible orientations of the substrate from docking (Figure 8A–D) resemble the reference binding mode of the co-crystallized ligand in the SULT1E1 X-ray structure (Figure 8F, PDB-id: 4JVN). The slot-like substrate pockets orient the substrate in a horizontal position in SULT1E1 (Figure 8A) and more vertically in SULT2A1 (Figure 8B). The substrate pockets of SULT4A1 (Figure 8C) and SULT6B1 (Figure 8D) are more voluminous and open. In SULT6B1, GSA can even adapt two distinct catalytically competent orientations.

In all SULTs a hydrogen bond is formed between the substrate hydroxy group and the catalytic histidine that is crucial for the reaction (Figure 8E). The docking poses suggest a difference in the distance and therefore in the quality of the hydrogen bond (Table 2). We suggest that the apparent different orientations of GSA in the SULT isoforms are caused by the different substrate pocket shapes. The less restrictive pockets in SULT4A1 and SULT6B1 allow for stronger hydrogen bonding, as suggested by a lower O_{GSA}-N_{His} atom distance. The increased O_{GSA}–S_{PAPS} atom distance can likely be reduced as the cofactor adopts a more favorable orientation towards the substrate.

Table 2. Distances of the hydroxy moiety of GSA in the binding modes suggested by docking.

SULT Isoform	Substrate Pose	$d(O_{GSA}-N_{His})$ [b][Å]	$d(O_{GSA}-S_{PAPS})$ [b][Å]
SULT1E1	X-ray [a]	3.0	3.3
SULT1E1	1	3.4	3.6
SULT2A1	1	3.4	3.8
SULT4A1	1	2.8	4.2
SULT6B1	1	2.5	4.7
SULT6B1	2	2.6	5.0

[a] Reference; [b] distance between indicated atoms.

4. Discussion

A set of fission yeast strains was created that contain expression constructs for each of the human SULT genes (Table 1). Sulfation activities of the twelve strains expressing human SULT1 or SULT2 enzymes were confirmed by whole-cell biotransformations using the known standard substrates 4-nitrophenol (for SULT1A2, SULT1A3 SULT1C2, and SULT1C3a), 1-naphthol (for SULT1A1, SULT1C3d, and SULT1E1), 7-hydroxycoumarin (for SULT1B1, SULT1C4, and SULT2A1), and DHEA (for SULT2B1a and SULT2B1b), respectively (exemplary results in Figure 1). These results confirm that the intracellular level of the cofactor PAPS is sufficiently high for sulfation reactions in fission yeast, as was previously demonstrated in similar experiments in baker's yeast [6].

Recently, we reported the successful use of permeabilized fission yeast cells (enzyme bags) for biotransformations catalyzed by human CYPs [43] or UGTs [17]. Such an assay design has the advantages of higher sensitivity and shorter reaction times, as substrates, cofactors, and products are not hampered by various biological membranes but can freely move between the assay medium and the inside of the cells. For comparison, the activity of SULT1C3d towards the standard substrate 1-naphthol was monitored with both enzyme bags and whole-cell biotransformation assays. Whole-cell assay resulted in no detection of the sulfated substrate, while in enzyme bags the sulfation of 1-naphthol was confirmed, which underlined the efficiency of enzyme bags assay. On the downside, the (sometimes expensive) cofactors need to be supplied to the reaction mixture. Thus, enzyme bag assays are well suited for enzymatic studies, whereas whole-cell biotransformations are to be preferred for (large scale) metabolite productions as they are cheaper and can be upscaled much easier. However, in contrast to membrane-bound human CYPs and UGTs, human SULTs are soluble proteins and might therefore be washed out of enzyme bags more easily. In our original study on the generation of enzyme bags from recombinant fission yeast cells, we demonstrated that upon permeabilization with 0.3% (*v*/*v*) Triton X-100, endogenous glucose 6-phosphate dehydrogenase (G6PDH) activity levels remain unaffected while small molecules can easily pass into and out of the cells [46]. There are three putative enzymes with G6PDH activity in fission yeast (gcd1, zwf1, and SPAC3C7.13c), which have sizes between 54 and 57 kDa [47]; thus, soluble proteins of this size (and possibly also slightly smaller ones) are expected to remain inside the enzyme bags. With the possible exception of SULT6B1, human SULTs exist as dimers of 61 to 82 kDa [2], so their size is expected to be compatible with the enzyme bag approach. We therefore tested this assay format using SULT-expressing fission yeast strains and the cofactor PAPS. We could not only show that this method is applicable for human SULTs, but we even observed activity of SULT4A1 towards 1-naphthol (Figure 2), thereby demonstrating the first enzymatic activity for this enzyme. Additionally, GSA was found to be successfully converted to its sulfate utilizing SULT4A1 and SULT6B1.

In general, probe substrates for drug metabolizing enzymes are compounds that are efficiently converted into readily detectable products. Detection methods that are used to monitor such conversions include light or UV absorbance, fluorescence, mass spectrometry, radiometry, and bioluminescence [48]. With respect to the latter, many proluciferin probe substrates are available which are (more or less

selectively) metabolized by certain CYPs or UGTs to reaction products that emit photons upon a second reaction step catalyzed by luciferase. However, a similar test system for the determination of SULT activities was not yet described. Since there is a significant overlap in the substrate selectivities of the human UGT and SULT families, it was reasonable to assume that at least one of the two available UGT proluciferin substrates may also be metabolized by SULTs. Sulfation reactions using these probe substrates together with the S9 fraction of human liver cells indeed demonstrated that GSA, but not GSB, is converted in a PAPS-dependent manner (Figure 3). Individual testing of the recombinant fission yeast strains showed that this reaction is catalyzed by SULT1E1, SULT2A1, SULT4A1, and SULT6B1 (Figures 4 and 5). Thus, a new probe reaction for these four enzymes was identified. This is especially noteworthy for SULT4A1 and SULT6B1, as its availability is expected to aid in the search for physiological substrates of these two enzymes. In addition, our data suggest that GSA sulfation by S9 fractions of human liver cells is mainly due to SULT2A1 activity.

In order to investigate the GSA activity trends, we constructed catalytically competent homology models for SULT4A1 and SULT6B1 with the novelty of PAPS cofactor accommodation (Figures 6 and 7). Structural comparison of the four GSA-metabolizing SULT isoforms identified different active site shapes. In SULT1E1 and SULT2A1, the substrate pocket is more slot-like, whereas it is more voluminous in SULT4A1 and SULT6B1. Molecular docking of GSA suggests that the less restrictive active sites in SULT4A1 and SULT6B1 enhance substrate binding and thereby increase its sulfation rate (Figure 8). The docking poses suggest varying lengths of the catalytically important hydrogen bond formed between the substrate hydroxy group and the catalytic histidine (Table 2), which are likely due to the different substrate pocket shapes of these four enzymes.

Taken together, in this study we show that all 14 human SULTs may be functionally expressed in fission yeast *S. pombe*. Moreover, we demonstrate for the first time that SULT4A1 and SULT6B1 are indeed catalytically active enzymes and we present test substrates for each of them. It is expected that this knowledge will contribute to the identification of physiologically important substrates of these enzymes and will thus contribute to elucidating their functions.

References

1.   Di, L.; Kerns, E.H. *Drug-Like Properties: Concepts, Structure Design and Methods from ADME to Toxicity Optimization*; Academic Press: London, UK, 2016.

2.   Coughtrie, M.W.H. Function and organization of the human cytosolic sulfotransferase (SULT) family. *Chem. Biol. Interact.* **2016**, *259*, 2–7. [CrossRef]

3.   Buhl, A.E.; Waldon, D.J.; Baker, C.A.; Johnson, G.A. Minoxidil sulfate is the active metabolite that stimulates hair follicles. *J. Investig. Dermatol.* **1990**, *95*, 553–557. [CrossRef]

4.   Tibbs, Z.E.; Rohn-Glowacki, K.J.; Crittenden, F.; Guidry, A.L.; Falany, C.N. Structural plasticity in the human cytosolic sulfotransferase dimer and its role in substrate selectivity and catalysis. *Drug Metab. Pharmacokinet.* **2015**, *30*, 3–20. [CrossRef] [PubMed]

5.   Taskinen, J.; Ethell, B.T.; Pihlavisto, P.; Hood, A.M.; Burchell, B.; Coughtrie, M.W. Conjugation of catechols by recombinant human sulfotransferases, UDP-glucuronosyltransferases, and soluble catechol O-methyltransferase: Structure-conjugation relationships and predictive models. *Drug Metab. Dispos.* **2003**, *31*, 1187–1197. [CrossRef] [PubMed]

6. Nishikawa, M.; Masuyama, Y.; Nunome, M.; Yasuda, K.; Sakaki, T.; Ikushiro, S. Whole-cell-dependent biosynthesis of sulfo-conjugate using human sulfotransferase expressing budding yeast. *Appl. Microbiol. Biot.* **2018**, *102*, 723–732. [CrossRef] [PubMed]

7. Falany, C.N.; Xie, X.; Wang, J.; Ferrer, J.; Falany, J.L. Molecular cloning and expression of novel sulphotransferase-like cDNAs from human and rat brain. *Biochem. J.* **2000**, *346 Pt 3*, 857–864. [CrossRef]

8. Allali-Hassani, A.; Pan, P.W.; Dombrovski, L.; Najmanovich, R.; Tempel, W.; Dong, A.; Loppnau, P.; Martin, F.; Thornton, J.; Edwards, A.M.; et al. Structural and chemical profiling of the human cytosolic sulfotransferases. *PLoS Biol.* **2007**, *5*, e97. [CrossRef]

9. Hossain, M.I.; Marcus, J.M.; Lee, J.H.; Garcia, P.L.; Gagne, J.P.; Poirier, G.G.; Falany, C.N.; Andrabi, S.A. SULT4A1 Protects Against Oxidative-Stress Induced Mitochondrial Dysfunction in Neuronal Cells. *Drug Metab. Dispos.* **2019**, *47*, 949–953. [CrossRef] [PubMed]

10. Freimuth, R.R.; Wiepert, M.; Chute, C.G.; Wieben, E.D.; Weinshilboum, R.M. Human cytosolic sulfotransferase database mining: Identification of seven novel genes and pseudogenes. *Pharm. J.* **2004**, *4*, 54–65. [CrossRef]

11. Petrotchenko, E.V.; Pedersen, L.C.; Borchers, C.H.; Tomer, K.B.; Negishi, M. The dimerization motif of cytosolic sulfotransferases. *FEBS Lett.* **2001**, *490*, 39–43. [CrossRef]

12. Takahashi, S.; Sakakibara, Y.; Mishiro, E.; Kouriki, H.; Nobe, R.; Kurogi, K.; Yasuda, S.; Liu, M.C.; Suiko, M. Molecular cloning, expression and characterization of a novel mouse SULT6 cytosolic sulfotransferase. *J. Biochem.* **2009**, *146*, 399–405. [CrossRef]

13. Zollner, A.; Dragan, C.A.; Pistorius, D.; Muller, R.; Bode, H.B.; Peters, F.T.; Maurer, H.H.; Bureik, M. Human CYP4Z1 catalyzes the in-chain hydroxylation of lauric acid and myristic acid. *Biol. Chem.* **2009**, *390*, 313–317. [CrossRef]

14. Durairaj, P.; Fan, L.; Du, W.; Ahmad, S.; Mebrahtu, D.; Sharma, S.; Ashraf, R.A.; Liu, J.; Liu, Q.; Bureik, M. Functional expression and activity screening of all human cytochrome P450 enzymes in fission yeast. *FEBS Lett.* **2019**, *593*, 1372–1380. [CrossRef] [PubMed]

15. Durairaj, P.; Fan, L.; Machalz, D.; Wolber, G.; Bureik, M. Functional characterization and mechanistic modeling of the human cytochrome P450 enzyme CYP4A22. *FEBS Lett.* **2019**, *593*, 2214–2225. [CrossRef]

16. Durairaj, P.; Fan, L.; Sharma, S.S.; Jie, Z.; Bureik, M. Identification of new probe substrates for human CYP20A1. *Biol. Chem.* **2020**, *401*, 361–365. [CrossRef]

17. Yang, F.; Machalz, D.; Wang, S.; Li, Z.; Wolber, G.; Bureik, M. A common polymorphic variant of UGT1A5 displays increased activity due to optimized cofactor binding. *FEBS Lett.* **2018**, *592*, 1837–1846. [CrossRef]

18. Wood, V.; Gwilliam, R.; Rajandream, M.A.; Lyne, M.; Lyne, R.; Stewart, A.; Sgouros, J.; Peat, N.; Hayles, J.; Baker, S.; et al. The genome sequence of Schizosaccharomyces pombe. *Nature* **2002**, *415*, 871–880. [CrossRef]

19. Sambrook, J.; Russell, D.W. *Molecular Cloning: A Laboratory Manual*; CSHL Press: Woodbury, NY, USA, 2001.

20. Alfa, C.; Fantes, P.; Hyams, J.; McLeod, M.; Warbrick, E. *Experiments with Fission Yeast. A Laboratory Course Manual*; Cold Spring Harbor Press: Cold Spring Harbor, NY, USA, 1993.

21. Dragan, C.-A.; Zearo, S.; Hannemann, F.; Bernhardt, R.; Bureik, M. Efficient conversion of 11-deoxycortisol to cortisol (hydrocortisone) by recombinant fission yeast Schizosaccharomyces pombe. *FEMS Yeast Res.* **2005**, *5*, 621–625. [CrossRef]

22. Maundrell, K. Thiamine-repressible expression vectors pREP and pRIP for fission yeast. *Gene* **1993**, *123*, 127–130. [CrossRef]

23. Maundrell, K. nmt1 of fission yeast. A highly transcribed gene completely repressed by thiamine. *J. Biol. Chem.* **1990**, *265*, 10857–10864. [PubMed]

24. Okazaki, K.; Okazaki, N.; Kume, K.; Jinno, S.; Tanaka, K.; Okayama, H. High-frequency transformation method and library transducing vectors for cloning mammalian cDNAs by trans-complementation of Schizosaccharomyces pombe. *Nucleic Acids Res.* **1990**, *18*, 6485–6489. [CrossRef]

25. Losson, R.; Lacroute, F. Plasmids carrying the yeast OMP decarboxylase structural and regulatory genes: Transcription regulation in a foreign environment. *Cell* **1983**, *32*, 371–377. [CrossRef]

26. Roy, A.; Kucukural, A.; Zhang, Y. I-TASSER: A unified platform for automated protein structure and function prediction. *Nat. Protoc.* **2010**, *5*, 725–738. [CrossRef] [PubMed]

27. Yang, J.; Yan, R.; Roy, A.; Xu, D.; Poisson, J.; Zhang, Y. The I-TASSER Suite: Protein structure and function prediction. *Nat. Methods* **2015**, *12*, 7–8. [CrossRef]

28. Zhang, Y. I-TASSER server for protein 3D structure prediction. *BMC Bioinform.* **2008**, *9*, 40. [CrossRef]

29. Consortium, U. UniProt: A worldwide hub of protein knowledge. *Nucleic Acids Res.* **2019**, *47*, D506–D515. [CrossRef]

30. Roy, A.; Yang, J.; Zhang, Y. COFACTOR: An accurate comparative algorithm for structure-based protein function annotation. *Nucleic Acids Res.* **2012**, *40*, W471–W477. [CrossRef]

31. Zhang, C.; Freddolino, P.L.; Zhang, Y. COFACTOR: Improved protein function prediction by combining structure, sequence and protein-protein interaction information. *Nucleic Acids Res.* **2017**, *45*, W291–W299. [CrossRef] [PubMed]

32. Yang, J.; Roy, A.; Zhang, Y. Protein-ligand binding site recognition using complementary binding-specific substructure comparison and sequence profile alignment. *Bioinformatics* **2013**, *29*, 2588–2595. [CrossRef] [PubMed]

33. Gamage, N.U.; Duggleby, R.G.; Barnett, A.C.; Tresillian, M.; Latham, C.F.; Liyou, N.E.; McManus, M.E.; Martin, J.L. Structure of a human carcinogen-converting enzyme, SULT1A1. Structural and kinetic implications of substrate inhibition. *J. Biol. Chem.* **2003**, *278*, 7655–7662. [CrossRef] [PubMed]

34. Teramoto, T.; Sakakibara, Y.; Inada, K.; Kurogi, K.; Liu, M.C.; Suiko, M.; Kimura, M.; Kakuta, Y. Crystal structure of mSULT1D1, a mouse catecholamine sulfotransferase. *FEBS Lett.* **2008**, *582*, 3909–3914. [CrossRef]

35. Jones, G.; Willett, P.; Glen, R.C.; Leach, A.R.; Taylor, R. Development and validation of a genetic algorithm for flexible docking. *J. Mol. Biol.* **1997**, *267*, 727–748. [CrossRef]

36. Gosavi, R.A.; Knudsen, G.A.; Birnbaum, L.S.; Pedersen, L.C. Mimicking of estradiol binding by flame retardants and their metabolites: A crystallographic analysis. *Env. Health Perspect.* **2013**, *121*, 1194–1199. [CrossRef]

37. Halgren, T.A.; Nachbar, R.B. Merck molecular force field. IV. conformational energies and geometries for MMFF94. *J. Comput. Chem.* **1996**, *17*, 587–615. [CrossRef]

38. Seidel, T.; Ibis, G.; Bendix, F.; Wolber, G. Strategies for 3D pharmacophore-based virtual screening. *Drug Discov. Today Technol.* **2010**, *7*, e221–e228. [CrossRef] [PubMed]

39. Wolber, G.; Langer, T. LigandScout: 3-d pharmacophores derived from protein-bound Ligands and their use as virtual screening filters. *J. Chem. Inf. Model* **2005**, *45*, 160–169. [CrossRef]

40. Wolber, G.; Sippl, W. Pharmacophore Identification and Pseudo-Receptor Modelling. In *The Practice of Medicinal Chemistry*, 4th ed.; Wermuth, C.G., Rognan, D., Eds.; Elsevier Ltd.: Philadelphia, PA, USA, 2015; pp. 489–507.

41. Gamage, N.; Barnett, A.; Hempel, N.; Duggleby, R.G.; Windmill, K.F.; Martin, J.L.; McManus, M.E. Human sulfotransferases and their role in chemical metabolism. *Toxicol. Sci.* **2006**, *90*, 5–22. [CrossRef]

42. Kurogi, K.; Sakakibara, Y.; Suiko, M.; Liu, M.C. Sulfation of vitamin D-3-related compounds-identification and characterization of the responsible human cytosolic sulfotransferases. *FEBS Lett.* **2017**, *591*, 2417–2425. [CrossRef] [PubMed]

43. Yan, Q.; Machalz, D.; Zollner, A.; Sorensen, E.J.; Wolber, G.; Bureik, M. Efficient substrate screening and inhibitor testing of human CYP4Z1 using permeabilized recombinant fission yeast. *Biochem. Pharm.* **2017**, *146*, 174–187. [CrossRef]

44. Rakers, C.; Schumacher, F.; Meinl, W.; Glatt, H.; Kleuser, B.; Wolber, G. In Silico Prediction of Human Sulfotransferase 1E1 Activity Guided by Pharmacophores from Molecular Dynamics Simulations. *J. Biol. Chem.* **2016**, *291*, 58–71. [CrossRef]

45. Zhang, Y.; Skolnick, J. TM-align: A protein structure alignment algorithm based on the TM-score. *Nucleic Acids Res.* **2005**, *33*, 2302–2309. [CrossRef] [PubMed]

46. Weyler, C.; Bureik, M.; Heinzle, E. Selective oxidation of UDP-glucose to UDP-glucuronic acid using permeabilized Schizosaccharomyces pombe expressing human UDP-glucose 6-dehydrogenase. *Biotechnol. Lett.* **2016**, *38*, 477–481. [CrossRef]

47. Lock, A.; Rutherford, K.; Harris, M.A.; Hayles, J.; Oliver, S.G.; Bahler, J.; Wood, V. PomBase 2018: User-driven reimplementation of the fission yeast database provides rapid and intuitive access to diverse, interconnected information. *Nucleic Acids Res.* **2019**, *47*, D821–D827. [CrossRef]

48. Cali, J.J.; Ma, D.; Wood, M.G.; Meisenheimer, P.L.; Klaubert, D.H. Bioluminescent assays for ADME evaluation: Dialing in CYP selectivity with luminogenic substrates. *Expert Opin. Drug Metab. Toxicol.* **2012**, *8*, 1115–1130. [CrossRef]

3.3 Manuscript Ⅲ: "Human Sulfotransferase Assays with PAPS Production in situ"

Yanan Sun, Lukas Corbinian Harps, Matthias Bureik, Maria Kristina Parr

Abstract: For *in vitro* investigations on human sulfotransferase (SULT) catalyzed phase II metabolism, the costly cofactor 3′-phosphoadenosine-5′-phosphosulfate (PAPS) is generally needed. In the present study, we developed and optimized a new approach that combines SULT-dependent biotransformation using recombinant and permeabilized fission yeast cells (enzyme bags) with PAPS production *in situ* applying quality by design principles. In the initial application of the procedure, yeast cells expressing human SULT1A3 were used for the production of 4′-hydroxypropranolol-4-*O*-sulfate from 4-hydroxypropranolol. The optimized protocol was then successfully transferred to other sulfonation reactions catalyzed by SULT2A1, SULT1E1, or SULT1B1. The concomitant degradation of some sulfoconjugates was investigated, and further optimization of the reaction conditions was performed in order to reduce product loss. Also, the production of stable isotope labelled sulfoconjugates was demonstrated utilizing isotopically labelled substrates or ^{34}S-sulfate. Overall, this new approach results in higher space-time yields while at the same time reducing experimental cost.

Human Sulfotransferase Assays With PAPS Production *in situ*

Yanan Sun[1,2†], Lukas Corbinian Harps[1†], Matthias Bureik[2]* and Maria Kristina Parr[1]*

[1]*Pharmaceutical and Medicinal Chemistry (Pharmaceutical Analyses), Institute of Pharmacy, Freie Universitaet Berlin, Berlin, Germany,* [2]*School of Pharmaceutical Science and Technology, Health Sciences Platform, Tianjin University, Tianjin, China*

For *in vitro* investigations on human sulfotransferase (SULT) catalyzed phase II metabolism, the costly cofactor 3′-phosphoadenosine-5′-phosphosulfate (PAPS) is generally needed. In the present study, we developed and optimized a new approach that combines SULT-dependent biotransformation using recombinant and permeabilized fission yeast cells (enzyme bags) with PAPS production *in situ* applying quality by design principles. In the initial application of the procedure, yeast cells expressing human SULT1A3 were used for the production of 4′-hydroxypropranolol-4-*O*-sulfate from 4-hydroxypropranolol. The optimized protocol was then successfully transferred to other sulfonation reactions catalyzed by SULT2A1, SULT1E1, or SULT1B1. The concomitant degradation of some sulfoconjugates was investigated, and further optimization of the reaction conditions was performed in order to reduce product loss. Also, the production of stable isotope labelled sulfoconjugates was demonstrated utilizing isotopically labelled substrates or [34]S-sulfate. Overall, this new approach results in higher space-time yields while at the same time reducing experimental cost.

Keywords: fission yeast, *in vitro* metabolism, method optimization, PAPS, sulfonation, SULT, quality by design, isotopic labelling

INTRODUCTION

The study of metabolic pathways of drug substances in humans relies both on *in vivo* and *in vitro* experiments. After administration drugs are either directly excreted unchanged or metabolized first. The main specimen for excretion of most drugs and metabolites is urine. The parent drugs often show shorter detection windows due to extensive metabolism. Therefore, in toxicological, forensic or doping control analysis metabolites are often used as target analytes in urine samples (Balcells et al., 2017; Esquivel et al., 2019). Even though *in vivo* techniques are widely applied in anti-doping research, the high expenditure and unpredicted toxicological effect of many prohibited drugs are considerable drawbacks. In the last two decades, modern *in vitro* techniques became a viable alternative and furthermore a great extension to *in vivo* studies (Ekins et al., 2000). Moreover, they allow for precise reaction phenotyping. In *in vitro* studies, tissues or fractions of tissues like liver microsomes or homogenized liver fractions are commonly applied. In recent years, biosynthesis of sulfoconjugates using genetically modified microorganisms has been developed as well (Taskinen et al., 2003; Nishikawa et al., 2018). Metabolism of drug substances occurs in the complementary phases I and II. While enzymes of phase I metabolism transform parent compounds by hydroxylation, oxidation, or reduction, phase II metabolism consists of the attachment of small moieties to the target molecules, thus allowing them to be excreted from the body rapidly and efficiently. The majority of phase II metabolites are glucuronide- or sulfoconjugates. The formation of the latter species is catalyzed

by sulfotransferases (SULTs), which for their activity depend on the cofactor 3'-phosphoadenosine-5'-phosphosulfate (PAPS).

For laboratory use PAPS is highly expensive (approx. 286 US$/mg). This fact might contribute to the limited number of sulfonation studies as compared with research on glucuronidation. In biological sulfonation, conversion of inorganic sulfate into the high-energy cofactor PAPS is a prerequisite. In this pathway, adenosine triphosphate (ATP) sulfonation is initially catalyzed by ATP-sulfurylase to generate adenosine-5'-phosphosulfate (APS), which is subsequently phosphorylated by APS kinase to yield PAPS (Burkart et al., 2000). Afterwards, the sulfo-group is transferred from PAPS to the parent drug or its phase I metabolite in a reaction catalyzed by a SULT enzyme. The released 3'-phosphoadenosine-5'-phosphate (PAP) is subsequently dephosphorylated and re-phosphorylated in several enzymatically catalyzed steps to regenerate ATP (Robbins and Lipmann, 1958). In animal cells, ATP sulfurylase and APS kinase are expressed as a bifunctional enzyme named PAPS synthase (PAPSS), whereas in bacteria, yeasts, fungi, and plants, the two enzymes are generally encoded by separate genes (Besset et al., 2000).

In the budding yeast *Saccharomyces cerevisiae* ATP sulfurylase and APS kinase are encoded by the genes MET3 and MET14, respectively (Masselot and Surdin-Kerjan, 1977; Cherest et al., 1985; Cherest et al., 1987; Mountain and Korch, 1991). In the fission yeast *Schizosaccharomyces pombe* there is a MET14 homologue which is predicted to encode a APS kinase (Lock et al., 2019). While this has yet to be demonstrated experimentally, PAPS synthesis in *S. pombe* as such has already been reported (Song and Roe, 2008). Previously, all 14 human SULTs have been functionally expressed in *S. pombe* and, moreover, using this microbial host the functionality of SULT4A1 and SULT6B1 was demonstrated for the first time (Sun et al., 2020). In comparison to whole-cell biotransformation, sulfonation of drugs with permeabilized recombinant fission yeast cells (enzyme bags) provided higher sensitivity and shorter reaction times. However, the required PAPS addition makes this approach expensive for extensive substrate screening or for up-scaling of biosynthetic metabolite production. In this study, we investigated the possibility of generating PAPS by endogenous fission yeast enzymes in the presence of (comparatively cheaper) ATP and ammonium sulfate. For this purpose, the experimental conditions were first optimized using SULT1A3 and 4-hydroxypropranolol (4HP) as model compound. Further verification was then performed with several other SULTs and substrates.

MATERIAL AND METHODS

Chemicals and Reagents

Na_2HPO_4 and $CaCl_2 \bullet 2 H_2O$ were purchased from Riedel de Haen (Seelze, Germany). KH_2PO_4, $CuSO_4 \bullet 5 H_2O$, H_3BO_3, potassium hydrogen phthalate, Na_2SO_4, nicotinic acid, $MnSO_4 \bullet H_2O$, and KI were from Merck (Darmstadt, Germany). $ZnSO_4 \bullet 7 H_2O$ was purchased from Acros (Geel, Belgium). Tris, agar,

NH_4HCO_3, NH_4Cl, $FeCl_3 \bullet 6 H_2O$, $MgCl_2 \bullet 6 H_2O$, glucose, Triton-X100, and biotin were from Roth (Karlsruhe, Germany). Inositol was from Th.Geyer (Berlin, Germany), and $MoO_4 \bullet 2 H_2O$ was purchased from Alfa Aesar (Kandel, Germany). Dehydroepiandrosterone (DHEA) was obtained from Steraloids (Newport, RI, United States). 4HP, ATP, and citric acid were purchased from Sigma Aldrich (Steinheim, Germany). 7-Hydroxycoumarin (7HC) and formic acid were purchased from TCI (Zwijndrecht, Belgium). ^{34}S labelled $(NH_4)_2SO_4$ and D_9-Salbutamol (D_9-SA) were purchased from Sigma-Aldrich (Taufkirchen, Germany), D_6-DHEA was obtained from Sigma-Aldrich (Saint Louis, MO, United States). Acetonitrile was from Fischer Scientific (Geel, Belgium), and $HCOONH_4$ was from VWR Chemicals (Damstadt, Germany). Ultrapure water was prepared with a Milli-Q water purification system LaboStar 2-DI/UV from SG Wasseraufbereitung und Regenerierstation GmbH (Barsbüttel, Germany). All other chemicals and reagents used were also of the highest grade available.

Fission Yeast Strains, Media and General Techniques

The recombinant fission yeast strains YN3, YN4, YN20, and YN25 used in this project were described before (Sun et al., 2020). The preparation of media and basic manipulation methods of *S. pombe* were carried out as described (Alfa et al., 1993). Briefly, strains were generally cultivated at 30°C in Edinburgh Minimal Medium (EMM). EMM was prepared with NH_4Cl (93.5 mM), glucose (2% w/v), Na_2HPO_4 (15.5 mM), potassium hydrogen phthalate (14.7 mM) and standard amounts of salt, vitamin and mineral stock solutions. Liquid cultures were kept shaking at 230 rpm.

Biotransformation With Enzyme Bags

This was essentially done as described before (Sun et al., 2020) with slight modifications. Briefly, fission yeast strains were grown in 10 ml liquid culture of EMM at 30°C and 230 rpm for 24 h. Incubation of main cultures in 250 ml Erlenmeyer flasks was performed subsequently. For each assay a certain number of cells were transferred to micro centrifuge tubes or falcons, pelleted and incubated in 0.3% Triton-X100 in Tris-KCl buffer (200 mM KCl, 100 mM Tris-Cl pH 7.8) at 30°C for 60 min at 230 rpm to allow for permeabilization. Cells were then washed thrice with NH_4HCO_3 buffer (50 mM, pH 7.8) and directly used for SULT-dependent reactions. Enzyme bags were resuspended in 200 μL of aqueous NH_4HCO_3 buffer (50 mM, pH 7.8) or phosphate buffer (50 mM, pH 7.8) containing PAPS or ATP, ammonium sulfate, magnesium chloride and substrate as indicated. Biotransformations were carried out at 37°C in a shaking incubator (300 rpm). Enzymatic reactions were stopped by short sharp centrifugation at 14,100 rcf for 2 min and 200 μL of sample in 1.5 ml micro centrifuge tubes were directly frozen at −20°C. After defrosting, samples were centrifuged again (14,100 rcf, 2 min). Supernatants were directly analyzed by ultra-high performance liquid chromatography tandem mass spectrometry (UHPLC-MS/MS) or diluted with a mixture of acetonitrile and ultrapure water

(50/50, v/v) prior to analysis. Negative control samples were incubated without cofactors (ATP, $(NH_4)_2SO_4$, and $MgCl_2$) or without cells, respectively.

Multifactorial Optimization

The optimization process was performed applying quality-by-design (QbD) principles. Design of experiments (DoE) was used for multivariate statistical analysis aiming to ensure robust protocol conditions. It started with a broad systematic screening of the influence of several factors on the incubation of 4HP with YN20 (SULT1A3): ATP concentration (1–50 mM, while $(NH_4)_2SO_4$ concentration was always kept to the half of ATP concentration), incubation time (3–72 h), cell number per incubation, pre-incubation time, and magnesium chloride concentration (1–100 mM) were altered. Results of the pre-screening disclosed some limits and trends of the factors. For further optimization a Box-Behnken design was used to investigate the effect of the five dependent variables in biotransformation and to optimize the experimental conditions to achieve the highest yield. The variables in this design involved ATP concentration (11–20 mM), magnesium chloride concentration (10–100 mM), pre-incubation time (i.e. incubation without substrate for either 0, 3, or 5 h), incubation time (3–24 h), and cell number (either 5×10^7, 1.25×10^8, 2.5×10^8, or 5×10^8 per 200 µl). Considering the outcome and prediction of pre-screening and first round of optimization two further rounds of fine tuning were performed subsequently. The best conditions of round two and three as well as predicted optimal conditions were then compared as proof of concept and re-evaluated focusing on incubation time in particular. Also, both NH_4HCO_3 and phosphate buffer systems were evaluated. Product formation was monitored by UHPLC-MS/MS and results of the same analytes were compared *via* peak area. Statistical data analysis and parts of experimental design were carried out using Minitab (RRID: SCR_014483, Statistical Software, Coventry, United Kingdom) software program.

Biosynthesis of Isotope-Labelled Metabolites and Evaluation of *in situ* PAPS Generation

D_6-DHEA (100 µM) and D_9-SA (100 µM) were used as substrates in enzyme bags experiments. Enzyme bags experiments were also carried out with DHEA (100 µM) and SA (100 µM) utilizing $(NH_4)_2{}^{34}SO_4$ (5.5 mM) and ATP (11 mM) as educts for the cofactor PAPS. Production of labelled sulfoconjugates was monitored by UHPLC-MS/MS.

Degradation Experiments

Degradation of an already sulfonated metabolite in enzyme bags experiment was tested by incubating 7-hydroxycoumarin sulfate (7HCSU) with either YN3 or YN4 for 5 h at 37°C. All experiments were carried out in duplicates.

Optimized Enzyme Bags Biosynthesis

Based on the optimization experiments the final enzyme bag method used 2.5×10^8 precultured and pelleted fission yeast cells that are permeabilized using 200 µL of Triton-X100 [0.3% in

Tris-KCl buffer (200 mM KCl, 100 mM Tris-Cl pH 7.8)] at 30°C for 60 min at 230 rpm. After washing with NH_4HCO_3 buffer (50 mM, pH 7.8, three times) enzyme bags were resuspended in 200 µL of aqueous NH_4HCO_3 buffer (50 mM, pH 7.8) and supplied with ATP at 11 mM, ammonium sulfate at 22 mM, and magnesium chloride at 20 mM. Following substrate addition (final concentration of 100 µM in incubation solution) mixtures are incubated at 37°C at 300 rpm. Sharp centrifugation at 14,100 rcf for 2 min followed by a freeze-thaw cycle at −20°C and a second centrifugation at 14,100 rcf for 2 min yielded the sulfoconjugates in the supernatant.

UHPLC-MS/MS Instrumentation and Analytical Methods

Separation was conducted on a 1290 Infinity UHPLC System (Agilent Technologies, Waldbronn, Germany) with an Agilent InfinityLab Poroshell 120 Phenyl Hexyl (100×2.1 mm, 2.7 µm) column or an Agilent InfinityLab Poroshell 120 C18-EC (2.1×50 mm, 1.9 µm) column. As mass detector an Agilent 6495 Triple Quadrupole MS/MS was utilized. The details of the chromatographic separation conditions, the MS/MS operating parameters and the transitions for all analytes are listed in the supplemental information (**Supplementary Tables S1–S3**). Presented peak areas were provided by transitions of highest intensity (quantifier).
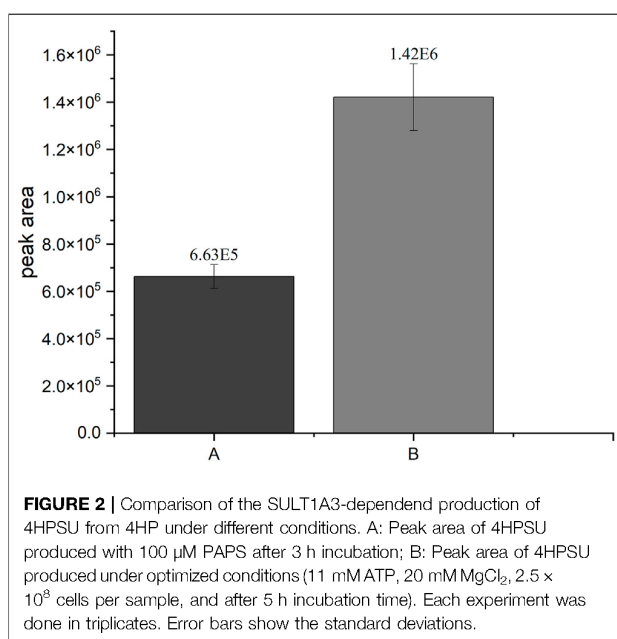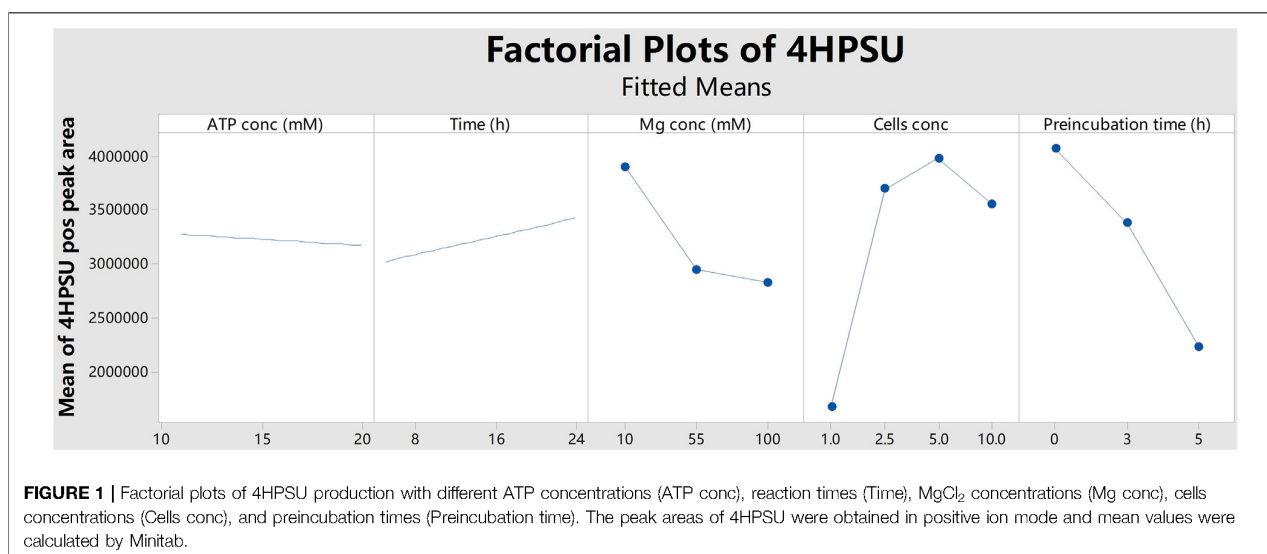
Statistical Analysis

All data are presented as mean ± SD. Statistical analysis was done using Origin 2021 (Originlab Corporation, Northampton, MA. United States).

RESULTS

Optimization of Reaction Conditions for Sulfoconjugate Production With Enzyme Bags

Initially, a sulfonation assay of 4HP (for reaction schemes see **Supplementary Figure S1**) by SULT1A3 (strain YN20) with external PAPS (100 µM) was carried out as described (Sun et al., 2020). For substitution of the cofactor PAPS by ATP and SO_4^{2-} and optimization of the product yields multifactorial screening supported by Minitab software was started with five factors: ATP concentration, $MgCl_2$ concentration, number of cells, reaction incubation time, and time of preincubation without substrate. Initial results indicated that a reduction of yield was correlated with longer preincubation time (**Figure 1**). Therefore, later rounds were performed without any preincubation. Two optimization rounds were conducted within a more targeted range of each factor using Box-Behnken design. More specifically, ATP concentrations of 11 mM or 15 mM, cell numbers of 1.25×10^8, 2.5×10^8, or 5×10^8 per assay, $MgCl_2$ concentrations of 10 mM, 20 mM or 30 mM, and incubation times from 5 to 72 h were tested. The optimal conditions obtained were 11 mM ATP, 2.5×10^8 cells per sample, 20 mM $MgCl_2$, and 5 h incubation time. The experiments under the optimal conditions gave over two times
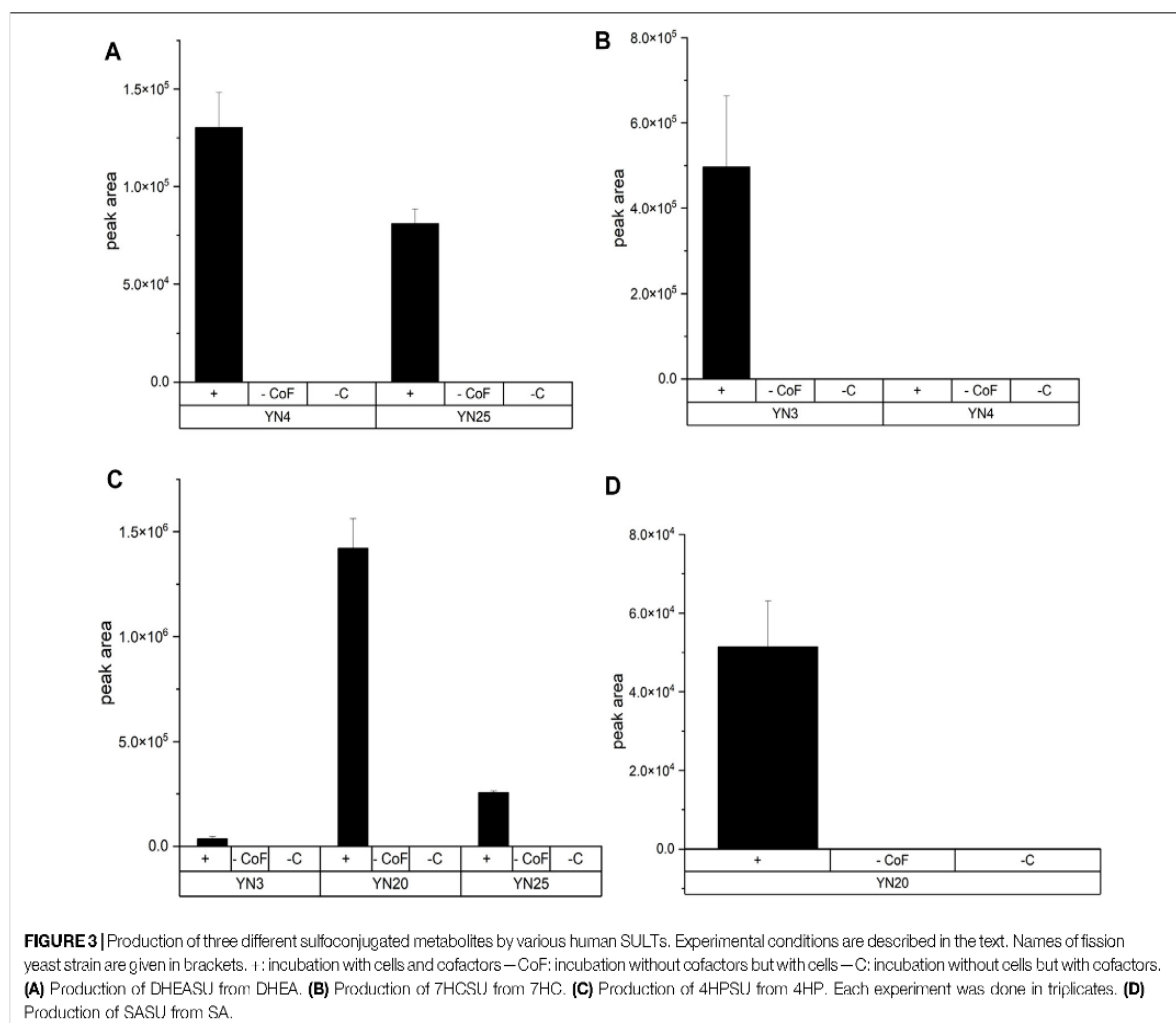
FIGURE 1 | Factorial plots of 4HPSU production with different ATP concentrations (ATP conc), reaction times (Time), $MgCl_2$ concentrations (Mg conc), cells concentrations (Cells conc), and preincubation times (Preincubation time). The peak areas of 4HPSU were obtained in positive ion mode and mean values were calculated by Minitab.

FIGURE 2 | Comparison of the SULT1A3-dependend production of 4HPSU from 4HP under different conditions. A: Peak area of 4HPSU produced with 100 µM PAPS after 3 h incubation; B: Peak area of 4HPSU produced under optimized conditions (11 mM ATP, 20 mM $MgCl_2$, 2.5 × 10^8 cells per sample, and after 5 h incubation time). Each experiment was done in triplicates. Error bars show the standard deviations.

higher peak areas of 4-hydroxypropranolol-4-O-sulfate (4HPSU) in comparison to the initial reaction with external PAPS (**Figure 2**). Thus, a standard protocol was established which allows substrate sulfonation with human SULTs recombinantly expressed in fission yeast using ATP and $(NH4)_2SO_4$ instead of PAPS.

Evaluation of Optimal Conditions for Additional Substrates and Enzyme Isoforms

As proof of concept the above-mentioned standard protocol developed with the SULT1A3 (YN20) and 4HP was then applied to 7HC, DHEA, salbutamol (SA) and 4HP using various SULTs (**Figure 3**). Experimental conditions were as follows: 11 mM ATP, 5.5 mM $(NH_4)_2SO_4$, 100 µM substrate, 20 mM $MgCl_2$, and 2.5 × 10^8 cells per sample in NH_4HCO_3 buffer (pH 7.8). Substrates were incubated with SULTs reported in literature to metabolize the respective substrates (Miyano et al., 2005; Gamage et al., 2006; Ko et al., 2012; Nishikawa et al., 2018). DHEA was transformed to dehydroepiandrosterone sulfate (DHEASU) by SULT1E1 (YN25) and SULT2A1 (YN4). The strain with the latter enzyme provided a higher space-time yield. In case of the substrates SA, 7HC, and 4HP with various enzyme isoforms phenolic sulfonated metabolites were found in all experiments except in incubations of 7HC with SULT2A1 (YN4). The generation of 4HPSU was catalysed by SULT1B1 (YN3), SULT1E1 (YN25), and SULT1A3 (YN20). In same order yields were ascending. SA sulfonation to salbutamol sulfate (SASU) was successfully performed by SULT1A3 (YN20). 7HCSU was generated by SULT1B1 (YN3). Blank incubations served as negative controls. All blank incubations either without cofactors (-CoF) or without cells (-C) did not result in any detection of sulfonated metabolites.

In the past, recombinant fission yeast strains that express human UDP glucuronosyltransferases were successfully used for the production of stable isotope-labelled glucuronides (Dragan et al., 2010; Buchheit et al., 2011). In order to demonstrate the usefulness of our new protocol for the production of stable isotope-labelled sulfometabolites, biotransformations with D_6-DHEA, D_9-salbutamol (D_9-SA), and $(NH_4)_2^{34}SO_4$ were conducted in the present study (**Figure 4** and **Figure 5**). Non-labelled DHEA or D_6-DHEA were subjected to SULT2A1-dependend enzyme bag biotransformations either with $(NH_4)_2SO_4$ or $(NH_4)_2^{34}SO_4$. Results of UHPLC-MS/MS analysis proved same retention time of DHEASU, D_6-DHEASU, and DHEA-^{34}S-SU (**Figures 4A,C,E**) the respective pattern of mass transitions (**Figures 4B,D,F**) showed the successful production of non-labelled and isotope-labelled
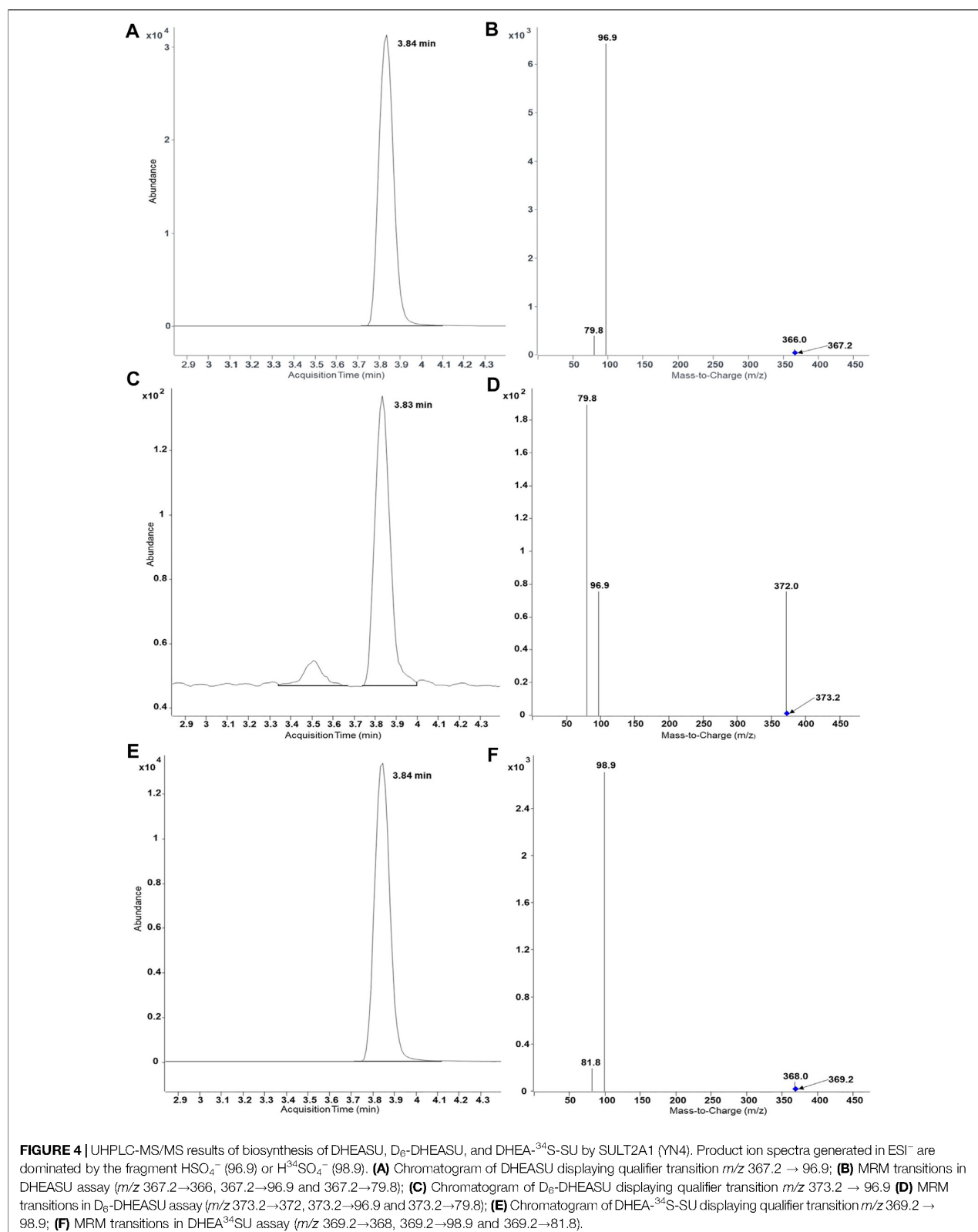
FIGURE 3 | Production of three different sulfoconjugated metabolites by various human SULTs. Experimental conditions are described in the text. Names of fission yeast strain are given in brackets. +: incubation with cells and cofactors −CoF: incubation without cofactors but with cells −C: incubation without cells but with cofactors. **(A)** Production of DHEASU from DHEA. **(B)** Production of 7HCSU from 7HC. **(C)** Production of 4HPSU from 4HP. Each experiment was done in triplicates. **(D)** Production of SASU from SA.

sulfometabolites. The same strategy was performed using non-labelled SA and D$_9$-SA with SULT1A3 (YN20) as well (**Figure 5**).

Further Optimization of Buffer, (NH$_4$)$_2$SO$_4$ and Substrate Concentrations

Unexpectedly, the sulfonation of 7HC by SULT2A1 (YN4) could not be shown using above mentioned conditions, even though the enzyme is known to metabolize this substrate (Nishikawa et al., 2018; Sun et al., 2020). It was suspected that product lability might be a reason. In order to confirm this suspicion, degradation assays were performed. Indeed, the incubation of 7HCSU with enzyme bags generated using YN3 at pH 7.8 led to more than 99% loss of the compound within 5 hours. By contrast, degradation tests in buffer without cells proved good stability of 7HCSU (**Supplementary Figure S2**). Apparently, there are endogenous fission yeast enzymes which can catalyze a cleavage of this sulfated metabolite.
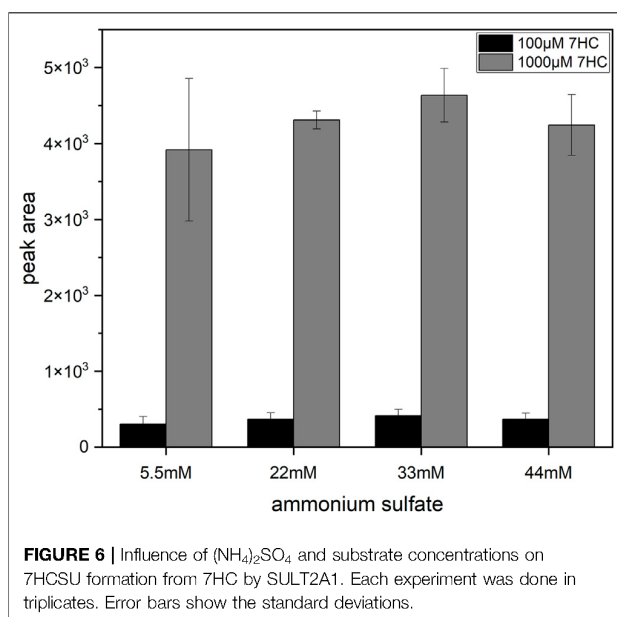
Further investigations of the degradation of 7HCSU were performed by incubating permeabilized YN3 cells either in NH$_4$HCO$_3$ buffer (at pH 7.8 or 7.4) or in phosphate buffer (at pH 7.8, 7.4, or 6.5). The results showed that in pH 7.8 phosphate buffer 7HCSU displays the smallest amount of degradation (**Supplementary Figure S3**). With the intention of avoiding total degradation of 7HCSU and increasing sulfonation yield of 7HC by SULT2A1 (YN4), and also with the purpose for exploring the possibility of further optimization of the general protocol, enzyme bag assays were subsequently conducted at higher substrate concentrations (7HC at 100 µM or 1 mM), higher (NH$_4$)$_2$SO$_4$ concentrations (5.5, 22, 33, or 44 mM), and also in phosphate buffer (pH 7.8). The results demonstrated that the peak area of 7HCSU reached the highest levels at 1 mM substrate concentration, while the influence of the (NH$_4$)$_2$SO$_4$ concentration on the yield was minor (**Figure 6**). The same optimization with higher substrate and ammonium sulfate concentrations was performed for the biotransformation of 4HP with SULT1A3 (YN20) as well. In this case, no particularly obvious differences were found among the different conditions (**Supplementary Figure S4**).

FIGURE 4 | UHPLC-MS/MS results of biosynthesis of DHEASU, D_6-DHEASU, and DHEA-^{34}S-SU by SULT2A1 (YN4). Product ion spectra generated in ESI$^-$ are dominated by the fragment HSO$_4^-$ (96.9) or H^{34}SO$_4^-$ (98.9). **(A)** Chromatogram of DHEASU displaying qualifier transition m/z 367.2 → 96.9; **(B)** MRM transitions in DHEASU assay (m/z 367.2→366, 367.2→96.9 and 367.2→79.8); **(C)** Chromatogram of D_6-DHEASU displaying qualifier transition m/z 373.2 → 96.9 **(D)** MRM transitions in D_6-DHEASU assay (m/z 373.2→372, 373.2→96.9 and 373.2→79.8); **(E)** Chromatogram of DHEA-^{34}S-SU displaying qualifier transition m/z 369.2 → 98.9; **(F)** MRM transitions in DHEA^{34}SU assay (m/z 369.2→368, 369.2→98.9 and 369.2→81.8).

FIGURE 5 | UHPLC-MS/MS results of biosynthesis of SASU, D_9-SASU, and SA-^{34}S-SU by SULT1A3 (YN20). Product ion spectra generated in ESI$^-$ are dominated by the fragment HSO_4^- (96.9) or $H^{34}SO_4^-$ (98.9). **(A)** Chromatogram of SASU shows ion transition m/z 318.0 → 97; **(B)** MRM transitions in SASU assay (m/z 318.0 →97.0 and 318.0 →80.0); **(C)** Chromatogram of D_9-SASU shows m/z 327.0 → 97.0; **(D)** MRM transitions in D_9-SASU assay (m/z 327.0 →97.0 and 327.0 →79.8); **(E)** Chromatogram of SA-^{34}S-SU shows m/z 320.0 → 99.0; **(F)** MRM transitions in SASU assay (m/z 320.0→99.0 and 320.0→82.0).

FIGURE 6 | Influence of $(NH_4)_2SO_4$ and substrate concentrations on 7HCSU formation from 7HC by SULT2A1. Each experiment was done in triplicates. Error bars show the standard deviations.

Final Protocol

The final protocol (**Figure 7**) for this sulfonation assay uses 20 mM Mg^{2+}, 11 mM ATP, 5.5 mM SO_4^{2-}, and 2.5×10^8 cells per incubation in ammonium bicarbonate buffer at pH 7.8 for 5 h at 37°C. In the case of 4HP, the most efficient substrate concentration was 100 µm. Sulfonation of compounds with a low affinity to a SULT can be achieved by enhancing substrate concentration to 1 mM.

DISCUSSION

In this study, the successful replacement of the SULT cofactor PAPS by ATP and $(NH_4)_2SO_4$ in a recombinant sulfoconjugate biosynthesis system is reported. While production and regeneration of PAPS were previously described in a chemoenzymatic approach (An et al., 2017), in an enzymatic approach (Burkart et al., 2000), and in liver S9 fraction-based biosynthesis (Weththasinghe et al., 2018), this assay successfully combines both, PAPS (re-)generation and sulfonation of xenobiotics. Multifactorial optimization was performed applying DoE principles using the model substrate 4HP and human SULT1A3, which is expressed by recombinant fission yeast strain YN20 (**Figure 1**). Compared with the biosynthesis where PAPS was used as cofactor, the optimized method with ATP and $(NH_4)_2SO_4$ resulted in a more than doubled yield of product (**Figure 2**). At the same time, the cost per experiment was reduced by a factor of 60. Further optimization was performed using 4HP with SULT1A3 and 7HC with SULT2A1. Permeabilized fission yeast (enzyme bags) assays with PAPS regeneration combine the advantage of high sensitivity and low cost. Small molecules like substrates, cofactors, and products can move in and out of the cells freely. Meanwhile, the enzymes needed for sulfonation remain trapped within the enzyme bags and can therefore be employed to catalyze the reactions of interest.

The concentration of magnesium ions was observed to be one of the most crucial parameters in the optimization process. Magnesium is an essential electrolyte in the human body. As a cofactor, magnesium participates in more than 300 enzyme systems that modulate multiple biochemical reactions in the body (Gröber

FIGURE 7 | Optimized method for sulfotansferase catalyzed metabolite generation including PAPS replacement protocol.
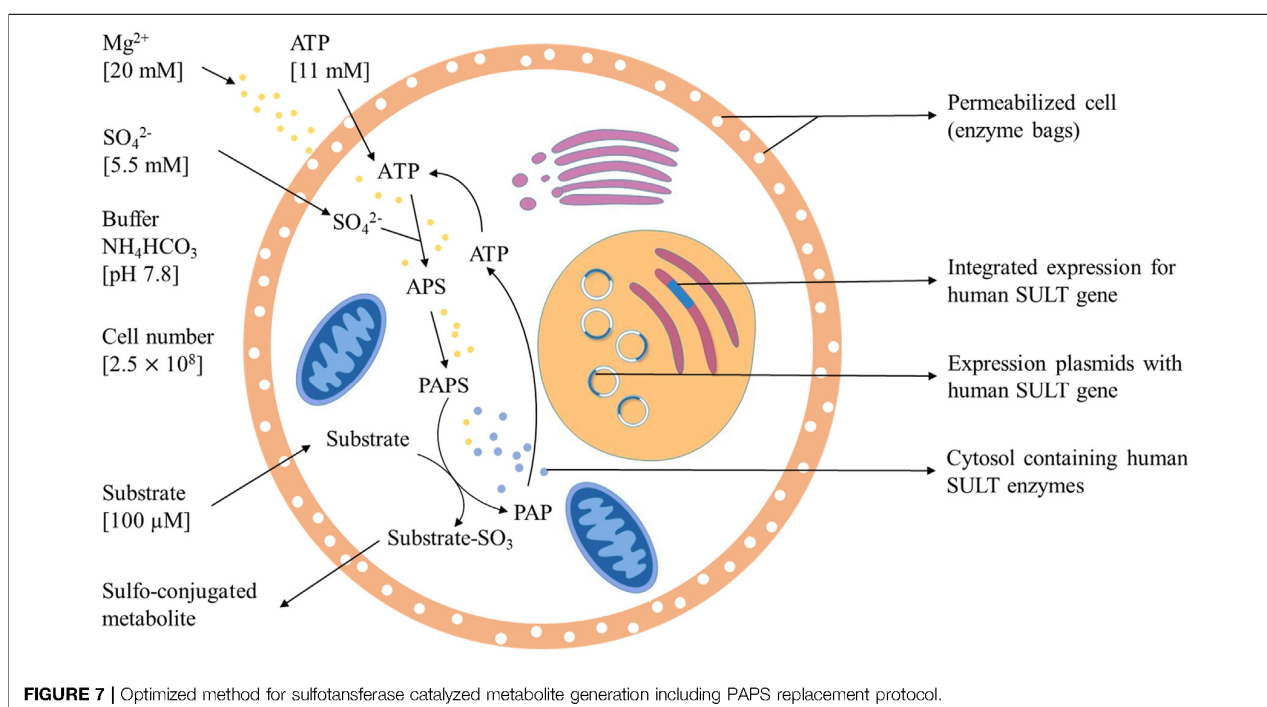
et al., 2015a). In biological systems that generate PAPS or sulfonated metabolites, magnesium functions as an assistant inorganic ion (Burkart et al., 2000; Weththasinghe et al., 2018). In this study, the concentration of $MgCl_2$ was tested in a range from 1 to 100 mM. Ultimately, 20 mM was found to be the optimal concentration. The results demonstrated that within certain limits, the $MgCl_2$ concentration had an evident impact on the yield of 4HPSU. Although the mechanism of magnesium in biological sulfonation is not yet completely understood, magnesium is reported to be essential for the pathway of PAPS synthesis in *S. cerevisiae* (Thomas and Surdin-Kerjan, 1997). It is reasonable to assume that magnesium either functions as an enzyme activator or is involved in ATP production within the sulfonation system (Swaminathan, 2003; Gröber et al., 2015b).

By screening several ATP concentrations, it was observed that higher ATP concentrations (≥ 50 mM) led to a significant decline of yield in sulfonated product formation. As a structural analogue of PAPS, ATP has been reported to competitively inhibit the sulfonation of human M and P phenol sulfotransferase (SULT1A3, SULT1A1) (Rens-Domiano and Roth, 1987; Dooley et al., 1994). This property might be responsible for the effects observed in here as well.

Afterwards, the standard protocol was applied to additional substrates and SULTs (**Figure 3**). Furthermore, production of stable isotope-labelled sulfometabolites, with D_6-DHEA, D_9-salbutamol (SA), and $(NH_4)_2^{34}SO_4$ were achieved applying the established protocol as well (**Figures 4, 5**). The competence of SULT2A1 to sulfonate 7HC was reported by Nishikawa (Nishikawa et al., 2018) and Sun (Sun et al., 2020). However, using our PAPS replacing protocol, the enzymatic activity of SULT2A1 towards 7HC could not be demonstrated under initial standard protocol conditions. A possible reason is a rapid degradation of the product 7HCSU, presumably by cleavage of the sulfate group. Therefore, the degradation of 7HCSU was subsequently investigated in reaction mixtures with and without cells (**Supplementary Figure S1**). Degradation was only found in assays with cells, which indicated that the degradation of 7HCSU is a result of enzymatical catalysis rather than of chemical instability. Less degradation was observed when phosphate buffer (pH 7.8) was used instead of hydrogen carbonate buffer, which is in line with earlier reports of sulfatase inhibition by phosphate (Lee and Van Etten, 1975; Bostick et al., 1978; Metcalfe et al., 1979). Furthermore, using phosphate buffer higher product yields were obtained with both SULT2A1 and SULT1B1. Therefore, for 7HC sulfonation experiments with enzyme bags, the usage of phosphate buffer (pH 7.8) is superior to that of NH_4HCO_3 buffer (pH 7.8).

In a previous study by Burkart et al. (2000) the generation of PAPS from ATP and inorganic sulfate was also achieved using genetically modified *E. coli*. Highest yields were obtained when the sulfate concentration dramatically exceeded that of ATP. Consequently, we increased the $(NH_4)_2SO_4$ concentration to 44 mM. However, the yield of 4HPSU did not show a significant rise with increasing $(NH_4)_2SO_4$ concentrations. This might indicate that the concentration of PAPS is not the main limiting factor of 4HPSU yield in this case.

Being a known hydroxysteroid converting SULT, SULT2A1 shows low affinity to phenolic compounds like 7HC (Tibbs et al.,

2015), which might explain the lack of sulfoconjugated metabolite in initial experiments. Therefore, the concentration of 7HC was increased to 1 mM to facilitate the enzymatic reaction. A remarkable increase of 7HCSU production (**Figure 6**) was observed. In this manner, the standard protocol was modified for biotransformation of low affinity substrates in enzyme bags.

The developed assay allows to determine whether a substrate is sulfonated by any one of the 14 human SULTs and also permits a comparison of their sulfonation activity. Due to the fact that the biosynthesized sulfoconjugates are not available as references, a quantitation of the results by UHPLC-MS/MS is not possible. Therefore, metabolite formation rates cannot be given in absolute values in this study.

The successful development of an optimized PAPS replacement protocol (details in **Figure 7**) provides an economic and efficient way for further research of SULT-depended phase II metabolism pathways of drugs. Bigger scale screening experiments will be performed to demonstrate broad applicability and to further evaluate the possibilities of this great sulfonation technique. The biotechnological generation of sulfonated compounds and metabolites may be achieved on reasonable costs applying this assay.

DATA AVAILABILITY STATEMENT

The original contributions presented in the study are included in the article/**Supplementary Material**, further inquiries can be directed to the corresponding authors.

AUTHOR CONTRIBUTIONS

Conceptualization, MP and MB; methodology, YS, LH, MB and MP; software, YS and LH; investigation, YS and LH, resources, MP, and MB; data curation, MP and MB; writing—original draft preparation, YS and LH; writing—review and editing, MP, and MB; visualization, YS and LH; supervision, MP, and MB; project administration, MP and MB; funding acquisition, MP and MB. All authors have read and agreed to the published version of the manuscript.

FUNDING

SUPPLEMENTARY MATERIAL

The Supplementary Material for this article can be found online at: https://www.frontiersin.org/articles/10.3389/fmolb.2022.827638/full#supplementary-material

REFERENCES

Alfa, C., Fantes, P., Hyams, J., McLeod, M., and Warbrick, E. (1993). *Experiments with Fission yeastA Laboratory Course Manual.* NY: Cold Spring Harbor Press, Cold Spring Harbor.

An, C., Zhao, L., Wei, Z., and Zhou, X. (2017). Chemoenzymatic Synthesis of 3'-Phosphoadenosine-5'-Phosphosulfate Coupling with an ATP Regeneration System. *Appl. Microbiol. Biotechnol.* 101, 7535–7544. doi:10.1007/s00253-017-8511-2

Balcells, G., Gómez, C., Garrostas, L., Pozo, Ó. J., and Ventura, R. (2017). Sulfate Metabolites as Alternative Markers for the Detection of 4-chlorometandienone Misuse in Doping Control. *Drug Test. Anal.* 9, 983–993. doi:10.1002/dta.2101

Besset, S., Vincourt, J.-B., Amalric, F., and Girard, J.-P. (2000). Nuclear Localization of PAPS Synthetase 1: a Sulfate Activation Pathway in the Nucleus of Eukaryotic Cells. *FASEB j.* 14, 345–354. doi:10.1096/fasebj.14.2.345

Bostick, W. D., Dinsmore, S. R., Mrochek, J. E., and Waalkes, T. P. (1978). Separation and Analysis of Arylsulfatase Isoenzymes in Body Fluids of Man. *Clin. Chem.* 24, 1305–1316. doi:10.1093/clinchem/24.8.1305

Buchheit, D., Drăgan, C.-A., Schmitt, E. I., and Bureik, M. (2011). Production of Ibuprofen Acyl Glucosides by Human UGT2B7. *Drug Metab. Dispos* 39, 2174–2181. doi:10.1124/dmd.111.041640

Burkart, M. D., Izumi, M., Chapman, E., Lin, C.-H., and Wong, C.-H. (2000). Regeneration of PAPS for the Enzymatic Synthesis of Sulfated Oligosaccharides. *J. Org. Chem.* 65, 5565–5574. doi:10.1021/jo0002660

Cherest, H., Nguyen, N. T., and Surdin-Kerjan, Y. (1985). Transcriptional Regulation of the MET3 Gene of *Saccharomyces cerevisiae. Gene* 34, 269–281. doi:10.1016/0378-1119(85)90136-2

Cherest, H., Kerjan, P., and Surdin-Kerjan, Y. (1987). The *Saccharomyces cerevisiae* MET3 Gene: Nucleotide Sequence and Relationship of the 5' Non-coding Region to that of MET25. *Mol. Gen Genet* 210, 307–313. doi:10.1007/bf00325699

Dooley, T. P., Mitchison, H. M., Munroe, P. B., Probst, P., Neal, M., Siciliano, M. J., et al. (1994). Mapping of Two Phenol Sulfotransferase Genes, STP and STM, to 16p: Candidate Genes for Batten Disease. *Biochem. Biophysical Res. Commun.* 205, 482–489. doi:10.1006/bbrc.1994.2691

Dragan, C. A., Buchheit, D., Bischoff, D., Ebner, T., and Bureik, M. (2010). Glucuronide Production by Whole-Cell Biotransformation Using Genetically Engineered Fission Yeast *Schizosaccharomyces pombe. Drug Metab. Dispos* 38, 509–515. doi:10.1124/dmd.109.030965

Ekins, S., Ring, B. J., Grace, J., McRobie-Belle, D. J., and Wrighton, S. A. (2000). Present and Future *In Vitro* Approaches for Drug Metabolism. *J. Pharmacol. Toxicol. Methods* 44, 313–324. doi:10.1016/s1056-8719(00)00110-6

Esquivel, A., Alechaga, É., Monfort, N., Yang, S., Xing, Y., Moutian, W., et al. (2019). Evaluation of Sulfate Metabolites as Markers of Intramuscular Testosterone Administration in Caucasian and Asian Populations. *Drug Test. Anal.* 11, 1218–1230. doi:10.1002/dta.2598

Gamage, N., Barnett, A., Hempel, N., Duggleby, R. G., Windmill, K. F., Martin, J. L., et al. (2006). Human Sulfotransferases and Their Role in Chemical Metabolism. *Toxicol. Sci.* 90, 5–22. doi:10.1093/toxsci/kfj061

Gröber, U., Schmidt, J., and Kisters, K. (2015). Magnesium in Prevention and Therapy. *Nutrients* 7, 8199–8226. doi:10.3390/nu7095388

Gröber, U., Schmidt, J., and Kisters, K. (2015). Magnesium in Prevention and Therapy. *Nutrients* 7, 8199–8226. doi:10.3390/nu7095388

Ko, K., Kurogi, K., Davidson, G., Liu, M.-Y., Sakakibara, Y., Suiko, M., et al. (2012). Sulfation of Ractopamine and Salbutamol by the Human Cytosolic Sulfotransferases. *J. Biochem.* 152, 275–283. doi:10.1093/jb/mvs073

Lee, G. D., and Van Etten, R. L. (1975). Purification and Properties of a Homogeneous Aryl Sulfatase A from Rabbit Liver. *Arch. Biochem. Biophys.* 166, 280–294. doi:10.1016/0003-9861(75)90389-6

Lock, A., Rutherford, K., Harris, M. A., Hayles, J., Oliver, S. G., Bähler, J., et al. (2019). PomBase 2018: User-Driven Reimplementation of the Fission Yeast Database Provides Rapid and Intuitive Access to Diverse, Interconnected Information. *Nucleic Acids Res.* 47, D821–D827. doi:10.1093/nar/gky961

Masselot, M., and Surdin-Kerjan, Y. (1977). Methionine Biosynthesis in *Saccharomyces cerevisiae. Mol. Gen. Genet.* 154, 23–30. doi:10.1007/bf00265572

Metcalfe, D. D., Corash, L. M., and Kaliner, M. (1979). Human Platelet Arylsulphatases: Identification and Capacity to Destroy SRS-A. *Immunology* 37, 723–729.

Miyano, J., Yamamoto, S., Hanioka, N., Narimatsu, S., Ishikawa, T., Ogura, K., et al. (2005). Involvement of SULT1A3 in Elevated Sulfation of 4-hydroxypropranolol in Hep G2 Cells Pretreated with β-naphthoflavone. *Biochem. Pharmacol.* 69, 941–950. doi:10.1016/j.bcp.2004.12.012

Mountain, H. A., and Korch, C. (1991). TDH2 Is Linked toMET3 on Chromosome X ofSaccharomyces Cerevisiae. *Yeast* 7, 873–880. doi:10.1002/yea.320070814

Nishikawa, M., Masuyama, Y., Nunome, M., Yasuda, K., Sakaki, T., and Ikushiro, S. (2018). Whole-cell-dependent Biosynthesis of Sulfo-Conjugate Using Human Sulfotransferase Expressing Budding Yeast. *Appl. Microbiol. Biotechnol.* 102, 723–732. doi:10.1007/s00253-017-8621-x

Rens-Domiano, S. S., and Roth, J. A. (1987). Inhibition of M and P Phenol Sulfotransferase by Analogues of 3'-Phosphoadenosine-5'-Phosphosulfate. *J. Neurochem.* 48, 1411–1415. doi:10.1111/j.1471-4159.1987.tb05679.x

Robbins, P. W., and Lipmann, F. (1958). Enzymatic Synthesis of Adenosine-5'-Phosphosulfate. *J. Biol. Chem.* 233, 686–690. doi:10.1016/s0021-9258(18) 64728-3

Song, J.-Y., and Roe, J.-H. (2008). The Role and Regulation of Trxl, a Cytosolic Thioredoxin in *Schizosaccharomyces pombe. J. Microbiol.* 46, 408–414. doi:10.1007/s12275-008-0076-4

Sun, Y., Machalz, D., Wolber, G., Parr, M. K., and Bureik, M. (2020). Functional Expression of All Human Sulfotransferases in Fission Yeast, Assay Development, and Structural Models for Isoforms SULT4A1 and SULT6B1. *Biomolecules* 10, 1517. doi:10.3390/biom10111517

Swaminathan, R. (2003). Magnesium Metabolism and its Disorders. *Clin. Biochem. Rev.* 24, 47–66.

Taskinen, J., Ethell, B. T., Pihlavisto, P., Hood, A. M., Burchell, B., and Coughtrie, M. W. H. (2003). Conjugation of Catechols by Recombinant Human Sulfotransferases, UDP-Glucuronosyltransferases, and Soluble Catechol O-Methyltransferase: Structure-Conjugation Relationships and Predictive Models. *Drug Metab. Dispos* 31, 1187–1197. doi:10.1124/dmd.31.9.1187

Thomas, D., and Surdin-Kerjan, Y. (1997). Metabolism of Sulfur Amino Acids in *Saccharomyces cerevisiae. Microbiol. Mol. Biol. Rev.* 61, 503–532. doi:10.1128/mmbr.61.4.503-532.1997

Tibbs, Z. E., Rohn-Glowacki, K. J., Crittenden, F., Guidry, A. L., and Falany, C. N. (2015). Structural Plasticity in the Human Cytosolic Sulfotransferase Dimer and its Role in Substrate Selectivity and Catalysis. *Drug Metab. Pharmacokinet.* 30, 3–20. doi:10.1016/j.dmpk.2014.10.004

Weththasinghe, S. A., Waller, C. C., Fam, H. L., Stevenson, B. J., Cawley, A. T., and McLeod, M. D. (2018). Replacing PAPS:In Vitrophase II Sulfation of Steroids with the Liver S9 Fraction Employing ATP and Sodium Sulfate. *Drug Test. Anal.* 10, 330–339. doi:10.1002/dta.2224

3.4 Manuscript Ⅳ: "Biosynthesis of Salbutamol-4'-O-sulfate as Reference for Identification of Intake Routes and Enantiopure Salbutamol Administration by Achiral UHPLC-MS/MS"

Annika Lisa Jendretzki, Lukas Corbinian Harps, Yanan Sun, Felix Bredendiek, Matthias Bureik, Ulrich Girreser, Xavier de la Torre, Francesco M. Botrè, and Maria Kristina Parr

Abstract: The aim of the study was a comprehensive and quantitative determination of salbutamol and its sulfo-conjugated major metabolite in urine samples using achiral ultrahigh performance liquid chromatography-tandem mass spectrometry (UHPLC-MS/MS). Therefore, salbut-amol-4'-O-sulfate was biosynthesized as reference using genetically modified fission yeast cells and the product was subsequently characterized by NMR and HRMS. In competitive sports sal-butamol is classified as prohibited drug, however inhalation at therapeutic doses is permitted with a maximum allowance of 600 µg/8h. In contrast the enantiopure levosalbutamol is prohibited at any condition. For analytical discrimination the amount of salbutamol and its main metabolite excreted in the urine was studied. As proof of concept a longitudinal study in one healthy volunteer was performed in order to investigate excreted amounts and to study potential discrimination using achiral chromatography. Discrimination of administration of racemic salbutamol or the enantiopure levosalbutamol was not achieved by solely analyzing salbutamol as parent compound. However, a distinction was possible by evaluation of the proportion of salbutamol-4'-O-sulfate in relation to salbutamol. Therefore, reference material of metabolites is of great importance in doping control, especially for threshold substances.

separations

MDPI

Article

Biosynthesis of Salbutamol-4′-*O*-sulfate as Reference for Identification of Intake Routes and Enantiopure Salbutamol Administration by Achiral UHPLC-MS/MS

Annika Lisa Jendretzki [1,†], Lukas Corbinian Harps [1,†], Yanan Sun [1], Felix Bredendiek [1,2], Matthias Bureik [3], Ulrich Girreser [4], Xavier de la Torre [5], Francesco M. Botrè [5,6] and Maria Kristina Parr [1,*]

[1] Institute of Pharmacy, Freie Universität Berlin, Königin-Luise-Straße 2+4, 14195 Berlin, Germany; annika.jendretzki@fu-berlin.de (A.L.J.); lukas.harps@fu-berlin.de (L.C.H.); suny72@zedat.fu-berlin.de (Y.S.); f.bredendiek@fu-berlin.de (F.B.)

[2] Core Facility BioSupraMol, Department of Biology, Chemistry, Pharmacy, Freie Universität Berlin, 14195 Berlin, Germany

[3] School of Pharmaceutical Science and Technology, Tianjin University, 92 Weijin Road, Nankai District, Tianjin 300072, China; matthias@tju.edu.cn

[4] Institute of Pharmacy, Christian-Albrechts University Kiel, Gutenbergstr. 76, 24118 Kiel, Germany; girreser@pharmazie.uni-kiel.de

[5] Laboratorio Antidoping FMSI, Largo Onesti 1, 00197 Rome, Italy; x.delatorre@labantidoping.it (X.d.l.T.); f.botre@labantidoping.it (F.M.B.)

[6] REDs—Research and Expertise on Antidoping Sciences, ISSUL—Institute de Sciences du Sport, Université de Lausanne, Synathlon 3224—Quartier Centre, 1015 Lausanne, Switzerland

[*] Correspondence: maria.parr@fu-berlin.de; Tel.: +49-30-838-57686

[†] These authors contributed equally to this work.

Abstract: The aim of the study was a comprehensive and quantitative determination of salbutamol and its sulfoconjugated major metabolite in urine samples using achiral ultrahigh performance liquid chromatography-tandem mass spectrometry (UHPLC-MS/MS). Therefore, salbutamol-4′-*O*-sulfate was biosynthesized as a reference using genetically modified fission yeast cells, and the product was subsequently characterized by NMR and HRMS. In competitive sports, salbutamol is classified as a prohibited drug; however, inhalation at therapeutic doses is permitted with a maximum allowance of 600 µg/8 h. In contrast, the enantiopure levosalbutamol is prohibited under any condition. For analytical discrimination, the amount of salbutamol and its main metabolite excreted in the urine was studied. As proof of concept, a longitudinal study in one healthy volunteer was performed in order to investigate excreted amounts and to study potential discrimination using achiral chromatography. Discrimination of administration of racemic salbutamol or the enantiopure levosalbutamol was not achieved by solely analyzing salbutamol as the parent compound. However, a distinction was possible by evaluation of the proportion of salbutamol-4′-*O*-sulfate in relation to salbutamol. Therefore, reference material of metabolites is of great importance in doping control, especially for threshold substances.

Keywords: reference synthesis; salbutamol-4′-*O*-sulfate; doping control analysis; bioanalysis; biosynthesis; metabolite identification; green synthesis; qNMR; achiral ultrahigh performance liquid chromatography tandem mass spectrometry

1. Introduction

Salbutamol (albuterol) is a widely known β_2-sympathomimetic drug commonly prescribed for the treatment of asthmatic patients. It is available as a racemic preparation and was recently also approved as the pure enantiomer levosalbutamol ((*R*)-salbutamol), which is the pharmacologically active enantiomer (chemical structures in Figure 1). However, a clinically relevant advantage of levosalbutamol as opposed to racemic formulations has not been shown [1].
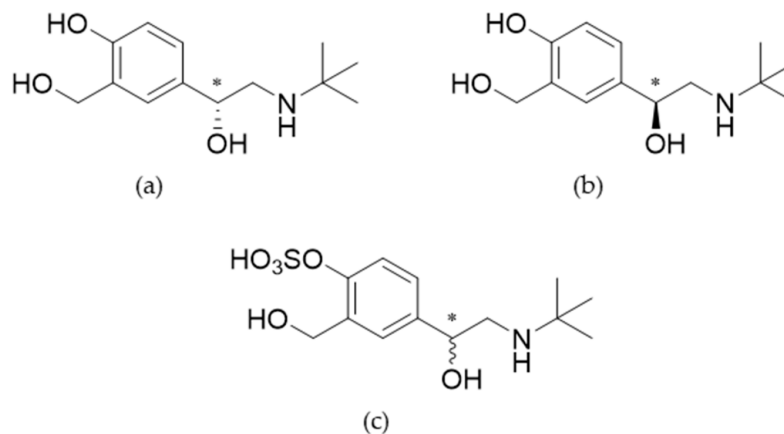
Figure 1. Chemical structures of (*R*)-salbutamol (**a**), (*S*)-salbutamol (**b**), racemic salbutamol-4′-*O*-sulfate (**c**), stereocenter (*).

In sports, salbutamol is prohibited as per the Prohibited List by the World Anti-Doping Agency (WADA) in and out of competition. To allow for therapeutical use, the inhalation administration of doses not exceeding 600 μg per 8 h (1600 μg per 24 h) is considered non-prohibited [2]. Concomitantly, a urinary concentration of 1000 ng/mL for urinary excreted salbutamol as a free substance or glucuronide conjugate is set as the threshold for doping control samples [3]. In contrast, any administration of enantiopure levosalbutamol is prohibited. To identify and quantify substances or their metabolites by means of mass spectrometric analysis, appropriate reference standards are of great importance for reliable and accurate results [4,5].

Biological synthesis utilizing recombinant human enzymes was successfully performed and described for several host organisms [6]. Furthermore, the suitability of genetically modified *Schizosaccharomyces pombe* (*S. pombe*) for preparative scale metabolite synthesis was demonstrated in whole-cell biotransformation experiments [7]. The benefits of using biocatalysts in human metabolite synthesis starting from the parent drug are selectivity of the reaction site, generating further knowledge by screening for suitable enzymes, and building a fundament for greener synthesis approaches. Since most enzymatic processes take place in aqueous solution, the use of hazardous organic solvents is reduced.

The main metabolic pathway of salbutamol is sulfonation by sulfotransferases (SULTs), more precisely by the phenol–sulfotransferase SULT1A3, while SULT1A1, SULT1B1, and SULT1C4 do not show activity towards this compound [1,8–10]. Sulfotransferases catalyze the transfer of a sulfonate group from the cofactor 3′-phosphoadenosine-5′phosphosulfate (PAPS) to the substrate, generally leading to inactive metabolites [8]. These enzymes are found in the liver, small intestine, kidneys, and lungs. Most abundant in the small intestine are SULT1B1 and SULT1A3, whereas in the liver, SULT1A1 is the major enzyme isoform, and only a minor amount of SULT1A3 is present. Lungs and kidneys contain only low levels of SULTs [8,11–13]. The biotransformation of salbutamol by SULT1A3 is a stereoselective process. (*R*)-salbutamol is favored by the enzyme and metabolized up to twelve times faster than the (*S*)-enantiomer [1,14]. Additionally, it has been reported, that (*S*)-salbutamol acts as a competitive inhibitor of the phenol–sulfotransferase, which leads to reduced sulfonation and thus to higher plasma concentrations of (*R*)-salbutamol when applied as racemate [15]. Mareck et al. [16] reported that glucuronidation of salbutamol only occurs for up to 3% after oral administration and glucuronidated metabolites were undetectable after inhalation.

Renal excretion is the major pathway to clear salbutamol and its metabolites from the body [17,18]. In this study, the proportions of free salbutamol and its major metabolite salbutamol-4′-*O*-sulfate were investigated in urine samples via achiral liquid chromatography coupled to tandem mass spectrometry. To quantify the sulfonated metabolite and thus

the total amount of salbutamol recovered in the samples, the reference substance, which was not commercially available, was biosynthesized utilizing genetically modified *S. pombe* and characterized by UHPLC-QTOF-MS and NMR. Absolute quantitation of the reference was performed by NMR as well. Additionally, it was demonstrated that discrimination of an administration of racemic salbutamol and levosalbutamol was not possible using achiral chromatography methods solely evaluating the amount of free salbutamol or its glucuronide conjugate. Orally administered levosalbutamol would not be identified as an adverse analytical finding in doping-control analysis. Considering the proportion of salbutamol and its sulfoconjugate, discrimination between levosalbutamol and racemic salbutamol was possible with an achiral chromatography method.

2. Materials and Methods

2.1. Chemicals and Reagents

Salbutamol hemisulfate (>98.0%) was obtained from TCI Europe (Zwijndrecht, Belgium). Levalbuterol hydrochloride (>98%), hydrochloric acid (35%, analytical grade), citric acid, ATP, and salbutamol-(tert-butyl-d_9)-acetate were obtained from Sigma Aldrich (Taufkirchen, Germany). Methanol (MeOH, LC-MS grade) and potassium hydrogen phthalate were purchased from Thermo Fisher Scientific (Hennigsdorf, Germany). Ammonium formate (HCOONH$_4$, LC-MS grade) and ammonium chloride were from VWR Chemicals (Darmstadt, Germany). D(+)-glucose, ammonium hydrogen carbonate, disodium hydrogen phosphate, ferric chloride hexahydrate, potassium chloride, magnesium chloride hexahydrate, D(+)-biotin, agar, Triton-X100 and Tris were purchased from Carl Roth GmbH (Karlsruhe, Germany). Ammonium sulfate, sodium sulfate, nicotinic acid, boric acid, copper sulfate pentahydrate, manganese sulfate, and potassium iodide were obtained from Merck (Darmstadt, Germany). Molybdic acid was purchased from Alfa Aesar (Kandel, Germany), and inositol was from Th. Geyer (Berlin, Germany). D_6-DMSO (>99.8%) was purchased from Deutero (Kastellaun, Germany). Ultrapure water was prepared with a Milli-Q water purification system LaboStar 2-DI/UV from SG Wasseraufbereitung und Regenerierstation GmbH (Barsbüttel, Germany) equipped with LC-Pak Polisher and a 0.22-μm membrane point-of-use cartridge (Millipak®, Th Geyer, Berlin, Germany). SalbuHEXAL® N was obtained from Hexal AG (Holzkirchen, Germany), and Cyclocaps® Salbutamol from PB Pharma GmbH (Meerbusch, Germany). Xopenex HFA was purchased from Sunovion Pharmaceuticals Inc. (Marlborough, Massachusetts, United States), and SALBU-BRONCH® Elixir 1 mg/mL from Infectopharm Arzneimittel und Consilium GmbH (Heppenheim, Germany).

2.2. Synthesis of Salbutamol-4′-O-sulfate as Reference

A suitable reference for quantitation of salbutamol-4′-O-sulfate was not commercially available. Therefore, it was synthesized following a biochemical approach developed by Sun et al. [10,19] utilizing a genetically modified fission yeast (*S. pombe*) strain (YN20), which expressed recombinant human SULT1A3 with minor modifications. Briefly, the fission yeast strain expressing SULT1A3 was precultured in 10 mL liquid Edinburgh Minimal Medium (EMM) at 30 °C, 230 rpm, and then transferred to a flask with 400 mL liquid EMM to grow a main culture. Subsequently, a certain number of cells was transferred to a centrifuge tube and centrifuged at 4 °C, 4500 *rcf* for 5 min. The supernatant was then discarded, and the cells were incubated in 0.3% Triton-X100 in Tris-KCl buffer (200 mM KCl, 100 mM Tris, pH 7.8) at 30 °C with agitation for one hour to permeabilize the cells. The cells were then washed thrice with NH$_4$HCO$_3$ buffer (50 mM, pH 7.8) and resuspended to a concentration of 2.5×10^8 cells per mL in 19.8 mL of a reaction mixture containing ATP (11 mM), (NH$_4$)$_2$SO$_4$ (5.5 mM), MgCl$_2$ (20 mM) in NH$_4$HCO$_3$ buffer (50 mM, pH 7.8). The reaction was started by adding 200 μL of a substrate stock solution (100 mM) to the mixture (final concentration 1 mM), which was then incubated with agitation for 17 h at 37 °C to allow biotransformation. Finally, the reaction mixture was centrifuged at 4 °C, 3320 *rcf* for 5 min, and the supernatant containing the product was collected. The cells

were washed twice with water, and the content of the merged supernatants was purified on a silica gravity column and additionally by semi-preparative HPLC separation. Details of the purification are described in Table A1 in Appendix A.1.

2.3. Characterization of Salbutamol-4′-O-sulfate
2.3.1. UHPLC-QTOF-MS

High-resolution accurate mass analysis of the biosynthesized salbutamol-4′-O-sulfate was performed in targeted MS/MS mode (2 Hz MS^1; 3 Hz MS^2) on an Agilent 6550 iFunnel QTOF-MS (G6550A; Agilent Technologies Inc., Santa Clara, CA, USA) coupled to an Agilent 1290 Infinity II UHPLC system (Agilent Technologies, Waldbronn, Germany). Ionization was achieved utilizing an electrospray ionization (ESI) source (Dual Agilent Jetstream) in positive and negative modes. Source parameters were 3500 V capillary voltage, 500 V nozzle voltage, drying gas temperature 170 °C, drying gas flow 17 L/min, nebulizer 10 psi, sheath gas temperature 375 °C, and sheath gas flow 12 L/min. The UHPLC was equipped with an Agilent Poroshell 120 phenyl–hexyl column (3.0 mm I.D. × 100 mm; 1.9 μm), gradient elution was performed at a flow rate of 0.400 mL/min at 35 °C column temperature and started with 5% B (20 mM ammonium formate in MeOH) and 95% A (20 mM ammonium formate in water) for 1 min. The gradient evolved in 4 min to 40% B, then in 2 min to 95% B, and was then kept at 95% B for 1.9 min before re-equilibration.

2.3.2. Nuclear Magnetic Resonance

^{1}H (400 MHz) and ^{13}C NMR (100 MHz) were recorded at 298 K on a Bruker Avance III 400 instrument (Bruker, Rheinstetten, Germany). ERETIC analysis was performed with 30° angle, 16 scans, and an interscan delay of 40 s. The frequency range was +/− 10 ppm, and 64k data points were generated. NMR integrals were referenced to NMR integrals of 10.05 mg 1,3,5-trimethoxybenzene (TraceCERT Lot#BCBO5470) in 0.605 mL d_6-DMSO counting in the content given by its batch analysis certificate. Analytes were dissolved in d_6-DMSO (99.8%) and measured in Wilmad economy-grade NMR sample tubes.

2.4. Proof of Concept: Longitudinal Case Study and Urine Analysis
2.4.1. Study Design

Different formulations of racemic salbutamol and pure levosalbutamol were administered to one healthy volunteer. Single doses of 600 μg of racemic salbutamol were applied by inhalation as aerosol (SA_MDI 6 × 100 μg; SalbuHEXAL® N) and as powder inhalation (SA_DPI, 3 × 200 μg; CYCLOCAPS® Salbutamol) to evaluate equivalence in excretion of the parent drug and its sulfoconjugated metabolite to the use of a metered dose inhaler (MDI) and a dry powder inhaler (DPI). Furthermore, levosalbutamol was administered pulmonary at a therapeutic dose of 90 μg (LSA_MDI_TD, 2 × 45 μg; Xopenex HFA®) and a high dose of 630 μg (LSA_MDI, 14 × 45 μg; Xopenex HFA®). Additionally, oral administrations of 2 mg of racemic salbutamol as a liquid (SAP, 2 mL as drops; SALBU-BRONCH® Elixir 1 mg/mL) and 1 mg of levosalbutamol hydrochloride (LSAP, 2 mL of a 0.5 mg/mL levosalbutamol solution) were performed. Administrations were carried out at least one week apart to ensure full washout. Urine was collected pre- and for up to 6 days post-administration. All urine samples were collected as they accrued throughout at least the first 48 h after administration. Afterward, morning urines were collected. Excreted volumes and corresponding collection periods were recorded. Aliquots of the urine samples were stored at −20 °C until analysis.

2.4.2. Matrix Assisted Calibration

Matrix-assisted calibration was performed with the biosynthesized salbutamol-4′-O-sulfate reference. Calibration levels in a range of 1.86 ng/mL to 186 ng/mL for salbutamol-4′-O-sulfate and 0.83 ng/mL to 1665 ng/mL for salbutamol were prepared with analyte-free urine.

2.4.3. Sample Preparation

For sample preparation, urine sample aliquots were thawed at room temperature. To 200 μL of the urine sample, 700 μL methanol and 100 μL internal standard (IS) solution containing d_9-salbutamol were added to a final concentration of 500 ng/mL. Samples were then cooled for 10 min at -20 °C, centrifuged at 14,100 *rcf* for 5 min, and the supernatant was transferred to 1.5 mL glass vials for analysis. Calibration solutions were prepared accordingly. Urine samples were diluted with analyte-free urine prior to sample preparation if the results exceeded the highest calibration level.

2.4.4. Specific Gravity of Urine Samples

The specific gravity of all urine samples was determined using a Kruess Handrefrak-tometer HRMT 18 (A. KRÜSS Optronic GmbH, Hamburg, Germany). Measurements were performed at 22 °C. The device was calibrated with demineralized water prior to sample analysis.

2.4.5. Instruments and Chromatographic Conditions for Urine Analysis

All quantitative urine analyses were carried out by ultrahigh performance liquid chromatography-tandem mass spectrometry (UHPLC-MS/MS) using a 1290 Infinity II UHPLC-System (Agilent Technologies, Waldbronn, Germany) coupled to a 6495 iFunnel triple quadrupole (QQQ) MS (G6495B; Agilent Technologies, Santa Clara, CA, USA). Chromatography was performed utilizing an Agilent InfinityLab Poroshell 120 phenyl-hexyl column (3.0 mm I.D. × 100 mm; 1.9 μm) at a temperature of 35 °C. Multistep gradient elution was performed using 20 mM ammonium formate in water (A) and 20 mM ammonium formate in methanol (B) at a flow rate of 0.400 mL/min. Gradient elution started and was kept for 1 min at 5% B, increased to 40% B in four minutes, and then in 1 min to 95% B and was kept at 95% B for 1.9 min before re-equilibration at 5% B. Post time was set to 2.5 min. The tandem mass spectrometer was operated in positive and negative electrospray ionization (ESI+ and ESI−) modes using multiple reaction monitoring (MRM). Detailed parameters for all analytes are available in Table 1.

Table 1. Operating conditions for electrospray ionization in UHPLC-QQQ-MS. Precursors, product ions, and collision energies used in multiple reaction monitoring modes. Transitions of the highest intensity were set as quantifier (*).

Electrospray Ionization			
Gas temperature	170 °C		
Gas flow	17 L/min		
Nebulizer	10 psi		
Sheath gas temperature	400 °C		
Sheath gas flow	12 L/min		
Capillary voltage	4000 V		
Nozzle voltage	500 V		
MRM			
	Precursor Ion [*m/z*]	**Product Ion [*m/z*]**	**Collision Energy [eV]**
Salbutamol	$[M+H]^+ = 240.0$	222.1	8
		166.1	12
		148.1 *	16
		121.1	25
		91.0	48
		77.1	56
Salbutamol-4'-*O*-sulfate	$[M+H]^+ = 320.0$	240.0 *	4
		222.0	16
		166.0	16
		148.0	32
		77.0	80
	$[M-H]^- = 318.0$ [1]	238.0	25
d_9-Salbutamol	$[M+H]^+ = 249.2$	231.1	8
		166.1	12
		148.1	16
		121.1	25
Salbutamol glucuronide	$[M+H]^+ = 416.0$ [1]	298.0	12
		240.0	18
		224.0	29
		222.0	20
		148.0	20
	$[M-H]^- = 414.0$ [1]	396.0	18
		220.0	25
		146.0	25

[1] not considered in this study since their mass transitions did not add value to the discussed results.

2.4.6. Method Characterization

The UHPLC-MS/MS method was previously described, and basic validation was performed by Harps et al. [5]. Retention time stability, matrix effect (ME), and precision were monitored in this study. Sample preparation was evaluated by performing experiments on recovery.

Experiments on ME were performed. Therefore, samples free from the matrix were prepared, and the target analytes were spiked at the very end of the sample preparation. Two different concentrations of salbutamol (104 ng/mL and 1040 ng/mL) and salbutamol-4'-*O*-sulfate (12 ng/mL and 116 ng/mL) in urine or water, which were within the calibration range were chosen, and samples were generated as triplicates. ME calculations were carried out according to Matuszewski et al. [20].

$$ME\% = \frac{Peak\ area\ matrix\ matched\ calibration}{Peak\ area\ neat\ solvent\ calibration} \times 100$$

Recovery of the analytes was evaluated by comparing the peak areas of samples spiked before sample preparation to samples spiked with the target analytes after sample preparation. All samples contained an analyte-free matrix. Recovery for two different concentrations for each analyte was evaluated, and samples were generated in triplicate. For salbutamol concentrations in urine were 104 ng/mL and 1040 ng/mL and 12 ng/mL and 116 ng/mL salbutamol-4'-O-sulfate.

The precision of the quantitative UHPLC-QQQ-MS/MS method was evaluated for all calibration levels within the limits of quantitation. For each calibration level, triplicates were generated and analyzed on two different days. Thus, inter-day differences in precision were evaluated as well as precision over the two days.

2.5. Data Analysis

For the confirmation of the identity of the salbutamol and salbutamol-4'-O-sulfate peaks, qualifier–quantifier ratios and statistical evaluation were calculated in OriginPro® 2019 (Academic) (OriginLab Corporation, Northampton, MA, USA).

Specific gravity-adjusted concentrations (C_{SG-V}) were calculated using the mean specific gravity (SG_{mean}) determined from all urine samples of the volunteer, the determined concentration (C), and the specific gravity of the urine sample (SG_{sample}).

$$C_{SG-V} = \frac{SG_{mean} - 1}{SG_{sample} - 1} \times C$$

Adjusted concentration (C_{SG-N}) calculated with normal specific gravity (1.02):

$$C_{SG-N} = \frac{1.02 - 1}{SG_{sample} - 1} \times C$$

Additionally, urinary flow adjusted concentrations (C_{adj-UF}) were calculated by a factor (f) describing the relation of the mean urinary flow rate (UF_{mean}) of the volunteer throughout all collection periods and the urinary flow rate for the specific sample (UF_{sample}). The measured concentration (C) was multiplied by f to adjust the concentration.

$$f = \frac{UF_{sample}}{UF_{mean}}$$

Measured concentrations (C) were multiplied with f to adjust for the urinary flow.

$$C_{adj-UF} = f \times C$$

The individual excreted masses (m) of salbutamol and salbutamol-4'-O-sulfate (as salbutamol equivalent) were calculated by the following equation with excreted volumes of the urine (V) and the measured concentration of the analytes (C) for salbutamol as well as for the sulfoconjugate. The mass of the sulfoconjugate was calculated as salbutamol equivalent.

$$m = V \times C$$

The total excreted cumulative mass ($m_{excreted}$) was calculated back to the sum of excreted salbutamol ($m_{sal\,(t)}$) and salbutamol-4'-O-sulfate ($m_{metabol\,(t)}$) per collection period (t).

$$m_{excreted} = \sum m_{sal\,(t)} + \sum m_{metabol\,(t)}$$

Proportions of salbutamol-4'-O-sulfate and salbutamol were calculated in relation to the total amount of salbutamol excreted as both compounds. Amounts of salbutamol-4'-O-sulfate were always calculated back to the mass of salbutamol metabolized. All calculations were performed using Microsoft® Excel 16.71 (Munich, Germany).

3. Results

3.1. Biosynthesis and Characterization of Reference by UHPLC-QTOF-MS and NMR

Reference material was successfully synthesized using a biotechnological approach. While chemical synthesis by sulfonation of salbutamol using Py^*SO_3 yielded a mixture of several products besides non-reacted substrate, the biocatalyzed reaction is regioselective.

The product of biosynthesis was purified and subsequently characterized by UHPLC-QTOF-MS and NMR.

In ESI+ the accurate mass found for salbutamol-4′-*O*-sulfate $[M+H]^+$ at RT = 3.69 min was m/z 320.11599 (exact mass m/z 320.11623, mass error $\Delta m/z = -0.75$ ppm). MS^1 data in positive mode also showed the loss of SO_3 as in-source fragmentation for salbutamol-4′-*O*-sulfate. This phenomenon was also observed in negative electrospray ionization mode, albeit to a considerably lesser extent. In QTOF-MS experiments, the sulfate showed higher stability in the ionization source injected from a neat solvent solution at the same ionization parameters in ESI−. The product ion spectra of salbutamol-4′-*O*-sulfate (A1 and A2) are displayed in Figure 2 (targeted MS^2). Product ion spectra of salbutamol are also included for comparison (Figure 2B1,B2). After the loss of SO_3 ($[M+H-SO_3]^+$ m/z 240.1579) salbutamol-4′-*O*-sulfate showed a similar fragmentation as salbutamol. Additional water losses led to the product ions m/z 222.14806 ($[M+H-SO_3-H_2O]^+$) and m/z 204.13701 ($[M+H-SO_3-2H_2O]^+$). α-Cleavage between position 2 and 3 of the side chain led to m/z 166.08561 ($[C_9H_{10}O_3]^+$), with an additional loss of water yielded m/z 148.07512 ($[C_9H_8O_2]^+$).
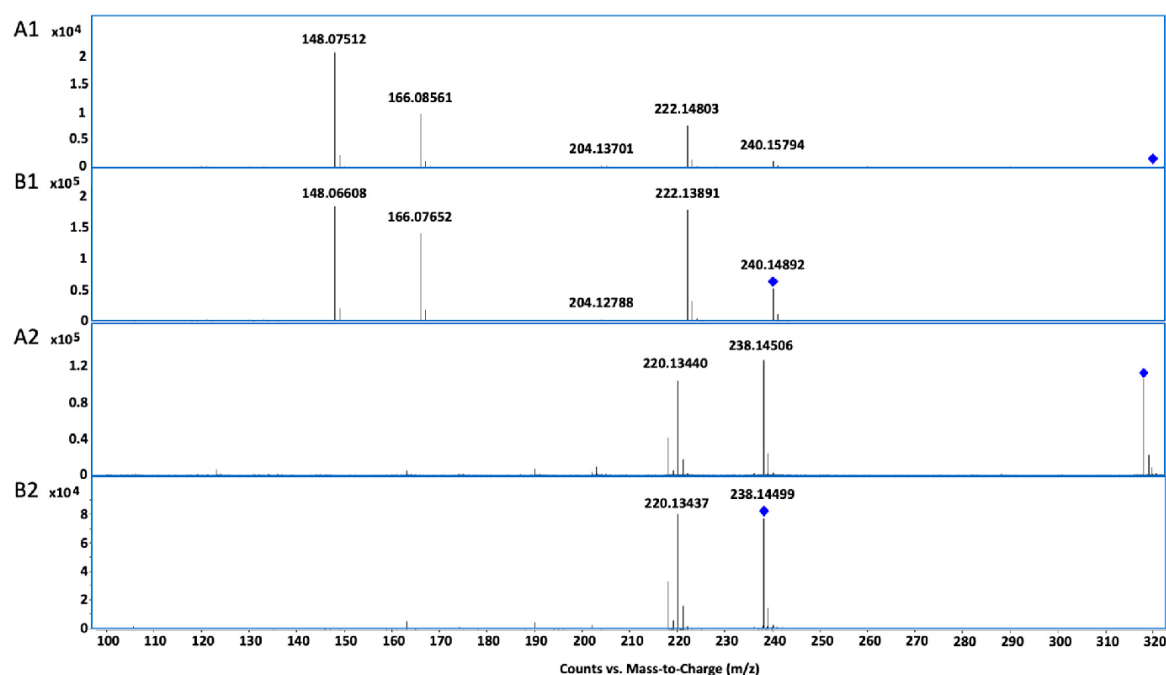
Figure 2. Product ion spectra (UHPLC-QTOF-MS) of salbutamol-4′-*O*-sulfate with 20 eV collision energy (**A1**) and salbutamol with 10 eV collision energy (**B1**) in positive mode and salbutamol-4′-*O*-sulfate with 20 eV collision energy (**A2**) and salbutamol with 10 eV collision energy (**B2**) in negative mode; blue rhombs indicate the respective precursor ion.

The fragmentation in negative mode (ESI−) behaves similarly, although only the loss of SO_3 ($[M-H-SO_3]^-$ m/z 238.14506) and an additional loss of water ($[M+H-SO_3-H_2O]^-$ m/z 220.13440) are observed with reasonable intensity at a collision energy of 10 eV.

Furthermore, ^{1}H and ^{13}C NMR shift data were collected for salbutamol hemisulfate salt and the biosynthesized sulfoconjugated salbutamol. The assignment of all signals was achieved unambiguously using 2D techniques like ^{1}H,^{1}H COSY, ^{1}H,^{13}C HSQC, and ^{1}H,^{13}C HMBC for the aliphatic ABX spin system and the AMX system of the aromatic protons. The chemical shifts and couplings are summarized in Table 2. The carbon attached to the phenol group of the sulfonated hydroxy group (the ipso position) was shielded by 3.84 ppm, and the chemical shifts of the carbon atoms ortho and para to the sulfonation site were in contrast, deshielded in a range of 4.53 to 7.30 ppm. Chemical shifts near other potential sulfonation sites, like the amine function or the benzylic or aliphatic hydroxy group, were only marginally changed. Diagnostic shift differences are marked in bold in Table 2.

Table 2. Chemical shifts (δ_H, δ_C in ppm, 400 MHz ^{1}H and 100 MHz ^{13}C NMR), signal splitting and coupling constants (in Hz) of salbutamol hemisulfate (30 mM) and salbutamol-4'-O-sulfate (5 mM) in d_6-DMSO at 298 K referenced to internal d_5-DMSO (δ_H 2.50 ppm) or d_6-DMSO (δ_C 39.5 ppm) and chemical shift differences observed upon sulfonation ($\Delta\delta = \delta_{Osulfate} - \delta_{OH}$) for the aromatic ring signals.

Position	Salbutamol [a] ^{1}H	Salbutamol ^{13}C	Salbutamol-4'-O-sulfate [a] ^{1}H	Salbutamol-4'-O-sulfate ^{13}C	Chemical Shift Differences $\Delta\delta = \delta_{Osulfate} - \delta_{OH}$ ^{1}H	^{13}C
1	4.72, dd [b], 10.0, 2.8 Hz	69.71	4.77, dd [b], 10.2, 2.6 Hz	69.69	+0.05	−0.02
2	2.74/2.83, AB d [b] 11.8, 10.0, 2.8 Hz	49.14	2.69/2.81 [c]	49.67	−0.05/−0.02	+0.53
4		53.89		54.68 [d]		+0.79
5	1.20, s	26.12	1.23, s	25.91	+0.03	−0.21
1'		132.93		137.46		**+4.53**
2'	7.31, d, 2.3 Hz	125.88	7.43, d, 2.1 Hz	124.86	+0.12	−1.02
3'		128.10		134.57		**+6.47**
3'-CH$_2$	4.47, s	58.24	4.55, s	58.30	+0.08	+0.06
4'		153.43		149.59		**−3.84**
5'	6.73, d, 8.3 Hz	114.16	7.27. d, 8.3 Hz	121.46	**+0.54**	**+7.30**
6'	7.07, dd, 8.3, 2.3 Hz	124.96	7.20, dd 8.3, 2.1 Hz	121.50	+0.13	−3.46

[a] exchangeable protons at 4.97, 6.85, and 9.26 ppm, very broad singlets (OH, NH$_2$, and aryl-OH), exchangeable signals of the 4'-O-sulfate not identified. [b] The coupling constants of the ABX system were analyzed in first order. [c] analysis of the coupling constants is not possible due to excessive overlap. [d] chemical shift extracted from the HMBC spectrum.

3.2. Metabolite Identification in Urine Samples

The excretion of salbutamol and salbutamol-4'-O-sulfate was monitored in post-administration urines using UHPLC-MS/MS. For identification, ratios, and ranges of qualifier–quantifier peak areas were calculated for salbutamol and salbutamol-4'-O-sulfate references using the data from the matrix-assisted calibration. The tolerances for the qualifier–quantifier ratios were set according to the WADA criteria for identification in tandem mass spectrometry [21]. The defined tolerance windows are based on the abundance of the diagnostic ions (qualifier) to the reference (quantifier). For a relative abundance of diagnostic ions in the range of >50–100%, a difference of 10% (absolute); for a relative abundance >25–50%, 20% (relative); and for relative abundances <25%, 5% (absolute) is allowed (Table 3).

Table 3. Qualifier–quantifier ratio ranges for salbutamol and salbutamol-4'-*O*-sulfate transitions based on WADA regulations, precursor ion (ESI+) for salbutamol m/z 240.0, salbutamol-4'-*O*-sulfate m/z 320.0.

Product Ion (m/z)	77.1	91.0	121.1	166.1	222.1
salbutamol	12.1–22.1	4.0–14.0	5.1–15.1	26.4–39.6	59.8–79.8

Product Ion (m/z)	148.0	166.0	222.0
salbutamol-4'-*O*-sulfate	44.8–64.8	15.2–25.2	29.9–44.9

The median values for the qualifier-quantifier ratios found in the analysis of the calibration were used as reference values. The distribution of the qualifier–quantifier ratios of the calibration and the samples are shown in Figure 3. The requirement for the assignment of a peak to one of the targeted analytes was that at least two qualifier–quantifier peak area ratios were within the given range. This was achieved in all samples within the calibrated concentration range, thus clearly identifying salbutamol and salbutamol-4'-*O*-sulfate.
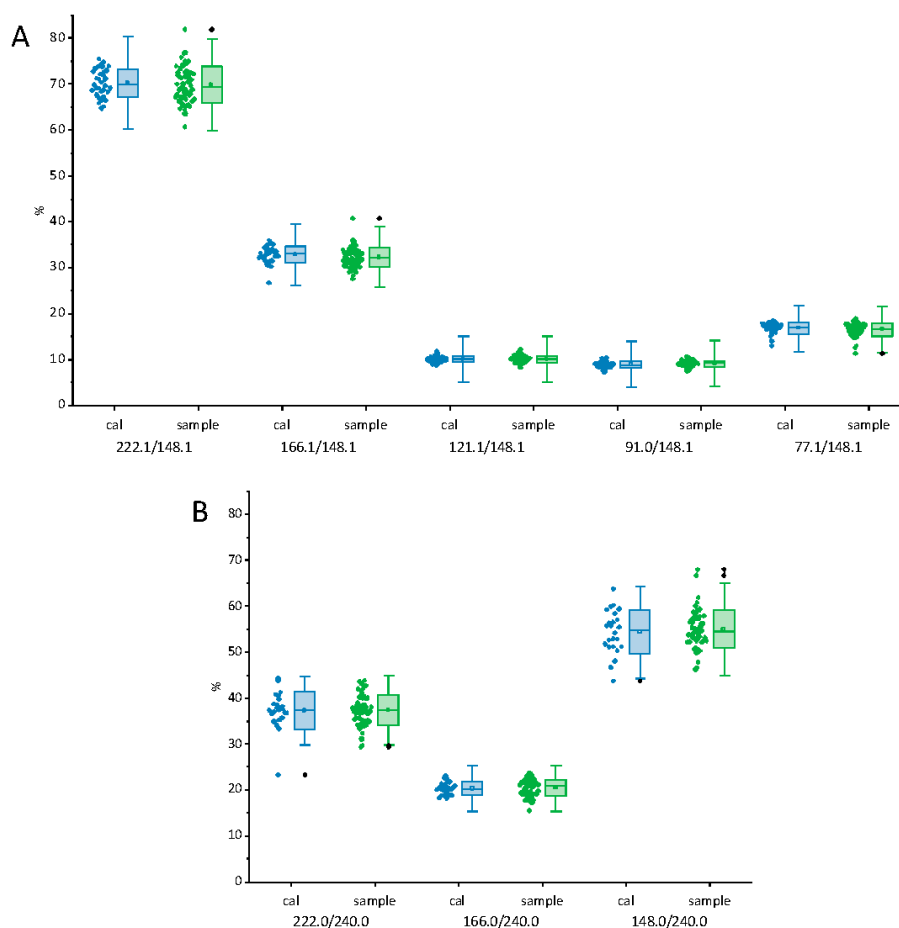
Figure 3. Distribution of the qualifier–quantifier ratios of matrix-assisted calibration (cal) and urine samples of (**A**) salbutamol and (**B**) salbutamol-4'-*O*-sulfate. Box shows standard deviation, whisker shows tolerances for qualifier–quantifier ratios (10% absolute tolerance for ratios >50–100%, 10% relative for ratios >25–50%, and 5% absolute for ratios <25%), solid line in box is median, and empty square in box is mean value. Black rhombs in line with box highlight outliers next to the box.

Except for the qualifier–quantifier ratio of 148.0 to 240.0 (Figure 3B), the distribution showed a lower scatter in the calibration samples. Qualifier–quantifier ratios in the quantitation of salbutamol-4'-*O*-sulfate gave a higher scatter than the ratios in salbutamol analysis. Throughout the measurements, the distribution of the qualifier–quantifier ratios showed only a few outliers, of which not all were outside the set tolerance limits from Table 3. Out of the three highlighted outliers in Figure 3A, two qualifier–quantifier ratios of 222.1/148.1 and 166.1/148.1 from two different samples (127 ng/mL and 3.7 ng/mL, respectively) were above the upper tolerance limit. In a further sample (1.7 ng/mL), the ratio of 77.1/148.1 was below the lower tolerance limit. All outliers were related to trace level concentration of salbutamol. Regarding the distribution of the qualifier–quantifier ratios of salbutamol-4'-*O*-sulfate shown in Figure 3B, two outliers from the calibration (level 1 and 3, respectively) were found, one at 222.0/240.0 and one at 148.0/240.0, both showing ratio below the lower tolerance limit. Four outliers were found in the qualifier–quantifier distribution of the samples, two at 222.0/240.0 and below and two at 148.0/240.0 and above the tolerance limits with concentrations of 3.5, 6.8, 5.9, and 5.6 ng/mL, respectively. Not any sample from the volunteer nor any calibration sample showed more than one outlier.

3.3. UHPLC-QQQ-MS/MS Method Characterization

The mean values of the retention times of the analytes were 3.502 min for salbutamol-4'-*O*-sulfate and 4.079 min for salbutamol, with maximum deviations of 0.034 min and 0.021 min, respectively. Retention time stability has been proven, and the tolerance of 1% of the retention time was not exceeded. Chromatograms of salbutamol and salbutamol-4'-*O*-sulfate are shown in Figure 4.
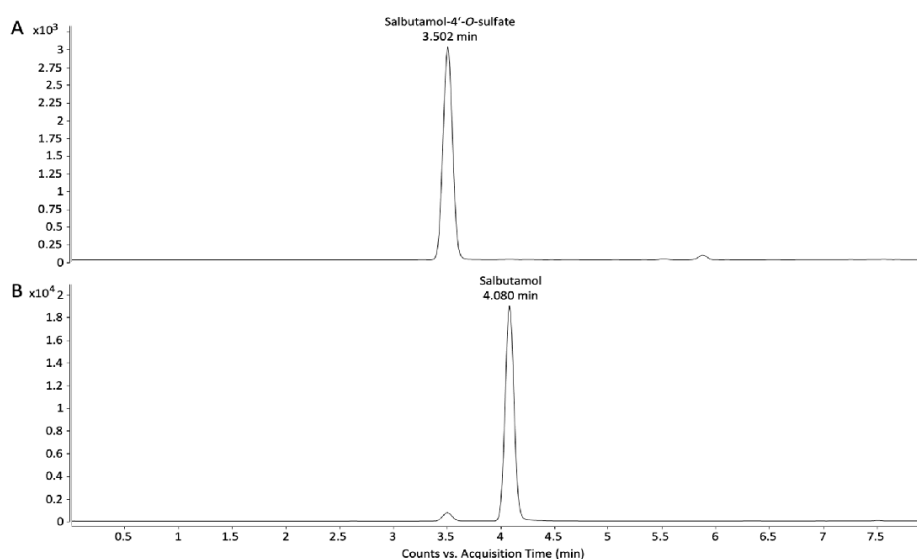
Figure 4. Chromatograms of salbutamol-4'-*O*-sulfate (**A**) and salbutamol (**B**). The transitions shown in the chromatograms are m/z 320.0 → 240.0 for salbutamol-4'-*O*-sulfate and m/z 240.0 → 148.1 for salbutamol, which were chosen as quantifiers. Due to the in-source fragmentation of salbutamol-4'-*O*-sulfate, the quantifier peak of salbutamol can also be detected at the retention time of the sulfoconjugate.

Evaluating the precision for salbutamol-4'-*O*-sulfate and salbutamol in all calibration levels, variation coefficients were from 2.4% to 7.3% and from 2.7% to 11.1%, respectively. Differences in precision between two days (inter-day precision) for salbutamol-4'-*O*-sulfate was from 0.2% to 11.4% and for salbutamol from 0.2% to 18.2%. The overall precision, as well as the inter-day precision, did not exceed 20%.

ME was found to be 68.4% for 12 ng/mL and 70.3% for 116 ng/mL for salbutamol-4′-O-sulfate in urine. For 104 ng/mL and 1040 ng/mL salbutamol in urine, 86.1% and 93.7% were found, respectively.

Recovery in the sample preparation was for the low level 97.4% for salbutamol and 99.9% for salbutamol-4′-O-sulfate and for the high level, 94.6% and 104.4%, respectively.

3.4. Evaluation of Urinary Excretion Profiles

3.4.1. Inhalation of Salbutamol through Dry Powder Inhaler vs. Metered Dose Inhaler

An equal dose (600 µg) of salbutamol was applied using a DPI and an MDI to assess the equivalence of different inhalation devices. Excretion of salbutamol and the sulfoconjugate appears to be equivalent for administration by MDI and DPI. Hence, only results from the MDI trial were used for comparison of inhalation of racemic salbutamol and levosalbutamol. The results of this trial are shown in Appendix A.2 (Table A2).

3.4.2. Urinary Excretion Rates

Following oral application of the racemic and enantiopure preparation, the highest excretion rate of salbutamol occurred in the collection period between 2–4 h and for inhalation administration after 1–2 h. When applied pulmonary as levosalbutamol, the maximum excretion rate tended to appear earlier, more precisely within the first hour after administration. Excretion rate maxima of salbutamol-4′-O-sulfate, on the other hand, appeared at a similar time for oral racemic and pulmonary enantiomeric application with a maximum excretion rate after 2–4 h, whereas pulmonary application of racemic salbutamol led to the highest excretion rate within 1–2 h post-administration. In contrast to the oral administration of racemic salbutamol, when applied as oral levosalbutamol, the maximum excretion rate for the sulfoconjugate occurred within the first-hour post-administration. Renal excretion rates of racemic salbutamol, levosalbutamol, and their sulfoconjugated metabolites after pulmonary and oral administration are shown in Figure 5.
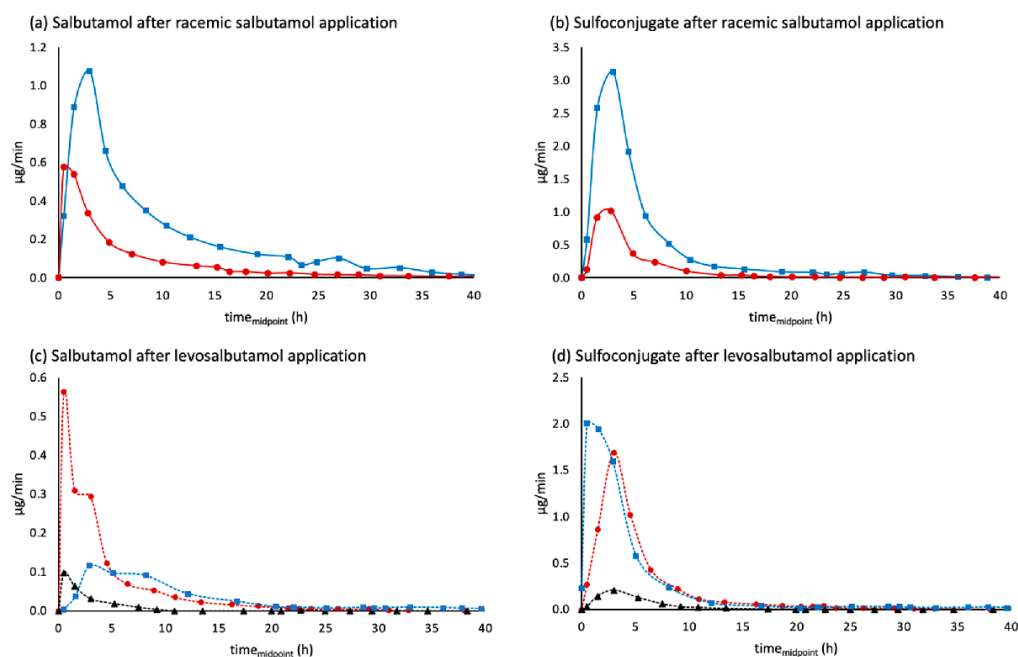
Figure 5. Urinary excretion rates of (**a**,**c**) salbutamol, (**b**,**d**) salbutamol-4′-O-sulfate after administration of racemic salbutamol (**a**,**b**) or levosalbutamol (**c**,**d**). Administration via inhalation of 600 µg (SA_MDI_2) or 630 µg (LSA_MDI) is shown as red circles and 90 µg (LSA_MDI_TD) as black triangles. Oral administration of 2 mg (SAP) or 1 mg (LSAP) is shown as blue squares.

Excreted parent compound and sulfonated metabolite were successfully determined for up to 70 h post administration for orally applied racemic salbutamol (SAP), 60 h for oral levosalbutamol (LSAP), and 46 h for inhaled racemic drug (SA_MDI). After pulmonary administration of 630 µg levosalbutamol (LSA_MDI) quantitative measurements for unchanged salbutamol were possible for 32 h and for 90 µg levosalbutamol (LSA_MDI_TD) 24 h post administration. Salbutamol-4'-*O*-sulfate, on the other hand, was also determined in later samples than the parent compound when pure levosalbutamol was applied with a quantitation window of 48 h for a high dose 630 µg and 46 h for a therapeutic dose of 90 µg levosalbutamol. Concentrations measured in later samples were below the calibrated range (0.83 ng/mL to 1665 ng/mL for salbutamol and 1.86 ng/mL to 186 ng/mL for sulfoconjugate), but identification of the analytes was still possible even at the later excretion times. The total renally excreted amount and the time of the highest excretion rate $t_{max\ (urine)}$ are shown in Table 4.

Table 4. Maximum excretion rates and absolute excreted amounts of salbutamol as parent compound and sulfate metabolite.
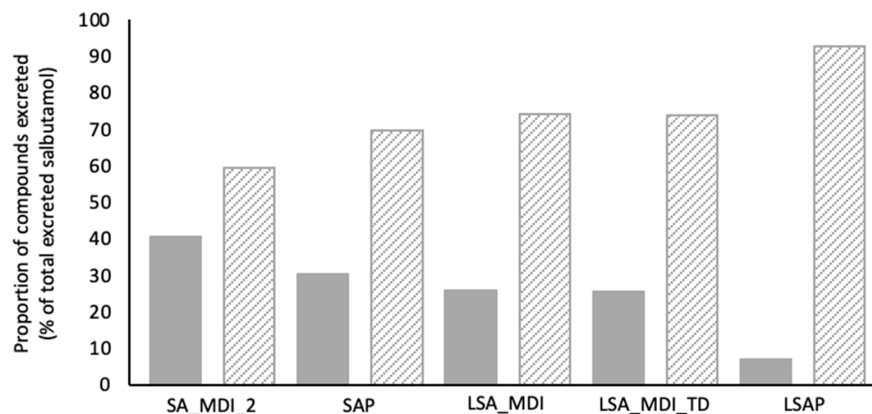
	Salbutamol	Salbutamol-4'-*O*-sulfate
$t_{max\ (urine)}$		
Oral racemate 2 mg (SAP)	3 h	3 h
Inhaled aerosol racemate 600 µg (SA_MDI_2)	1.5 h	1.5 h
Oral levosalbutamol 1 mg (LSAP)	3 h	0.5 h
Inhaled levosalbutamol 630 µg (LSA_MDI)	0.5 h	3 h
Inhaled levosalbutamol 90 µg (LSA_MDI_TD)	0.5 h	3 h
Total urinary excretion [1]		
Oral racemate 2 mg (SAP) [1]	449 µg (22.5%)	1030 µg (51.5%)
Inhaled aerosol racemate 600 µg (SA_MDI_2) [1]	203 µg (33.8%)	298 µg (49.6%)
Oral levosalbutamol 1 mg (LSAP) [1]	65 µg (6.5%)	847 µg (84.7%)
Inhaled levosalbutamol 630 µg (LSA_MDI) [1]	129 µg (20.5%)	371 µg (58.9%)
Inhaled levosalbutamol 90 µg (LSA_MDI_TD) [1]	19 µg (21.1%)	55 µg (61.1%)

[1] Salbutamol-4'-*O*-sulfate calculated as amount of salbutamol that was sulfonated. Percentages are in relation to applied dose.

3.4.3. Proportions of Salbutamol and Salbutamol-4'-*O*-sulfate

The proportion of the excreted compounds related to the total excreted amount is shown in Figure 6. For all administrations, the majority was excreted as the sulfoconjugated metabolite, while 7–45% of the excreted amount was recovered as an unchanged parent compound. After administration of levosalbutamol, the excreted proportion of salbutamol-4'-*O*-sulfate was higher than after application of racemic salbutamol for pulmonary as well as oral administration.

Figure 6. Proportion of salbutamol as parent compound (solid bars) and salbutamol-4′-*O*-sulfate (dashed bars) excreted in relation to total excreted salbutamol. SA_MDI_2—600 µg inhaled racemic salbutamol, SAP—2 mg orally administered racemic salbutamol, LSA_MDI—630 µg inhaled levosalbutamol and LSA_MDI_TD—90 µg inhaled levosalbutamol (therapeutic dose), LSAP—1 mg orally administered levosalbutamol.

3.4.4. Salbutamol-4′-*O*-sulfate in Relation to Unchanged Salbutamol

In the first hour after pulmonary application of racemic salbutamol and levosalbutamol, two to three times more unconjugated salbutamol than sulfate-metabolite was recovered in the urine. During the following collection periods, the correlation reversed, and salbutamol-4′-*O*-sulfate predominated the excreted amount. However, differences in the sulfate metabolite proportion for racemic formulation and the pure enantiomer were observed. Proportions of excreted salbutamol-4′-*O*-sulfate in relation to unconjugated salbutamol are shown in Figure 7, exemplary for administration by inhalation. Proportions after oral administration are shown in Appendix A.3 (Figure A1). For the entire time of renal elimination, the proportion of salbutamol-4′-*O*-sulfate did not exceed 75% and shifted towards salbutamol again after twelve hours when racemic salbutamol was inhaled whereas for pure levosalbutamol, the metabolite proportion climbed up to 95% for a supratherapeutical (630 µg) dose and 84% for a therapeutical dose (90 µg) levosalbutamol. When administered orally as a racemate, the sulfonated metabolite predominated the excreted amount throughout twelve hours post-administration. In later samples, a slight shift towards an equal amount of both analytes and a slight tendency towards unchanged salbutamol was observed. In contrast, after oral administration of levosalbutamol the sulfate proportion was higher than 85% from the very beginning of urinary excretion and did not fall below 72%, showing that most of the compound was renally excreted as the sulfoconjugate at all collection times.
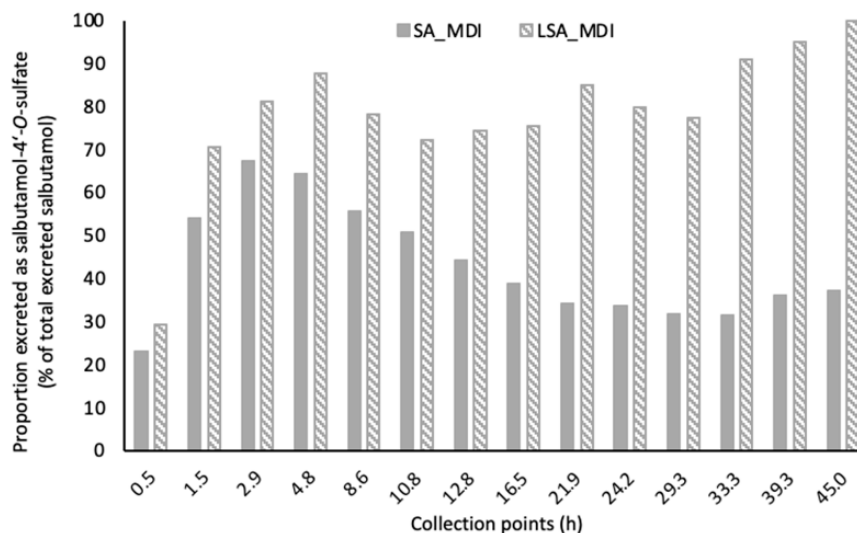
Figure 7. Time profile of proportion of salbutamol-4′-*O*-sulfate excreted in urine in relation to total salbutamol excreted. SA MDI—600 μg inhaled racemic salbutamol. LSA MDI—630 μg inhaled levosalbutamol. Salbutamol-4′-*O*-sulfate was calculated as the salbutamol equivalent.
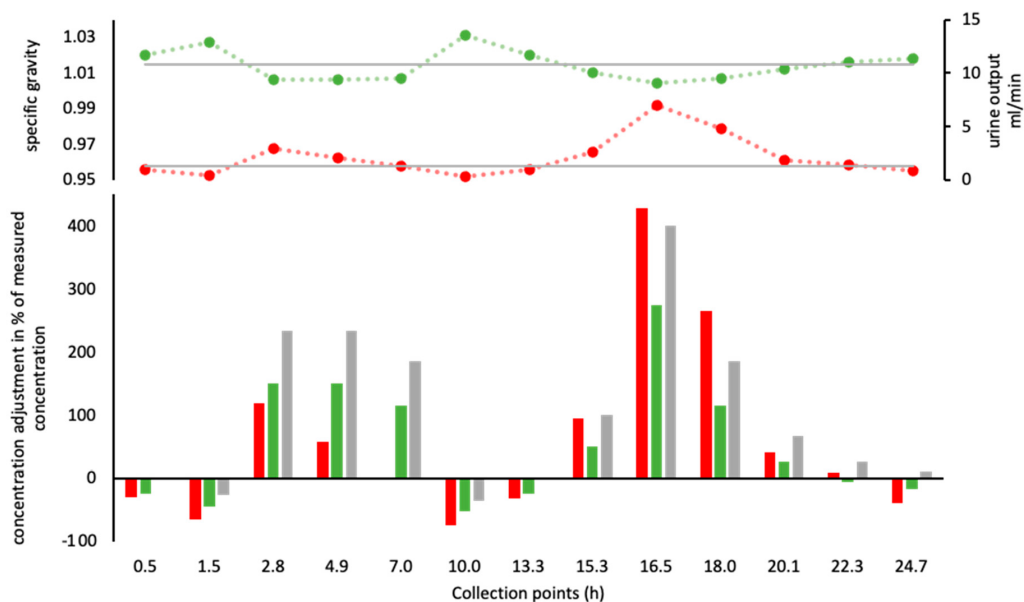
3.4.5. Adjustment by the Specific Gravity of the Urine and by Urinary Flow Rate

The specific gravity (SG) of all urine samples was measured. Concentrations were then corrected with the SG to compensate for dilution or concentration of the urine resulting from high or low liquid intake or physical activity. Uncorrected concentrations of salbutamol and salbutamol-4′-*O*-sulfate, as well as SG and urinary flow rate and the adjusted concentrations, are exemplary for inhaled racemic salbutamol in Figure 8. The other trials are shown in Figure A2 (Appendix A.3).

A high urinary flow rate of the volunteer resulted in a low specific gravity of the sample. This correlation is shown by a mirror-like appearance of the upper graphs in Figures 8 and 9. When the urinary flow rate was higher than the average for the volunteer and the specific gravity lower than average, the adjusted concentration of salbutamol was estimated to be higher than measured and vice versa (Figure 9).
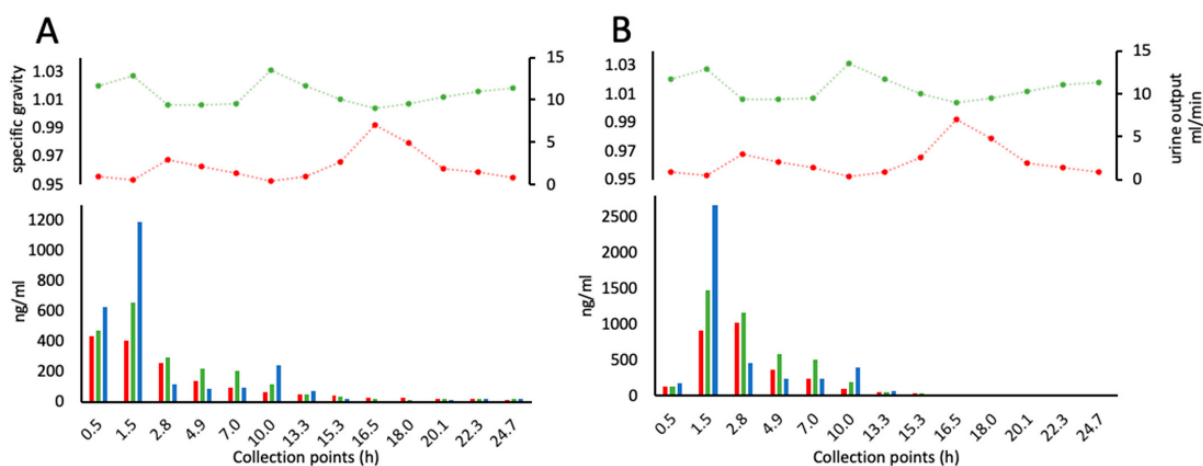
Figure 8. Salbutamol (**A**) and salbutamol-4′-*O*-sulfate (**B**) uncorrected concentrations (blue) and adjusted concentrations by the specific gravity of the urines (green) and by the urinary flow rate (red) after inhalation of 600 μg racemic salbutamol.

Figure 9. Percentage adjustment of measured concentration by volunteer average specific gravity (SG, green), volunteer average urinary flow rate (UF, red), and average specific gravity used by WADA (grey). Dotted graphs show the SG of the sample (green) and the UF of the collection period (red). Grey lines show volunteer average SG and UF.

4. Discussion

4.1. Biosynthesis and Characterization of Salbutamol-4'-O-sulfate

To directly quantify salbutamol-4'-*O*-sulfate, reference material was biosynthesized and characterized by UHPLC-QTOF-MS and NMR. The lack of selectivity in sulfonation of the three hydroxy groups in salbutamol is a great challenge in chemical synthesis. Similar to analogous sympathomimetic drugs, the protection group strategies failed [22]. A highly selective approach was chosen utilizing recombinant human SULT1A3 expressed in genetically modified fission yeasts. The incubation resulted in one mono-sulfonated product, and no further sulfonation byproducts were detected. Further considerations of green chemistry were met for the biosynthesis by using only aqueous solutions instead of organic solvents [23]. However, a bottleneck is the consumption of chemicals in the purification process.

The accurate mass of one-time sulfonated salbutamol was successfully detected in QTOF analysis. Furthermore, fragmentation experiments (MS/MS) verified the successful conjugation of the SO_3-moiety by enzymatic synthesis in *S. pombe*. Although the sulfonation site was expected to be at the phenolic hydroxy group due to the use of the phenol-sulfotransferase 1A3, mass spectrometric experiments could not provide sufficient confirmation as fragmentation analysis did not reveal diagnostic evidence. To prove the exact sulfonation site of salbutamol, ^{1}H, and ^{13}C NMR shift data were collected for salbutamol hemisulfate salt and the biosynthesized sulfoconjugate of salbutamol.

The problem of determining the sulfonation site in substituted phenols has already been described by Purchartová et al. [24], who demonstrated that direct proof was not possible. The position of sulfonation was identified indirectly by the effects of chemical shifts on neighboring atoms, most prominently on the carbon atoms. In general, for simple phenols and also more complex structures and natural products with higher substituted aromatic rings, the following effects upon sulfonation are observed in deuterated water, methanol, or dimethyl sulfoxide [24–26]: The carbon attached to the phenol group of the sulfonated hydroxy group (the ipso position) is shielded by 4 to 6 ppm, the chemical shifts

of the carbon atoms ortho and para to the sulfonation site, in contrast, are deshielded in a range of 3 to 7 ppm, the meta positions are not influenced to such a large extent. Similarly, the chemical shifts of the protons in ortho position of the sulfonation site are deshielded by 0.4 to 0.6 ppm; other protons in the ring system exhibit only a small low field shift in the range of 0.1 ppm. These effects were also observed without exception in the case of sulfonated salbutamol, and the chemical shifts near other potential sulfonation sites, like the amine function or the benzylic or aliphatic hydroxy group, were only marginally changed. Thus, the 4'-hydroxy group was clearly identified as a sulfonation site. Due to fast exchange processes, the protons of the amine and hydroxy functions were not observed as separate signals, which was considered independent proof of the sulfonation of the phenolic hydroxy group as well.

After biosynthesis and subsequent purification, the amount of salbutamol-4'-*O*-sulfate was determined by absolute quantitative NMR, which allows its use as a reference for metabolite determination in urine samples.

A reliable identification of salbutamol and salbutamol-4'-*O*-sulfate in the quantitation was achieved by monitoring the qualifier–quantifier ratios after forced fragmentation. Within the range of the quantitation in all matrix-assisted calibration samples and all samples from the volunteer, at least two qualifier–quantifier ratios were valid according to the WADA criteria. Considering the dilution while sample preparation, all outliers were related to concentrations at the trace level. The one exception was still at the trace level. Distribution in the qualifier–quantifier ratio of salbutamol-4'-*O*-sulfate showed a wider scattering and subsequent higher standard deviations for comparable ratio levels. In-source fragmentation, which might also be affected by the matrix of the urines, might reduce the precision in forced fragmentation by tandem MS/MS. Additionally, the higher sensitivity for salbutamol in this method may result in tighter distribution patterns. However, the WADA-based identification criteria in terms of qualifier–quantifier ratios as prerequisite for the quantitation was successfully achieved. The robustness of different urine matrices should be investigated in the future.

4.2. Basic Method Validation

Additionally, to carry over, as performed by Harps et al. [5], basic method validation was successfully performed in terms of retention time stability, matrix effect, recovery, and precision. The method was proven to be suitable for this study.

4.3. Proof of Concept: Achiral Analysis of Urinary Excreted Salbutamol and Salbutamol-4'-O-sulfate for Discrimination of Application Routes and Enantiomeric Composition of the Administered Drug

Considering the different routes of administration (i.e., oral (aqueous solution) versus inhalation (MDI)), it became apparent that the period for salbutamol and salbutamol-4'-*O*-sulfate in which the analytes were quantifiable was 1.5 times longer after oral administration. Similarly, a 1.2 times longer quantitation window was observed after oral administration of the racemic drug compared to oral administration of levosalbutamol. Likewise, the maximum excretion rate of the unchanged drug after oral administration of the racemic drug was 1.6 times higher than after levosalbutamol. The highest excretion rate of the sulfo-conjugate after application of a racemic drug was 10 times the maximum excretion rate of salbutamol-4'-*O*-sulfate after enantiopure administration. As the amount of administered racemic salbutamol was higher than the amount of levosalbutamol in oral applications, and the oral dosage was higher than the pulmonary applied dosage, the observed longer occurrence in urine and higher excretion rate was not surprising. By comparing the inhalation of similar doses (~600 μg) of racemic and enantiopure salbutamol, a shorter detection window for the parent compound was observed after enantiopure administration, whereas the quantitation window for the sulfoconjugate was slightly longer. Even after inhalation of 90 μg levosalbutamol, the salbutamol-4'-*O*-sulfate quantitation window was the same as for 600 μg inhaled racemic salbutamol, indicating a higher rate of metabolization for the enantiopure drug. After inhalation, higher excretion rates were observed for sulfonated

salbutamol after applying the enantiopure drug. While the highest excretion rates for the parent compound were similar for both formulations, t_{max} was observed sooner (0.5 h) after inhalation of levosalbutamol than after racemic salbutamol (1.5 h). This observation may be explained by a higher metabolization rate of the preferred (*R*)-salbutamol, leaving less parent drug to be excreted. For racemic salbutamol, the less preferred (*S*)-salbutamol might have led to a relatively higher excretion rate. Chiral analysis would be needed to prove this hypothesis finally.

After administration of levosalbutamol, the parent compound was sulfoconjugated to a greater extent than after racemic salbutamol. The highest amounts of sulfoconjugate were found when levosalbutamol was administered orally (84% of the dose was excreted as sulfoconjugate). This is in accordance with the literature that SULT1A3 is mainly localized in the jejunum [8,11]. According to literature, only 10–20% of an inhaled dose was delivered to the lungs, whereas the rest of the dose was swallowed, leading to high shares of salbutamol-4'-*O*-sulfate recovered in urine after inhalation of salbutamol [18,27,28]. In line with these findings in the current study, the application of levosalbutamol disregarded the dosage and administration pathway, leading to higher proportions of its sulfonated metabolite in the urine. Considering the same applied amount of levosalbutamol in racemic or enantiopure administration (LSAP 1 mg vs. SAP 2 mg), the results reflect and support the above-mentioned higher affinity of SULT1A3 towards (*R*)-salbutamol, which was already reported by Boulton et al. and Walle et al. [1,14]. Opposed to oral administration, after inhalation, less sulfoconjugate was formed from racemic salbutamol as well as from levosalbutamol. Due to the missing first-pass effect in the lungs [29], the truly pulmonary applied part of the dose contributes less to the generation of salbutamol-4'-*O*-sulfate. Further investigations may profit from the additional availability of serum samples and an enhanced number of participants.

In the analysis of urine samples, usually, the analyte's concentration in the urine is measured. However, the concentration of the analyte does not account for the excreted urine volumes, and subsequently, highly diluted or concentrated urines may compromise the assessments of the results. High or low intake of liquids, physical activity, and the loss of volume (sweating) impact the specific gravity of the excreted urine. Therefore, measured salbutamol and salbutamol-4'-*O*-sulfate concentrations were adjusted using two different methods, and the adjustments by the specific gravity of the urine sample or by the urinary flow rate showed both methods to be reasonably applicable. In this study changes in the urinary flow rate were also seen to be reflected in the specific gravity. However, the correction of the concentration was not always to the same extent for both methods highly depending on the chosen reference values.

The results of the study show that the main metabolite salbutamol-4'-*O*-sulfate is important to consider for urine analysis of salbutamol to allow for discrimination between the administration of racemic salbutamol or enantiopure levosalbutamol. Neither inhalation nor oral administration of levosalbutamol would be classified as an adverse analytical finding in doping control analysis by only evaluating the urinary excreted salbutamol. Applying the WADA rules for doping control analysis [2,3], concentrations or adjusted concentrations (specific gravity) of salbutamol did not exceed the WADA's decision limit (1200 ng/mL) throughout the study. However, considering the proportions of salbutamol-4'-*O*-sulfate for a distinction of oral administration vs. inhalation or racemic vs. levosalbutamol is a promising approach. Further studies, including more participants, should be performed to account for interindividual variations. Therefore, reference substances of phase II metabolites are of great value to correctly assess and identify the prohibited use of enantiopure drugs by achiral routine analysis.

5. Conclusions

The main metabolite of salbutamol, salbutamol-4'-*O*-sulfate, was successfully biosynthesized, characterized, and quantified in this study, which facilitated the quantitative analysis of the sulfoconjugated metabolite in urine. Different formulations of salbutamol

were applied in a case study in one healthy volunteer as proof of concept for discrimination of administration of racemic and enantiopure salbutamol by achiral analysis. The extent of metabolization was shown to be higher for levosalbutamol than for racemic salbutamol, reflected in higher sulfate proportions at all times of sample collection. Therefore, the evaluation of the proportion of salbutamol and salbutamol-4′-O-sulfate in urine was found to be a promising approach for the discrimination of the applied drug formulation or enantiomerical form.

Author Contributions: Conceptualization, A.L.J., L.C.H., F.M.B., X.d.l.T. and M.K.P.; methodology, A.L.J., L.C.H., Y.S., M.B. and U.G.; validation, A.L.J. and L.C.H.; formal analysis, A.L.J. and U.G.; investigation, A.L.J., L.C.H., F.B. and M.K.P.; resources, M.K.P., M.B. and F.M.B.; data curation, A.L.J.; writing—original draft preparation, A.L.J.; writing—review and editing, L.C.H., F.B., M.B., U.G., F.M.B., X.d.l.T. and M.K.P.; visualization, A.L.J. and F.B.; supervision, M.K.P., M.B. and F.M.B.; project administration, M.K.P.; funding acquisition, M.K.P., M.B. and F.M.B. All authors have read and agreed to the published version of the manuscript.

Institutional Review Board Statement: The study was conducted in accordance with the Declaration of Helsinki. The volunteer provided informed consent before participation.

Informed Consent Statement: Informed consent was obtained from all subjects involved in the study.

Data Availability Statement: Data are available from the authors upon request.

Conflicts of Interest: The authors declare no conflict of interest.

Appendix A.

Appendix A.1. Purification of Biosynthesized Salbutamol-4′-O-sulfate

After the biosynthesis, the solution containing the product was freeze-dried over 3 days. Subsequent steps are shown in Table A1.

Table A1. Purification conditions for biosynthesized salbutamol-4′-O-sulfate reference.

	Gravity Column Purification	**HPLC Purification**
Sample preparation	Dissolving dried remains in methanol, filtration	Evaporation of fractions containing product to reduce sample volume Filtration of silica remains
Stationary phase	Silica	C18
Column length	40 cm	25 cm
Column diameter	3.5 cm	1 cm
Particle size	n.a.	5 μm
Flow rate	n.a.	2.5 mL/min
Mobile phase	Isopropanol:ethyl acetate:ammonia (17.5%) 40:50:10 (V:V:V)	A: water B: acetonitrile 0–5 min: 3% B to 15% B 5–6.5 min: 15% B 6.5–16 min: 15% B to 27% B 16–20 min: 27% B to 45% B 20–22 min: 45% B to 95% B 25–27 min: 95% B to 3% B
Detection of product	Fraction analysis with LC-MS	UV detection 265 nm

n.a. not applicable.

Appendix A.2. Inhalation of Salbutamol through Dry Powder Inhaler vs. Metered Dose Inhaler

An equal dose (600 μg) of salbutamol was applied using a DPI and an MDI to assess the equivalence of different inhalation devices. Administration of racemic salbutamol with an MDI was performed in duplicate. The results for the excreted total salbutamol (salbutamol + sulfoconjugate) quantity and the shares excreted as unchanged drug and sulfonated metabolite are shown in Table A2. The amount of the dose recovered in the urine was 80% after administration as powder and 83–115% after using an MDI. The proportion of cumulative excreted salbutamol and salbutamol-4′-*O*-sulfate related to the total excreted amount of salbutamol was similar for both administration types. Excretion of salbutamol and the sulfoconjugate appears to be equivalent for administration by MDI and DPI. Hence, only results from the MDI trial were used for comparison of inhalation of racemic salbutamol and levosalbutamol.

Table A2. Cumulative proportion of compounds excreted after administration of salbutamol using dry powder inhaler or metered dose inhaler.

	DPI [1]	MDI [2]	MDI [2]_2
Percentage of dose recovered in urine [3]	80%	115%	83%
Proportion of parent compound [4]	42%	46%	41%
Proportion of salbutamol-4′-*O*-sulfate [4]	58%	54%	59%

[1] DPI—Dry powder inhaler. [2] MDI—Metered dose inhaler. [3] amount excreted as parent compound and sulfonated metabolite in relation to administered dose. [4] calculated as the percentage of overall amount excreted as salbutamol and salbutamol-4′-*O*-sulfate.

Inhalation by the two different application forms, i.e., DPI and MDI, were compared, and it was found to lead to the same proportion of parent compound and salbutamol-4′-*O*-sulfate for the total excreted amount. Administration by MDI was repeated due to an amount of more than 100% of the dose recovered in the urine. Possible reasons for values over 100% might be the release of a higher dose than specified by the manufacturer in the first puffs of a new inhaler. The repetition of the administration of 600 μg racemic salbutamol from an MDI led to a recovery of 83% of the dosage in the urine. The same MDI was used, supporting the assumption of the first doses released from the inhaler being higher than 100 μg per puff. However, another source for recovery over 100% might serve the relatively high uncertainty in urine volume determination. The volumetric device used was not qualified for high precision volume determination of very low amounts of urines. This uncertainty may contribute to inaccuracy for the total amount of recovered salbutamol in the first trial of inhalation application of 600 μg racemic salbutamol (SA_MDI). In the repetition of the trial (SA_MDI_2) the urine collection was performed utilizing more accurate equipment for low volumes, if necessary.

Appendix A.3. Appendix Figures
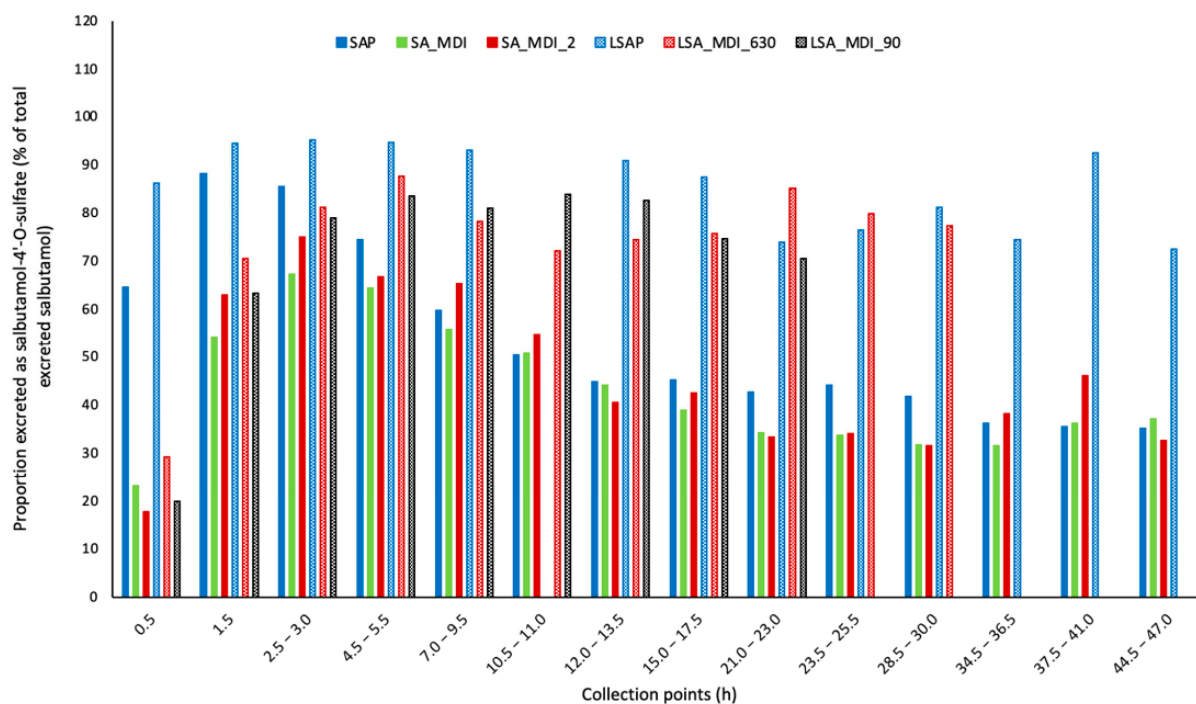
Figure A1. Time profile of proportion of salbutamol-4′-O-sulfate excreted in urine in relation to total salbutamol excreted. Salbutamol-4′-O-sulfate was calculated as salbutamol equivalent. SA_MDI—600 µg inhaled racemic salbutamol, SAP—2 mg oral racemic salbutamol, LSA_MDI—630 µg inhaled levosalbutamol and LSA_MDI_TD—90 µg inhaled levosalbutamol, LSAP—1 mg oral levosalbutamol.
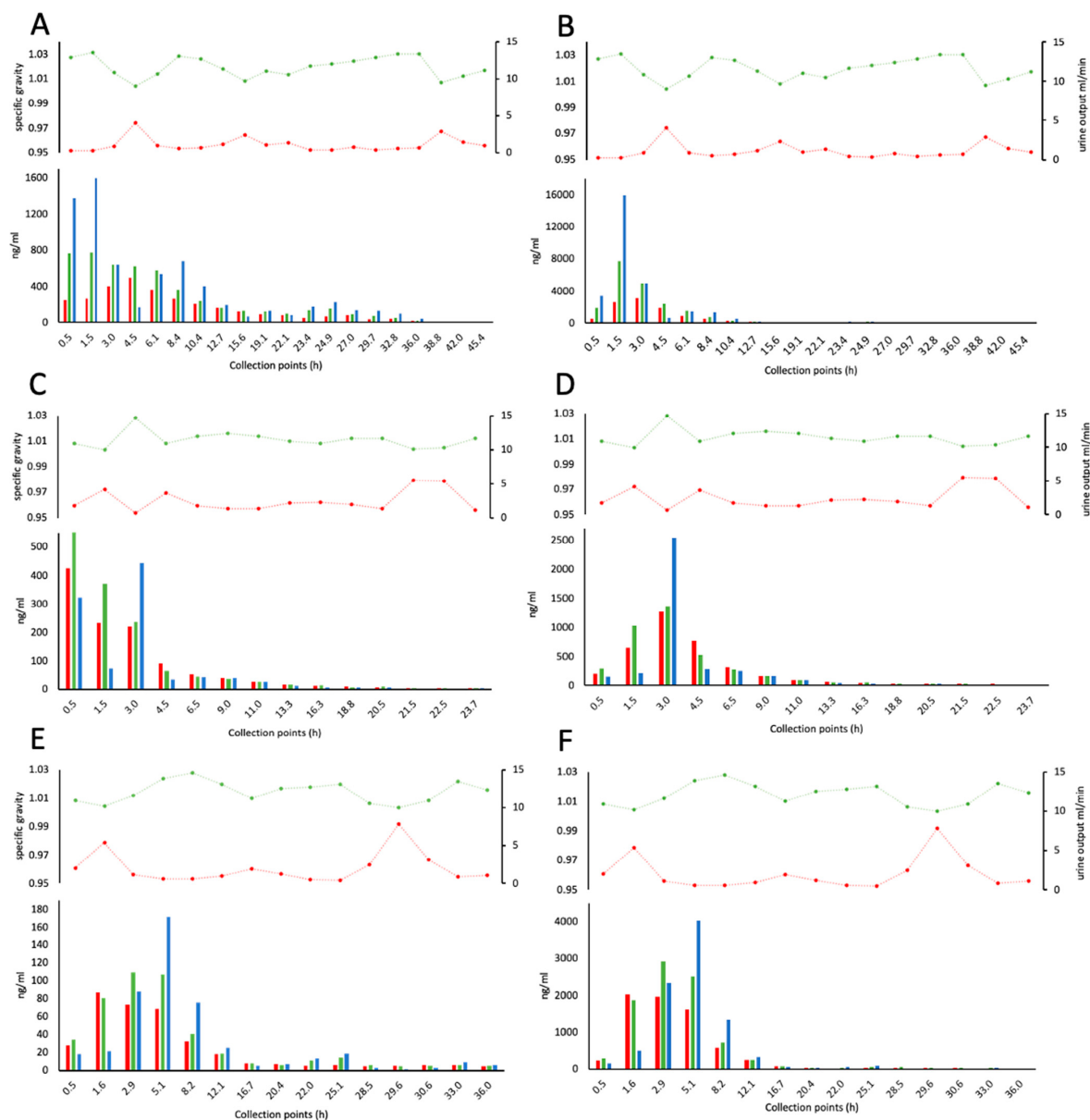
Figure A2. Salbutamol (**left**) and salbutamol-4′-O-sulfate (**right**) uncorrected concentrations (blue) and adjusted concentrations by the specific gravity of the urines (green) and by the urinary flow rate (red) after (**A,B**) oral administration of 2 mg racemic salbutamol, (**C+D**) inhalation 630 μg and (**E+F**) oral administration of 1 mg levosalbutamol. Specific gravity and urinary flow rate for the samples are shown as dotted lines.

References

1. Boulton, D.W.; Fawcett, J.P. The pharmacokinetics of levosalbutamol: What are the clinical implications? *Clin. Pharmacokinet.* **2001**, *40*, 23–40. [CrossRef]
2. World Anti-Doping Agency. WADA Prohibited List 2022. Available online: https://www.wada-ama.org/sites/default/files/resources/files/2022list_final_en.pdf (accessed on 5 July 2023).
3. World Anti-Doping Agency. WADA Technical Document TD2022DL. Available online: https://www.wada-ama.org/sites/default/files/2022-01/td2022dl_v1.0_final_eng_0.pdf (accessed on 5 July 2023).

4.   Mackay, L.G.; Kazlauskas, R. The importance of reference materials in doping-control analysis. *Anal. Bioanal. Chem.* **2011**, *401*, 483–492. [CrossRef]

5.   Harps, L.C.; Bizjak, D.A.; Girreser, U.; Zügel, M.; Steinacker, J.M.; Diel, P.; Parr, M.K. Quantitation of Formoterol, Salbutamol, and Salbutamol-4′-O-Sulfate in Human Urine and Serum via UHPLC-MS/MS. *Separations* **2023**, *10*, 368. [CrossRef]

6.   Winkler, M.; Geier, M.; Hanlon, S.P.; Nidetzky, B.; Glieder, A. Human Enzymes for Organic Synthesis. *Angew. Chem. Int. Ed.* **2018**, *57*, 13406–13423. [CrossRef]

7.   Drăgan, C.-A.; Peters, F.T.; Bour, P.; Schwaninger, A.E.; Schaan, S.M.; Neunzig, I.; Widjaja, M.; Zapp, J.; Kraemer, T.; Maurer, H.H.; et al. Convenient Gram-Scale Metabolite Synthesis by Engineered Fission Yeast Strains Expressing Functional Human P450 Systems. *Appl. Biochem. Biotechnol.* **2011**, *163*, 965–980. [CrossRef]

8.   Ko, K.; Kurogi, K.; Davidson, G.; Liu, M.Y.; Sakakibara, Y.; Suiko, M.; Liu, M.C. Sulfation of ractopamine and salbutamol by the human cytosolic sulfotransferases. *J. Biochem.* **2012**, *152*, 275–283. [CrossRef]

9.   Jacobson, G.A.; Raidal, S.; Robson, K.; Narkowicz, C.K.; Nichols, D.S.; Haydn Walters, E. Bronchopulmonary pharmacokinetics of (R)-salbutamol and (S)-salbutamol enantiomers in pulmonary epithelial lining fluid and lung tissue of horses. *Br. J. Clin. Pharmacol.* **2017**, *83*, 1436–1445. [CrossRef]

10. Sun, Y.; Harps, L.C.; Bureik, M.; Parr, M.K. Human Sulfotransferase Assays With PAPS Production in situ. *Front. Mol. Biosci.* **2022**, *9*, 827638. [CrossRef]

11. Teubner, W. *Charakterisierung von Sulfotransferasen im Gastrointestinaltrakt von Mensch und Ratte und Aktivierung von Promutagenen in V79-Zellen, die Eine Intestinale Form (1B1) des Menschen und der Ratte Exprimieren*; Universität Potsdam: Potsdam, Germany, 2001.

12. Gamage, N.; Barnett, A.; Hempel, N.; Duggleby, R.G.; Windmill, K.F.; Martin, J.L.; McManus, M.E. Human sulfotransferases and their role in chemical metabolism. *Toxicol. Sci.* **2006**, *90*, 5–22. [CrossRef]

13. Riches, Z.; Stanley, E.L.; Bloomer, J.C.; Coughtrie, M.W.H. Quantitative Evaluation of the Expression and Activity of Five Major Sulfotransferases (SULTs) in Human Tissues: The SULT "Pie". *Drug Metab. Dispos.* **2009**, *37*, 2255. [CrossRef]

14. Walle, T.; Eaton, E.A.; Walle, U.K.; Pesola, G.R. Stereoselective metabolism ofRS-albuterol in humans. *Clin. Rev. Allergy Immunol.* **1996**, *14*, 101–113. [CrossRef]

15. Boulton, D.W.; Fawcett, J.P. Pharmacokinetics and pharmacodynamics of single oral doses of albuterol and its enantiomers in humans. *Clin. Pharmacol. Ther.* **1997**, *62*, 138–144. [CrossRef]

16. Mareck, U.; Guddat, S.; Schwenke, A.; Beuck, S.; Geyer, H.; Flenker, U.; Elers, J.; Backer, V.; Thevis, M.; Schänzer, W. Determination of salbutamol and salbutamol glucuronide in human urine by means of liquid chromatography-tandem mass spectrometry. *Drug Test. Anal.* **2011**, *3*, 820–827. [CrossRef]

17. Boulton, D.W.; Fawcett, J.P. Enantioselective disposition of salbutamol in man following oral and intravenous administration. *Br. J. Clin. Pharmacol.* **1996**, *41*, 35–40. [CrossRef]

18. Ward, J.K.; Dow, J.; Dallow, N.; Eynott, P.; Milleri, S.; Ventresca, G.P. Enantiomeric disposition of inhaled, intravenous and oral racemic-salbutamol in man--no evidence of enantioselective lung metabolism. *Br. J. Clin. Pharmacol.* **2000**, *49*, 15–22. [CrossRef]

19. Sun, Y.; Machalz, D.; Wolber, G.; Parr, M.K.; Bureik, M. Functional Expression of All Human Sulfotransferases in Fission Yeast, Assay Development, and Structural Models for Isoforms SULT4A1 and SULT6B1. *Biomolecules* **2020**, *10*, 1517. [CrossRef]

20. Matuszewski, B.K.; Constanzer, M.L.; Chavez-Eng, C.M. Strategies for the assessment of matrix effect in quantitative bioanalytical methods based on HPLC-MS/MS. *Anal. Chem.* **2003**, *75*, 3019–3030. [CrossRef]

21. World Anti-Doping Agency. WADA Technical Document TD2021IDCR. Available online: https://www.wada-ama.org/sites/default/files/resources/files/td2021idcr_final_eng_0.pdf (accessed on 21 July 2021).

22. Orlovius, A.-K.L. *Sulfokonjugierte Sympathomimetika in der Dopinganalytik: Synthese, Charakterisierung und Analyse*; Rheinische Friedrich-Wilhelms-Universität Bonn: Bonn, Germany, 2014. Available online: https://hdl.handle.net/20.500.11811/6086 (accessed on 9 July 2023).

23. Kharissova, O.V.; Kharisov, B.I.; Oliva González, C.M.; Méndez, Y.P.; López, I. Greener synthesis of chemical compounds and materials. *R. Soc. Open Sci.* **2019**, *6*, 191378. [CrossRef]

24. Purchartová, K.; Valentová, K.; Pelantová, H.; Marhol, P.; Cvačka, J.; Havlíček, L.; Křenková, A.; Vavříková, E.; Biedermann, D.; Chambers, C.S.; et al. Prokaryotic and Eukaryotic Aryl Sulfotransferases: Sulfation of Quercetin and Its Derivatives. *ChemCatChem* **2015**, *7*, 3152–3162. [CrossRef]

25. Horst, M.; Hartog, A.; Morabet, R.; Marais, A.; Kircz, M.; Wever, R. Enzymatic Sulfation of Phenolic Hydroxy Groups of Various Plant Metabolites by an Arylsulfotransferase. *Eur. J. Org. Chem.* **2015**, *2015*, 534–541. [CrossRef]

26. Ragan, M.A. Phenol sulfate esters: Ultraviolet, infrared, 1H and 13C nuclear magnetic resonance spectroscopic investigation. *Can. J. Chem.* **1978**, *56*, 2681–2685. [CrossRef]

27. Melchor, R.; Biddiscombe, M.F.; Mak, V.H.; Short, M.D.; Spiro, S.G. Lung deposition patterns of directly labelled salbutamol in normal subjects and in patients with reversible airflow obstruction. *Thorax* **1993**, *48*, 506–511. [CrossRef]

28. Nishikawa, M.; Masuyama, Y.; Nunome, M.; Yasuda, K.; Sakaki, T.; Ikushiro, S. Whole-cell-dependent biosynthesis of sulfo-conjugate using human sulfotransferase expressing budding yeast. *Appl. Microbiol. Biotechnol.* **2018**, *102*, 723–732. [CrossRef]
29. Nakpheng, T.; Songkarak, S.; Suwandecha, T.; Sritharadol, R.; Chunhachaichana, C.; Srichana, T. Evidences for salbutamol metabolism by respiratory and liver cell lines. *Drug Metab. Pharmacokinet.* **2017**, *32*, 127–134. [CrossRef]

4   Declaration of Own Contribution

In the following, the author's contribution to the individual publications, which are included in this cumulative work, are disclosed:

Manuscript I:

- Cooperation in manuscript preparation and revision

Manuscript II：

- Conception and design of the experiments in cooperation with co-authors

- Construction of a complete set of recombinant fission yeast strains

- Execution of biotransformation experiments and evaluation of data.

- Preparation and revision of manuscript in cooperation with co-authors

Manuscript III：

- Conception, design, and execution of biotransformation experiments together with co-authors

- Cooperation for data analysis and evaluation

- Preparation of manuscript and revision in cooperation with co-authors

Manuscript IV：

- Design and execution of *in vitro* experiments

- Synthesis of sulfate metabolite with co-authors

- Revision of the manuscript in cooperation with co-authors

5 Discussion

The central focus of this work is SULT metabolism, encompassing various research fields such as anti-doping research, drug metabolism, *in vitro* studies, and biosynthesis. Three major aims of this work are outlined below: Firstly, to establish a complete set of human SULTs that fills the existing gaps in this field and provides a robust tool for *in vitro* studies on SULT metabolism. Secondly, to develop an economical and efficient biotransformation approach that enables broader participation in the *in vitro* study of SULT metabolism. Thirdly, to offer valuable insights to enhance the detection of prohibited drugs in sports and to contribute to anti-doping research. This work promotes the advancement of knowledge in the field of SULT metabolism. The achieved results have substantial implications for further understanding of metabolism, biochemistry, the practical application of biosynthesis, doping control analysis and fields where the knowledge or application of SULT metabolism is highly relevant.

The studies of SULTs and sulfonation can be dated back to the 1960s. In recent decades, many isoforms were isolated and identified due to genome sequencing projects [111-113]. *In vitro* studies generally use homogenized organ fractions, isolated enzymes or gene modified microorganisms such as *E. coli* [53] or budding yeast [20]. Nevertheless, a complete expressing system of human SULTs had not yet been constructed. To study human SULTs systematically and to conduct subsequent research, the first step in this work was to establish recombinant fission yeast strains for each human SULT. In Manuscript II, a gene-modified fission yeast strain NCYC2036 was employed as the parent strain. Both plasmids, pCAD1 and pREP1, with integrated cDNA encoding each of 14 human SULTs, were subsequently transformed. The successful utilization of permeabilized fission yeast cells (enzyme bags) for biotransformations catalyzed by human CYPs [65, 66] and UGTs [72] was reported by our group previously. Such an assay was developed for SULTs as well. The advantages of higher sensitivity and shorter retention time of enzyme bag compared to whole-cell biotransformation were verified by the activity monitoring of SULT1C3d. Using the recombinant fission yeast strains and the newly developed SULT activity assay, the catalytical activity of SULT4A1 and SULT6B1 was demonstrated for the first time. While SULT4A1 and SULT6B1 were identified in 2000 [35] and 2004 [114], respectively, no substrate had been reported for either enzyme until our

functional assay was applied. SULT4A1 possesses a different PAPS binding region and was reported to be unable to bind PAP(S) [35, 115]. Thus, it was assumed to be involved in the sulfation of non-classical substrates or perform a divergent function intracellularly [116]. A rare description of SULT6B1 can be found in literature, indicating that the functional characteristics of this isoform are still unrevealed. The results presented in this study demonstrate the enzymatic function of SULT4A1 and SULT6B1, and further research can be carried out based on these findings.

However, the requirement of exogenous PAPS in this assay results in high experimental costs, which hampers extensive substrate screening and upscaling for biosynthetic metabolite production. The development and optimization of an approach with *in situ* PAPS production is therefore desirable for a broader application of this method in metabolism and anti-doping research. Although the mechanism of PAPS synthesis in fission yeast *S. pombe* has not been completely revealed, the successful whole-cell biotransformation activity assay indicates sufficient PAPS production for sulfation reactions by fission yeast (Manuscript II). Previously, PAPS production was reported in a chemoenzymatic approach [117], an enzymatic approach [44], and in a liver S9 fraction-based biosynthesis [118]. In manuscript III, the successful combination of the (re-)generation of PAPS and the sulfonation of xenobiotics are described. Further method optimization resulted in a more than double product yield while reducing the cost per experiment by a factor of 60 compared with the biosynthesis using PAPS as cofactor. The developed method was successfully used for the production of stable isotopically labelled sulfate metabolites (D_6-DHEA sulfate, DHEA-^{34}S-Sulfate, D_9-salbutamol sulfate, and salbutamol-^{34}S-sulfate). This finding highlights the potential of the method developed in Manuscript Ⅲ for synthesizing labeled sulfate metabolites as reference materials.

In manuscript IV, a sulfate metabolite of salbutamol, salbutamol-4′-*O*-sulfate was synthesized based on the developed biosynthesis approach in Manuscript III, with some modifications to reach an upscaled production. The lack of selectivity in sulfonation at the three hydroxy groups of salbutamol presents a significant challenge in chemical synthesis. The strategies of using protection groups also failed [119]. However, biosynthesis performed with constructed recombinant human SULT1A3-expressed strain (Manuscript II) exhibited high selectivity, resulting in one mono-sulfonated product (salbutamol-4′-*O*-sulfate) without additional

sulfonation byproducts detected. After biosynthesis and subsequent purification, the exact structure was confirmed, and the amount of salbutamol-4′-O-sulfate was determined by absolute quantitative nuclear magnetic resonance spectroscopy (qNMR). The identified and quantitated salbutamol-4′-O-sulfate was successfully used as a reference material in the study of enantiopure salbutamol administration. However, challenges and drawbacks are obvious in this biosynthesis approach. The productivity of the salbutamol-4'-O-sulfate biosynthesis is relatively low. Hence, several batches of synthesis were required to obtain a sufficient amount of product for qNMR analysis. Another challenge is purification. The permeabilization and three washes with NH_4HCO_3 buffer in the developed enzyme bags method removed many small molecules and water-soluble peptides, resulting in a cleaner matrix compared to whole-cell biotransformation. Still, the remaining impurities require complex purification processes, involving liquid-solid extraction and gravity column chromatography, followed by semi-preparative high-performance liquid chromatography (HPLC). However, the qNMR data still revealed an approximate 80% impurity in the purified product.

The same biosynthesis approach used for salbutamol-4'-O-sulfate was applied to the synthesis of a potential phase II sulfate metabolite of methyltestosterone (MT), 17α-methyl-5β-androstan-3α,17β-diol, 3α-sulfate (S2), with slight modifications. The reaction was performed using 17α-methyl-5β-androstan-3α,17β-diol (M2) as the substrate, incubated with recombinant human SULT2A1-expressed cells. The detection using quadrupole time-flight-mass spectrometer (LC-QTOF) indicated the yield of one monosulfo-conjugate (S2) when the substrate concentration was 0.1 mM, but the yield of three sulfo-conjugates, including S2, when the substrate concentration was increased to 1 mM. LC-QTOF detection suggests that the other two sulfo-conjugates had the same retention time as 17α-methyl-5α-androstan-3β,17β-diol, 3α-sulfate (S3), and 17α-methyl-5β-androstan-3β,17β-diol, 3α-sulfate (S4), respectively. Whether the epimerization occurs at C3/C5, or analogues generated through additional reactions during the sulfonation lead to the formation of these additional sulfates, is still not known. Furthermore, as the stereochemistry at C5 is known to be highly stable [120], epimerization at C5 is unlikely to happen during biological sulfonation. GC-MS analysis of the three detected sulfo-conjugates after the enzymatic hydrolysis [121] and derivatization [100] indicated that they share the same configuration. This result suggests another potential explanation, the formation of a bis-sulfate

during biosynthesis. However, this hypothesis does not adequately explain the detection of three monosulfates in LC-QTOF, while no bis-sulfate was detected.

In conclusion, the results presented in this work advance the research on SULT metabolism, particularly in the context of *in vitro* investigation. Meanwhile, they contribute to refining methodologies in anti-doping research and metabolic studies. The novel biotransformation system and optimized biosynthesis approach developed in this study provide promising prospects for synthesizing various sulfate metabolites. This alternative approach holds potential as a viable option for producing essential reference materials, including those required for anti-doping analysis and metabolic study. Future studies building upon the outcomes of this research are eagerly anticipated.

6   Outlook

Future work may firstly focus on improving the biosynthesis approach by raising the productivity and developing a more efficient purification procedure. Solid phase extraction may be considered involving sulfonated product purification. The weak anion ion exchange cartridge (Oasis WAX, Waters) and Oasis HLB cartridge are two potential choices since their capability on purification of chemical synthesized sulfonated compounds [6, 100, 122] and sulfonated metabolites in urine samples [123, 124] was previously demonstrated. To increase the productivity of biosynthesized salbutamol-4'-*O*-sulfate, optimization and monitoring of reaction conditions are recommended. Implementing a bioreactor for monitoring pH value, temperature, substrate consumption, and conducting fed-batch reactions may be a worthwhile approach to explore.

For the biosynthesis of S2, there are still unexplained results that require further research. Structure confirmation of synthesized S2 and the other two unknown products need to be conducted by NMR analysis. Further biotransformation assays with incremental substrate (M2) concentrations are expected to reveal the best reaction conditions for the production of single sulfo-conjugate and multiple sulfo-conjugates. To understand the underlying reasons for the generation of those two unknown sulfo-conjugates of M2 *in vitro* sulfonation, *in silico* studies may be helpful. Moreover, a study of *in vivo* sulfonated metabolism of MT by detection of sulfate metabolites in urine excretion is desired for a deeper understanding of SULT metabolism and advancing anti-doping research.

7 Summary

This thesis extensively evaluates SULT metabolism and its significance in drug metabolism and anti-doping research. It demonstrates a complete strategy that encompasses the establishment of an experimental approach, method development, and method application. The study yields three key outcomes. First, a complete set of recombinant fission yeast strains capable of functionally expressing all 14 human SULTs was generated, and a corresponding biotransformation assay (enzyme bags) was developed. Second, the developed method was enhanced by implementing *in situ* production of PAPS and optimized to achieve higher efficiency. Third, direct detection and quantitation of a sulfate metabolite of salbutamol *in vivo* was achieved through an *in vitro* biosynthesis. These findings advance our knowledge of SULT metabolism, particularly in the realm of anti-doping research, leading to an accurate identification and quantitation of SULT metabolites.

In the present work, all results were obtained mainly through *in vitro* approach. The primary research method for *in vitro* studies involved the use of recombinant fission yeast *S. pombe*. Biotransformation experiments were conducted by incubating substrates with recombinant strains expressing individual human SULTs, either after permeabilization (enzyme bag) or as whole-cell biotransformation. These *in vitro* studies served various purposes, such as monitoring enzyme activity, exploring unknown biofunctions, optimizing methods, and generating reference materials.

Different analytical techniques were utilized to evaluate the samples generated through *in vitro* biosynthesis. Liquid chromatography coupled by electrospray ionization to a quadrupole time-flight-mass spectrometer (LC-ESI-QTOF-MS) was used to analyze and identify the produced metabolites. Liquid chromatography hyphenated by electrospray ionization to a triple quadrupole mass spectrometer (LC-ESI-QQQ-MS) was used to quantitate and determine metabolites. qNMR was applied to confirm the structure of synthesized reference materials and perform an absolute quantitation. Additionally, luminescence measurements were conducted to explore the activity of SULTs towards luminescent substrates.

The results presented in this thesis lay a solid foundation for further research on SULT metabolism. Further scientific fields that can benefit from the results include drug metabolism,

drug-drug interaction, metabolic-related disease research, and bioinformatics. The advanced analytical techniques described here significantly enhance the detection and identification of generated metabolites, improving the detection of misused compounds in anti-doping research. In summary, the results presented in this work hold great significance for SULT metabolism research and anti-doping analysis, with the potential to profoundly influence the relevant fields.

8 Zusammenfassung

In dieser Arbeit wird der SULT-Stoffwechsel und seine Bedeutung für den Arzneimittelstoffwechsel und die Anti-Doping-Forschung umfassend bewertet. Sie zeigt eine vollständige Strategie auf, die die Festlegung eines experimentellen Ansatzes, die Entwicklung einer Methode und die Anwendung der Methode umfasst. Die Studie führt zu drei wichtigen Ergebnissen. Erstens wurde ein vollständiger Satz rekombinanter Spalthefestämme erzeugt, die alle 14 menschlichen SULTs funktionell exprimieren können, und es wurde eine entsprechende Biotransformationsmethode (*enzyme bags*) entwickelt. Zweitens wurde die entwickelte Methode durch die Einführung der *in situ*-Produktion von PAPS verbessert und optimiert, um eine höhere Effizienz zu erreichen. Drittens wurde der direkte Nachweis und die Quantifizierung des Sulfatmetaboliten von Salbutamol *in vivo* durch eine *in vitro*-Biosynthese erreicht. Diese Ergebnisse haben unser Wissen über den SULT-Stoffwechsel erweitert, insbesondere im Bereich der Anti-Doping-Forschung, und führten zu einer genauen Identifizierung und Quantifizierung von SULT-Metaboliten.

In der vorliegenden Arbeit wurden alle Ergebnisse hauptsächlich durch einen *in vitro*-Ansatz erzielt. Die primäre Forschungsmethode für die *in vitro*-Studien war die Verwendung von rekombinanten Spalthefen *S. pombe*. Biotransformationsexperimente wurden durchgeführt, indem Substrate mit rekombinanten Stämmen inkubiert wurden, die einzelne menschliche SULTs exprimieren, entweder nach Permeabilisierung (*enzyme bags*) oder als Ganzzell-Biotransformation. Diese *in vitro*-Studien dienten verschiedenen Zwecken, wie der Überwachung der Enzymaktivität, der Erforschung unbekannter Biofunktionen, der Optimierung von Methoden und der Herstellung von Referenzmaterialien.

Zur Auswertung der durch die *in vitro*-Biosynthese gewonnenen Proben wurden verschiedene Analyseverfahren eingesetzt. Flüssigchromatographie, gekoppelt durch Elektrospray-Ionisierung mit einem Quadrupol-Zeitflug-Massenspektrometer (LC-ESI-QTOF-MS), wurde zur Analyse und Identifizierung der erzeugten Metaboliten verwendet. Die Flüssigchromatographie mit Elektrospray-Ionisierung auf einem Dreifach-Quadrupol-Massenspektrometer (LC-ESI-QQQ-MS) wurde zur Quantifizierung und Bestimmung der Metaboliten verwendet. qNMR wurde eingesetzt, um die Struktur der synthetisierten

Referenzmaterialien zu bestätigen und eine absolute Quantifizierung durchzuführen. Zusätzlich wurden Lumineszenzmessungen durchgeführt, um die Aktivität der SULTs gegenüber lumineszierenden Substraten zu untersuchen.

Die in dieser Arbeit vorgestellten Ergebnisse bilden eine solide Grundlage für die weitere Erforschung des SULT-Stoffwechsels. Weitere wissenschaftliche Bereiche, die von den Ergebnissen profitieren können, sind der Fremdstoffmetabolismus, die Wechselwirkung zwischen Medikamenten, die Erforschung von Krankheiten im Zusammenhang mit dem Stoffwechsel und die Bioinformatik. Die hier beschriebenen fortschrittlichen Analysetechniken verbessern den Nachweis und die Identifizierung der erzeugten Metaboliten erheblich, was die Aufdeckung missbräuchlich verwendeter Substanzen in der Anti-Doping-Forschung verbessert. Zusammenfassend lässt sich sagen, dass die in dieser Arbeit vorgestellten Ergebnisse von großer Bedeutung für die SULT-Stoffwechselforschung und die Anti-Doping-Analyse sind und das Potenzial haben, die entsprechenden Bereiche tiefgreifend zu beeinflussen.

9 References

[1]   Ljungqvist A. Brief History of Anti-Doping. *Medicine and sport science* 62 (2017) 1-10

[2]   Willick SE, Miller GD, Eichner D. The anti-doping movement. *PM&R* 8 (2016) S125-S132

[3]   Gomes RL, Meredith W, Snape CE, Sephton MA. Analysis of conjugated steroid androgens: deconjugation, derivatisation and associated issues. *Journal of pharmaceutical and biomedical analysis* 49 (2009) 1133-1140

[4]   Martinez-Brito D, Notarianni ML, Iannone M, De La Torre X, Botre F. Validation of steroid sulfates deconjugation for metabolic studies. Application to human urine samples. *Journal of pharmacological and toxicological methods* 106 (2020) 106938

[5]   Cawley AT, Kazlauskas R, Trout GJ, George AV. Determination of urinary steroid sulfate metabolites using ion paired extraction. *Journal of Chromatography B* 825 (2005) 1-10

[6]   Waller CC, Mcleod MD. A simple method for the small scale synthesis and solid-phase extraction purification of steroid sulfates. *Steroids* 92 (2014) 74-80

[7]   Garg N, Hansson A, Knych HK, Stanley SD, Thevis M, Bondesson U, Hedeland M, Globisch D. Structural elucidation of major selective androgen receptor modulator (SARM) metabolites for doping control. *Organic & biomolecular chemistry* 16 (2018) 698-702

[8]   Parr MK, Orlovius A-K, Guddat S, Gütschow M, Thevis M, Schänzer W. Sulfoconjugates of heavy volatile nitrogen containing doping substances for improved LC-MS/MS screening. *Recent Advances in Doping Analysis, Sportverl Strauß, Köln* 15 (2007) 97-102

[9]   Orlovius AK, Guddat S, Parr MK, Kohler M, Gütschow M, Thevis M, Schänzer W. Terbutaline sulfoconjugate: characterization and urinary excretion monitored by LC/ESI-MS/MS. *Drug testing and analysis* 1 (2009) 568-575

[10]   Orlovius A, Guddat S, Parr M, Koch A, Gütschow M, Thevis M, Schänzer W. Identification and monitoring of octopamine sulfoconjugate in urine by LC/(ESI)-MS/MS. *Recent advances in doping analysis (19). Cologne: Sportverlag Strauß* (2011) 34-43

[11]   Tibbs ZE, Rohn-Glowacki KJ, Crittenden F, Guidry AL, Falany CN. Structural plasticity in the human cytosolic sulfotransferase dimer and its role in substrate selectivity and catalysis. *Drug metabolism and pharmacokinetics* 30 (2015) 3-20

[12]   Blanchard RL, Freimuth RR, Buck J, Weinshilboum RM, Coughtrie MW. A proposed nomenclature system for the cytosolic sulfotransferase (SULT) superfamily. *Pharmacogenetics and Genomics* 14 (2004) 199-211

[13]   Wang T, Cook I, Leyh TS. The NSAID allosteric site of human cytosolic sulfotransferases. *Journal of Biological Chemistry* 292 (2017) 20305-20312

[14]   Hui Y, Luo L, Zhang L, Kurogi K, Zhou C, Sakakibara Y, Suiko M, Liu MC. Sulfation of afimoxifene, endoxifen, raloxifene, and fulvestrant by the human cytosolic sulfotransferases (SULTs): A systematic analysis. *Journal of pharmacological sciences* 128 (2015) 144-149

[15]   Shen F, Wen H-M, Shan C-X, Kang A, Dong B, Chai C, Zhang J-Y, Zhang Q, Li W. Sulfotransferase-catalyzed biotransformation of liguzinediol and comparison of its metabolism in different species using UFLC-QTOF-MS. *Journal of Chromatography B* 1089 (2018) 1-7

[16]   Arlt VM, Glatt H, Gamboa Da Costa G, Reynisson J, Takamura-Enya T, Phillips DH. Mutagenicity and DNA adduct formation by the urban air pollutant 2-nitrobenzanthrone. *Toxicol Sci* 98 (2007) 445-457

[17]   Glatt H, Meinl W. Sulfotransferases and acetyltransferases in mutagenicity testing: technical aspects. *Methods in enzymology* 400 (2005) 230-249

[18]   Glatt H, Meinl W. Pharmacogenetics of soluble sulfotransferases (SULTs). *Naunyn-Schmiedeberg's archives of pharmacology* 369 (2004) 55-68

[19]   Salman ED, Kadlubar SA, Falany CN. Expression and localization of cytosolic sulfotransferase (SULT) 1A1 and SULT1A3 in normal human brain. *Drug Metabolism and Disposition* 37 (2009) 706-709

[20]   Nishikawa M, Masuyama Y, Nunome M, Yasuda K, Sakaki T, Ikushiro S. Whole-cell-dependent biosynthesis of sulfo-conjugate using human sulfotransferase expressing budding yeast. *Applied microbiology and biotechnology* 102 (2018) 723-732

[21]   Teubner W, Meinl W, Florian S, Kretzschmar M, Glatt H. Identification and localization of soluble sulfotransferases in the human gastrointestinal tract. *Biochemical Journal* 404 (2007) 207-215

[22]   Meinl W, Meerman JH, Glatt H. Differential activation of promutagens by alloenzymes of human sulfotransferase 1A2 expressed in Salmonella typhimurium. *Pharmacogenetics and Genomics* 12 (2002) 677-689

[23]   Eisenhofer G, Coughtrie MW, Goldstein DS. Dopamine sulphate: an enigma resolved. *Clinical and experimental pharmacology & physiology. Supplement* 26 (1999) S41-53

[24]   Wang J, Falany JL, Falany CN. Expression and characterization of a novel thyroid hormone-sulfating form of cytosolic sulfotransferase from human liver. *Molecular pharmacology* 53 (1998) 274-282

[25]   Blanchard RL. Nomenclature and molecular biology of the human sulfotransferase family. *Human cytosolic sulfotransferases* 1 (2005) 1-26

[26]   Duniec-Dmuchowski Z, Rondini EA, Tibbs ZE, Falany CN, Runge-Morris M, Kocarek TA. Expression of the orphan cytosolic sulfotransferase SULT1C3 in human intestine: characterization of the transcript variant and implications for function. *Drug Metabolism and Disposition* 42 (2014) 352-360

[27]   Meinl W, Donath C, Schneider H, Sommer Y, Glatt H. SULT1C3, an orphan sequence of the human genome, encodes an enzyme activating various promutagens. *Food and chemical toxicology* 46 (2008) 1249-1256

[28]   Sakakibara Y, Yanagisawa K, Katafuchi J, Ringer DP, Takami Y, Nakayama T, Suiko M, Liu M-C. Molecular cloning, expression, and characterization of novel human sult1c sulfotransferases that catalyze the sulfonation of N-Hydroxy-2-acetylaminofluorene. *Journal of Biological Chemistry* 273 (1998) 33929-33935

[29]   Guidry AL, Tibbs ZE, Runge-Morris M, Falany CN. Expression, purification and characterization of human cytosolic sulfotransferase (SULT) 1C4. *Hormone molecular biology and clinical investigation* 29 (2017) 27-36

[30]   Coughtrie MWH. Function and organization of the human cytosolic sulfotransferase (SULT) family. *Chem Biol Interact* 259 (2016) 2-7

[31]   Kurogi K, Chepak A, Hanrahan MT, Liu M-Y, Sakakibara Y, Suiko M, Liu M-C. Sulfation of opioid drugs by human cytosolic sulfotransferases: metabolic labeling study and enzymatic analysis. *European journal of pharmaceutical sciences* 62 (2014) 40-48

[32]   Geese WJ, Raftogianis RB. Biochemical characterization and tissue distribution of human SULT2B1. *Biochemical and biophysical research communications* 288 (2001) 280-289

[33]   Meloche CA, Falany CN. Expression and characterization of the human 3β-hydroxysteroid sulfotransferases (SULT2B1a and SULT2B1b). *The Journal of steroid biochemistry and molecular biology* 77 (2001) 261-269

[34]   Dooley TP, Haldeman-Cahill R, Joiner J, Wilborn TW. Expression profiling of human sulfotransferase and sulfatase gene superfamilies in epithelial tissues and cultured cells. *Biochemical and biophysical research communications* 277 (2000) 236-245

[35]   Falany CN, Xie X, Wang J, Ferrer J, Falany JL. Molecular cloning and expression of novel sulphotransferase-like cDNAs from human and rat brain. *Biochemical Journal* 346 (2000) 857-864

[36]   Uhlen M, Oksvold P, Fagerberg L, Lundberg E, Jonasson K, Forsberg M, Zwahlen M, Kampf C, Wester K, Hober S. Towards a knowledge-based human protein atlas. *Nature biotechnology* 28 (2010) 1248-1250

[37]   Human Protein Atlas. (2023) https://www.proteinatlas.org/ENSG00000138068-SULT6B1/summary/sections, Access date: 02.08.2023

[38]   Kakuta Y, Pedersen LG, Carter CW, Negishi M, Pedersen LC. Crystal structure of estrogen sulphotransferase. *Nature structural biology* 4 (1997) 904-908

[39]   Bidwell LM, Mcmanus ME, Gaedigk A, Kakuta Y, Negishi M, Pedersen L, Martin JL. Crystal structure of human catecholamine sulfotransferase. *Journal of molecular biology* 293 (1999) 521-530

[40]   Kakuta Y, Petrotchenko EV, Pedersen LC, Negishi M. The sulfuryl transfer mechanism: crystal structure of a vanadate complex of estrogen sulfotransferase and mutational analysis. *Journal of Biological Chemistry* 273 (1998) 27325-27330

[41]   Ong E, Yeh J-C, Ding Y, Hindsgaul O, Fukuda M, Pedersen LC, Negishi M. Structure and function of HNK-1 sulfotransferase: identification of donor and acceptor binding sites by site-directed mutagenesis. *Journal of Biological Chemistry* 274 (1999) 25608-25612

[42]   Teramoto T, Sakakibara Y, Liu M-C, Suiko M, Kimura M, Kakuta Y. Snapshot of a Michaelis complex in a sulfuryl transfer reaction: Crystal structure of a mouse sulfotransferase, mSULT1D1, complexed with donor substrate and accepter substrate. *Biochemical and biophysical research communications* 383 (2009) 83-87

[43]   Pedersen LC, Petrotchenko E, Shevtsov S, Negishi M. Crystal structure of the human estrogen sulfotransferase-PAPS complex: evidence for catalytic role of Ser137 in the sulfuryl transfer reaction. *Journal of Biological Chemistry* 277 (2002) 17928-17932

[44]   Burkart MD, Izumi M, Chapman E, Lin CH, Wong CH. Regeneration of PAPS for the enzymatic synthesis of sulfated oligosaccharides. *The Journal of organic chemistry* 65

(2000) 5565-5574

[45] Günal S, Hardman R, Kopriva S, Mueller JW. Sulfation pathways from red to green. *Journal of Biological Chemistry* 294 (2019) 12293-12312

[46] Takahashi H, Kopriva S, Giordano M, Saito K, Hell R. Sulfur assimilation in photosynthetic organisms: molecular functions and regulations of transporters and assimilatory enzymes. *Annual review of plant biology* 62 (2011) 157-184

[47] Carroll KS, Gao H, Chen H, Stout CD, Leary JA, Bertozzi CR. A conserved mechanism for sulfonucleotide reduction. *PLoS biology* 3 (2005) e250

[48] Goettsch S, Badea RA, Mueller JW, Wotzlaw C, Schoelermann B, Schulz L, Rabiller M, Bayer P, Hartmann-Fatu C. Human TPST1 transmembrane domain triggers enzyme dimerisation and localisation to the Golgi compartment. *Journal of molecular biology* 361 (2006) 436-449

[49] Yokoyama Y, Sasaki Y, Terasaki N, Kawataki T, Takekawa K, Iwase Y, Shimizu T, Sanoh S, Ohta S. Comparison of drug metabolism and its related hepatotoxic effects in HepaRG, cryopreserved human hepatocytes, and HepG2 cell cultures. *Biological and pharmaceutical bulletin* 41 (2018) 722-732

[50] Gomez-Lechon M, Donato M, Castell J, Jover R. Human hepatocytes as a tool for studying toxicity and drug metabolism. *Current drug metabolism* 4 (2003) 292-312

[51] Gissen P, Arias IM. Structural and functional hepatocyte polarity and liver disease. *Journal of hepatology* 63 (2015) 1023-1037

[52] Duffus JH, Nordberg M, Templeton DM. Glossary of terms used in toxicology, (IUPAC Recommendations 2007). *Pure and Applied Chemistry* 79 (2007) 1153-1344

[53] Shimohira T, Kurogi K, Hashiguchi T, Liu M-C, Suiko M, Sakakibara Y. Regioselective production of sulfated polyphenols using human cytosolic sulfotransferase-expressing Escherichia coli cells. *Journal of bioscience and bioengineering* 124 (2017) 84-90

[54] Rydevik A, Lagojda A, Thevis M, Bondesson U, Hedeland M. Isolation and characterization of a β-glucuronide of hydroxylated SARM S1 produced using a combination of biotransformation and chemical oxidation. *Journal of pharmaceutical and biomedical analysis* 98 (2014) 36-39

[55] Karim A, Gerliani N, Aïder M. Kluyveromyces marxianus: An emerging yeast cell factory for applications in food and biotechnology. *International Journal of Food Microbiology* 333 (2020) 108818

[56] Eldarov M, Kishkovskaia S, Tanaschuk T, Mardanov A. Genomics and biochemistry of Saccharomyces cerevisiae wine yeast strains. *Biochemistry (Moscow)* 81 (2016) 1650-1668

[57] Avalueva E, Iup U, Tkachenko E, Sitkin S. Use of Saccharomyces boulardii in treating patients inflammatory bowel diseases (clinical trial). *Eksperimental'naia i Klinicheskaia Gastroenterologiia= Experimental & Clinical Gastroenterology* (2010) 103-111

[58] Mattanovich D, Branduardi P, Dato L, Gasser B, Sauer M, Porro D. Recombinant protein production in yeasts. *Recombinant gene expression* (2012) 329-358

[59] Hedges SB. The origin and evolution of model organisms. *Nature Reviews Genetics* 3 (2002) 838-849

[60] Hayles J, Nurse P. Introduction to fission yeast as a model system. *Cold Spring Harbor*

Protocols 2018 (2018) pdb. top079749

[61]   Muller S, Sandal T, Kamp-Hansen P, Dalboge H. Comparison of expression systems in the yeasts Saccharomyces cerevisiae, Hansenula polymorpha, Klyveromyces lactis, Schizosaccharomyces pombe and Yarrowia lipolytica. Cloning of two novel promoters from Yarrowia lipolytica. *Yeast* 14 (1998) 1267-1283

[62]   Chang F. Forces that shape fission yeast cells. *Molecular biology of the cell* 28 (2017) 1819-1824

[63]   Pretorius IS. Synthetic genome engineering forging new frontiers for wine yeast. *Critical reviews in biotechnology* 37 (2017) 112-136

[64]   Zollner A, Dragan CA, Pistorius D, Muller R, Bode HB, Peters FT, Maurer HH, Bureik M. Human CYP4Z1 catalyzes the in-chain hydroxylation of lauric acid and myristic acid. *Biological chemistry* 390 (2009) 313-317

[65]   Durairaj P, Fan L, Machalz D, Wolber G, Bureik M. Functional characterization and mechanistic modeling of the human cytochrome P450 enzyme CYP4A22. *FEBS Lett* 593 (2019) 2214-2225

[66]   Durairaj P, Fan L, Du W, Ahmad S, Mebrahtu D, Sharma S, Ashraf RA, Liu J, Liu Q, Bureik M. Functional expression and activity screening of all human cytochrome P450 enzymes in fission yeast. *FEBS Lett* 593 (2019) 1372-1380

[67]   Buchheit D, Schmitt EI, Bischoff D, Ebner T, Bureik M. S-Glucuronidation of 7-mercapto-4-methylcoumarin by human UDP glycosyltransferases in genetically engineered fission yeast cells. (2011)

[68]   Dragan CA, Buchheit D, Bischoff D, Ebner T, Bureik M. Glucuronide production by whole-cell biotransformation using genetically engineered fission yeast Schizosaccharomyces pombe. *Drug Metab Dispos* 38 (2010) 509-515

[69]   Dragan CA, Zearo S, Hannemann F, Bernhardt R, Bureik M. Efficient conversion of 11-deoxycortisol to cortisol (hydrocortisone) by recombinant fission yeast Schizosaccharomyces pombe. *FEMS yeast research* 5 (2005) 621-625

[70]   Maundrell K. Thiamine-repressible expression vectors pREP and pRIP for fission yeast. *Gene* 123 (1993) 127-130.

[71]   Heyer W-D, Sipiczki M, Kohli J. Replicating plasmids in Schizosaccharomyces pombe: improvement of symmetric segregation by a new genetic element. *Molecular and cellular biology* 6 (1986) 80-89

[72]   Sharma S, Durairaj P, Bureik M. Rapid and convenient biotransformation procedure for human drug metabolizing enzymes using permeabilized fission yeast cells. *Analytical biochemistry* 607 (2020) 113704

[73]   Birzniece V. Doping in sport: effects, harm and misconceptions. *Internal medicine journal* 45 (2015) 239-248

[74]   World Anti-Doping Agency. World Anti-Doping Code. (2021) https://www.wada-ama.org/en/resources/world-anti-doping-program/world-anti-doping-code, Access date: 20.05.2023

[75]   World Anti-Doping Agency. International Standard for Laboratories (ISL). (2021) https://www.wada-ama.org/en/resources/world-anti-doping-program/international-standard-laboratories-isl, Access date: 20.05.2023

[76]   De Kerkhof V. DH Steroid Profiling in Doping Analysis Universiteit Utrecht. *Utrecht,*

Netherlands (2001)

[77] Guddat S, Solymos E, Orlovius A, Thomas A, Sigmund G, Geyer H, Thevis M, Schänzer W. High‐throughput screening for various classes of doping agents using a new ‘dilute‐and‐shoot’ liquid chromatography‐tandem mass spectrometry multi‐target approach. *Drug testing and analysis* 3 (2011) 836-850

[78] Görgens C, Guddat S, Orlovius A-K, Sigmund G, Thomas A, Thevis M, Schänzer W. “Dilute-and-inject” multi-target screening assay for highly polar doping agents using hydrophilic interaction liquid chromatography high resolution/high accuracy mass spectrometry for sports drug testing. *Analytical and bioanalytical chemistry* 407 (2015) 5365-5379

[79] Gomez C, Pozo OJ, Marcos J, Segura J, Ventura R. Alternative long-term markers for the detection of methyltestosterone misuse. *Steroids* 78 (2013) 44-52

[80] Rzeppa S, Viet L. Analysis of sulfate metabolites of the doping agents oxandrolone and danazol using high performance liquid chromatography coupled to tandem mass spectrometry. *Journal of chromatography. B, Analytical technologies in the biomedical and life sciences* 1029-1030 (2016) 1-9

[81] Parr MK, Wuest B, Naegele E, Joseph JF, Wenzel M, Schmidt AH, Stanic M, De La Torre X, Botrè F. SFC-MS/MS as an orthogonal technique for improved screening of polar analytes in anti-doping control. *Analytical and bioanalytical chemistry* 408 (2016) 6789-6797

[82] Parr M, Sun Y, Harps L, Bureik M. Human sulfotransferase assays with PAPS production in situ. *Frontiers in Molecular Biosciences* 9-2022 107

[83] Aboushady D, Hanafi RS, Parr MK. Quality by Design approach for Enantioseparation of Terbutaline and its Sulfate Conjugate Metabolite for Bioanalytical Application using Supercritical Fluid Chromatography. *Journal of Chromatography A* (2022) 463285

[84] National Library of Medicine. NCBI Literature Resources. https://pubmed.ncbi.nlm.nih.gov/?term=sulfate+doping, 18.07.2023

[85] Pasqualini JR, Jayle M-F. Identification of 3β, 21-dihydroxy-5-pregnene-20-one disulfate in human urine. *The Journal of Clinical Investigation* 41 (1962) 981-987

[86] Arcos M, Lieberman S. 5-Pregnene-3β, 20α-diol-3-sulfate-20-(2'-acetamido-2'-deoxy-α-D-glucoside) and 5-Pregnene-3β, 20α-diol-3, 20-disulfate. Two Novel Urinary Conjugates. *Biochemistry* 6 (1967) 2032-2039

[87] Kuuranne T. Phase-II metabolism of androgens and its relevance for doping control analysis. *Handbook of experimental pharmacology* (2010) 65-75

[88] Gower D, Houghton E, Kicman A. Anabolic steroids: metabolism, doping and detection in equestrian and human sports. In: *Steroid Analysis*, Springer, (1995) 468-526

[89] Schänzer W. Metabolism of anabolic androgenic steroids. *Clinical chemistry* 42 (1996) 1001-1020

[90] Dehennin L, Lafarge P, Dailly P, Bailloux D, Lafarge J-P. Combined profile of androgen glucuro-and sulfoconjugates in post-competition urine of sportsmen: a simple screening procedure using gas chromatography-mass spectrometry. *Journal of Chromatography B: Biomedical Sciences and Applications* 687 (1996) 85-91

[91] Sakellariou P, Kiousi P, Fragkaki AG, Lyris E, Petrou M, Georgakopoulos C, Angelis

YS. Alternative markers for Methylnortestosterone misuse in human urine. *Drug testing and analysis* 12 (2020) 1544-1553

[92]   Strahm E, Baume N, Mangin P, Saugy M, Ayotte C, Saudan C. Profiling of 19-norandrosterone sulfate and glucuronide in human urine: Implications in athlete's drug testing. *Steroids* 74 (2009) 359-364

[93]   Torrado S, Roig M, Farré M, Segura J, Ventura R. Urinary metabolic profile of 19‑norsteroids in humans: glucuronide and sulphate conjugates after oral administration of 19‑nor‑4‑androstenediol. *Rapid Communications in Mass Spectrometry: An International Journal Devoted to the Rapid Dissemination of Up‑to‑the‑Minute Research in Mass Spectrometry* 22 (2008) 3035-3042

[94]   Piper T, Dib J, Putz M, Fusshöller G, Pop V, Lagojda A, Kuehne D, Geyer H, Schänzer W, Thevis M. Studies on the in vivo metabolism of the SARM YK11: Identification and characterization of metabolites potentially useful for doping controls. *Drug testing and analysis* 10 (2018) 1646-1656

[95]   Teubel J, Wüst B, Schipke CG, Peters O, Parr MK. Methods in endogenous steroid profiling–A comparison of gas chromatography mass spectrometry (GC–MS) with supercritical fluid chromatography tandem mass spectrometry (SFC-MS/MS). *Journal of Chromatography A* 1554 (2018) 101-116

[96]   Mumma RO. Preparation of sulfate esters. *Lipids* 1 (1966) 221-223

[97]   Joseph JP, Dusza JP, Bernstein S. Steroid conjugates I. The use of sulfamic acid for the preparation of steroid sulfates. *Steroids* 7 (1966) 577-587

[98]   Desoky AY, Hendel J, Ingram L, Taylor SD. Preparation of trifluoroethyl-and phenyl-protected sulfates using sulfuryl imidazolium salts. *Tetrahedron* 67 (2011) 1281-1287

[99]   Liu Y, Lien I-FF, Ruttgaizer S, Dove P, Taylor SD. Synthesis and protection of aryl sulfates using the 2, 2, 2-trichloroethyl moiety. *Organic letters* 6 (2004) 209-212

[100]   Rzeppa S, Heinrich G, Hemmersbach P. Analysis of anabolic androgenic steroids as sulfate conjugates using high performance liquid chromatography coupled to tandem mass spectrometry. *Drug testing and analysis* 7 (2015) 1030-1039

[101]   Sigmund G, Dib J, Tretzel L, Piper T, Bosse C, Schänzer W, Thevis M. Monitoring 2‑phenylethanamine and 2‑(3‑hydroxyphenyl) acetamide sulfate in doping controls. *Drug testing and analysis* 7 (2015) 1057-1062

[102]   Thevis M, Opfermann G, Schmickler H, Schänzer W. Mass spectrometry of steroid glucuronide conjugates. II—Electron impact fragmentation of 3‑keto‑4‑en‑and 3‑keto‑5α‑steroid‑17‑O‑β glucuronides and 5α‑steroid‑3α, 17β‑diol 3‑and 17‑glucuronides. *Journal of mass spectrometry* 36 (2001) 998-1012

[103]   Thevis M, Opfermann G, Schmickler H, Schänzer W. Mass spectrometry of steroid glucuronide conjugates. I. Electron impact fragmentation of 5α‑/5β‑androstan‑3α‑ol‑17‑one glucuronides, 5α‑estran‑3α‑ol‑17‑one glucuronide and deuterium‑labelled analogues. *Journal of mass spectrometry* 36 (2001) 159-168

[104]   Kharissova OV, Kharisov BI, Oliva González CM, Méndez YP, López I. Greener synthesis of chemical compounds and materials. *Royal Society open science* 6 (2019) 191378

[105]   Martinez CA, Rupashinghe SG. Cytochrome P450 bioreactors in the pharmaceutical industry: challenges and opportunities. *Current topics in medicinal chemistry* 13 (2013)

1470-1490

[106]   Roell M-S, Zurbriggen MD. The impact of synthetic biology for future agriculture and nutrition. *Current Opinion in Biotechnology* 61 (2020) 102-109

[107]   Liu J, Chen L, Joseph JF, Naß A, Stoll A, De La Torre X, Botrè F, Wolber G, Parr MK, Bureik M. Combined chemical and biotechnological production of 20βOH-NorDHCMT, a long-term metabolite of Oral-Turinabol (DHCMT). *Journal of inorganic biochemistry* 183 (2018) 165-171

[108]   Zollner A, Parr MK, Dragan CA, Dras S, Schlorer N, Peters FT, Maurer HH, Schanzer W, Bureik M. CYP21-catalyzed production of the long-term urinary metandienone metabolite 17beta-hydroxymethyl-17 alpha-methyl-18-norandrosta-1,4,13-trien-3-one: a contribution to the fight against doping. *Biol Chem* 391 (2010) 119-127

[109]   Weththasinghe SA. Synthesis and in vitro metabolism studies of selected steroids for anti-doping analysis. in: *Research School of Chemistry*, Australian National University,   (2020)

[110]   Ko K, Kurogi K, Davidson G, Liu MY, Sakakibara Y, Suiko M, Liu MC. Sulfation of ractopamine and salbutamol by the human cytosolic sulfotransferases. *The Journal of Biochemistry* 152 (2012) 275-283

[111]   Wilborn TW, Comer KA, Dooley TP, Reardon IM, Heinrikson RL, Falany CN. Sequence analysis and expression of the cDNA for the phenol-sulfating form of human liver phenol sulfotransferase. *Molecular pharmacology* 43 (1993) 70-77

[112]   Fujita K-I, Nagata K, Ozawa S, Sasano H, Yamazoe Y. Molecular cloning and characterization of rat ST1B1 and human ST1B2 cDNAs, encoding thyroid hormone sulfotransferases. *The journal of biochemistry* 122 (1997) 1052-1061

[113]   Comer KA, Falany JL, Falany C. Cloning and expression of human liver dehydroepiandrosterone sulphotransferase. *Biochemical Journal* 289 (1993) 233-240

[114]   Freimuth R, Wiepert M, Chute C, Wieben E, Weinshilboum R. Human cytosolic sulfotransferase database mining: identification of seven novel genes and pseudogenes. *The pharmacogenomics journal* 4 (2004) 54-65

[115]   Allali-Hassani A, Pan PW, Dombrovski L, Najmanovich R, Tempel W, Dong A, Loppnau P, Martin F, Thonton J, Edwards AM. Structural and chemical profiling of the human cytosolic sulfotransferases. *PLoS biology* 5 (2007) e97

[116]   Crittenden F, Thomas H, Ethen CM, Wu ZL, Chen D, Kraft TW, Parant JM, Falany CN. Inhibition of SULT4A1 expression induces up-regulation of phototransduction gene expression in 72-hour postfertilization zebrafish larvae. *Drug Metabolism and Disposition* 42 (2014) 947-953

[117]   An C, Zhao L, Wei Z, Zhou X. Chemoenzymatic synthesis of 3'-phosphoadenosine-5'-phosphosulfate coupling with an ATP regeneration system. *Appl Microbiol Biotechnol* 101 (2017) 7535-7544

[118]   Weththasinghe SA, Waller CC, Fam HL, Stevenson BJ, Cawley AT, Mcleod MD. Replacing PAPS: In vitro phase II sulfation of steroids with the liver S9 fraction employing ATP and sodium sulfate. *Drug testing and analysis* 10 (2018) 330-339

[119]   Orlovius A-KL. Sulfokonjugierte Sympathomimetika in der Dopinganalytik. in, Universitäts-und Landesbibliothek Bonn,   (2014)

[120]   Loke S, Liu L, Wenzel M, Scheffler H, Iannone M, De La Torre X, Schlörer N, Botrè

F, Keiler AM, Bureik M. New insights into the metabolism of methyltestosterone and metandienone: detection of Novel A-Ring reduced metabolites. *Molecules* 26 (2021) 1354

[121]   Roche. β-Glucuronidase/Arylsulfatase from Helix pomatia. in,   (2021) 5-6,

[122]   Okihara R, Mitamura K, Hasegawa M, Mori M, Muto A, Kakiyama G, Ogawa S, Iida T, Shimada M, Mano N. Potential corticoid metabolites: chemical synthesis of 3-and 21-monosulfates and their double-conjugates of tetrahydrocorticosteroids in the 5α-and 5β-series. *Chemical and Pharmaceutical Bulletin* 58 (2010) 344-353

[123]   Pranata A, Fitzgerald CC, Khymenets O, Westley E, Anderson NJ, Ma P, Pozo OJ, Mcleod MD. Synthesis of steroid bisglucuronide and sulfate glucuronide reference materials: Unearthing neglected treasures of steroid metabolism. *Steroids* 143 (2019) 25-40

[124]   Pozo OJ, Marcos J, Khymenets O, Pranata A, Fitzgerald CC, Mcleod MD, Shackleton C. SULFATION PATHWAYS: Alternate steroid sulfation pathways targeted by LC-MS/MS analysis of disulfates: application to prenatal diagnosis of steroid synthesis disorders. *Journal of molecular endocrinology* 61 (2018) M1-M12

10 Publications

10.1 Publications in scientific journals

<u>Sun Y,</u> Machalz D, Wolber G, Parr MK, Bureik M. Functional Expression of All Human Sulfotransferases in Fission Yeast, Assay Development, and Structural Models for Isoforms SULT4A1 and SULT6B1. *Biomolecules* 10 (2020) 1517

https://doi.org/10.3390/biom10111517

<u>Sun Y,</u> Harps L, Bureik M, Parr MK. Human sulfotransferase assays with PAPS production in situ. *Frontiers in Molecular Biosciences*   107

https://doi.org/10.3389/fmolb.2022.827638

Jendretzki AL, Harps LC, <u>Sun Y,</u> Bredendiek F, Bureik M, Girreser U, De La Torre X, Botrè FM, Parr MK. Biosynthesis of Salbutamol-4′-O-sulfate as Reference for Identification of Intake Routes and Enantiopure Salbutamol Administration by Achiral UHPLC-MS/MS. Separations 10 (2023) 427

https://doi.org/10.3390/separations10080427

10.2 Oral presentations in national and international conferences

<u>Sun, Y.</u>, Machalz, D., Wolber, G., Parr, M. K., & Bureik, M. Functional expression of all human sulfotransferases in fission yeast, assay development, and structural models for isoforms SULT4A1 and SULT6B1. The 2nd Advanced Chemistry World Congress, 14-15 June 2021.

<u>Sun, Y.</u>, Harps, L. C., Bureik, M., & Parr, M. K. (2022). Human Sulfotransferase Assays With PAPS Production *in situ*. Young Scientists present, 08 July 2022.

11 Appendix

11.1 List of figures

11.2 List of tables

12   Declaration of independence

Herewith I certify that I have prepared and written my thesis independently and that I have not used any sources and aids other than those indicated by me.

A doctoral procedure has never been completed at any other university or applied to another department.

Yanan Sun